Characterization of the Functional Roles of *Six2* During Kidney and Stomach Development

Michelle Maxey Self

Characterization of the Functional Roles of *Six2* During Kidney and Stomach Development

Karakterisering van de functionele rol van Six2 tijdens de ontwikkeling van de nier en de maag

Thesis

to obtain the degree of Doctor from the
Erasmus University Rotterdam
by command of the
rector magnificus

Prof.dr. S. W. J. Lamberts

and in accordance with the decision of the Doctorate Board

The public defense shall be held on
Wednesday 22 October 2008 at 13:45 o'clock

by

Michelle Maxey Self

born at Greenwood, Mississippi, USA

ERASMUS UNIVERSITEIT ROTTERDAM

Doctoral Committee

Promoter:

Prof.dr. F.G. Grosveld

Other members:

Prof.dr. M. von Lindern

Prof.dr. E. Zwarthoff

Prof.dr. G. Grosveld

Copromoter:

Dr. G. Oliver

CONTENTS

Self M, Lagutin O, Bowling B, Hendrix J, Cai Y, Dressler G, and Oliver G.
EMBO J. **25**, 5214-5228 (2006)

Chapter 3   59

Six2 defines and regulates a multipotent self-renewing nephron progenitor population throughout mammalian kidney development

Kobayashi A, Valerius MT, Mugford J, Carroll T, Self M, Oliver G, and McMahon A.
Cell Stem Cell **3**, 169-181 (2008)

Chapter 4   75

Six2 activity is required for the formation of the pyloric sphincter during mouse stomach development

Self M and Oliver G.
Manuscript in preparation

Scope of this thesis

A better understanding of the cellular and molecular mechanisms controlling different aspects of normal and pathological organogenesis is central to human health. To this end, the characterization of the functional roles of genes involved in mammalian organogenesis by using gain- and loss-of-function approaches in animal models is a powerful experimental approach. As described in this thesis, I identify the homeobox gene *Six2* as an important gene regulating different aspects of kidney and pyloric sphincter formation. The generated *Six2*-null mouse strain exhibits major phenotypic alterations in the development of these two structures.

Homeobox-containing genes have been shown to play key roles in a variety of developmental processes in multicellular organisms. The previously identified *Six/so* family of homeobox transcription factors in vertebrates includes six members (Six1-Six6). *Six2* was found to be expressed in many tissues during murine development including the developing eyes, kidneys, stomach, branchial arches, limb buds, otic and olfactory epithelia, somites, hindbrain, Rathke's pouch, and genital eminence. The development of many of these organs relies on mesenchymal-epithelial interactions.

Mammalian kidney organogenesis is a classical model of branching morphogenesis and reciprocal inductive interactions responsible for mesenchyme-to-epithelia transition. During kidney development, the metanephric mesenchyme responds to inductive signals emanating from the ureteric bud to generate the epithelia of the nephron, the functional excretory unit of the kidney. The metanephric mesenchyme is a multipotent renal progenitor cell population that is continuously replenished during nephron formation. The detailed analysis of the *Six2*-null kidney described in Chapter 2 allowed us to identify Six2 as a key factor responsible for the maintenance of this undifferentiated mesenchymal population. Furthermore, in Chapter 3 I described an important genetic interaction between *Six2* and *Wnt9b*, a member of the *Wnt* family of signaling molecules, during kidney organogenesis.

In Chapter 4, I investigated the functional role of *Six2* during stomach organogenesis, a process that in mammals is poorly understood. I determined that *Six2* activity is critical for the formation of the pyloric sphincter, a constriction of the stomach wall that is necessary to prevent intestinal reflux. Together, these results will add to our understanding of the fundamental causes of human developmental disorders such as Branchio-oto-renal syndrome, renal hypodysplasia, and infantile hypertrophic pyloric stenosis in which alterations in the functional activity of SIX2 may play a role.

Chapter 1

Introduction

During animal development, organogenesis is defined as the series of embryonic processes by which ectodermal, endodermal and mesodermal cells give rise to complete organs. The cells of an organ-forming region undergo differential development and movement to form an organ primordium or anlage. Key to facilitate our understanding of the mechanisms controlling these processes is the identification of genes involved in the development of different organs and the generation of animal models. The work presented in this thesis focused on deciphering the mechanisms regulating kidney and pyloric sphincter formation by using *Six2*, a homeobox-containing gene, as a molecular dissecting tool and the generated *Six2* mutant strain as an animal model.

1. Homeobox Genes

Homeodomain-containing proteins are transcription factors containing a conserved 60 amino acid-long sequence called the homeobox that functions to recognize and bind specific DNA target sequences[1-6]. Homeodomain proteins consist of three alpha helices that fold into a helix-turn-helix motif. The third helix contacts the major groove of the target DNA, and the N-terminal amino acid sequence makes contact with the minor groove[7-9]. A conserved motif, TAAT, is recognized by most homeodomains[5].
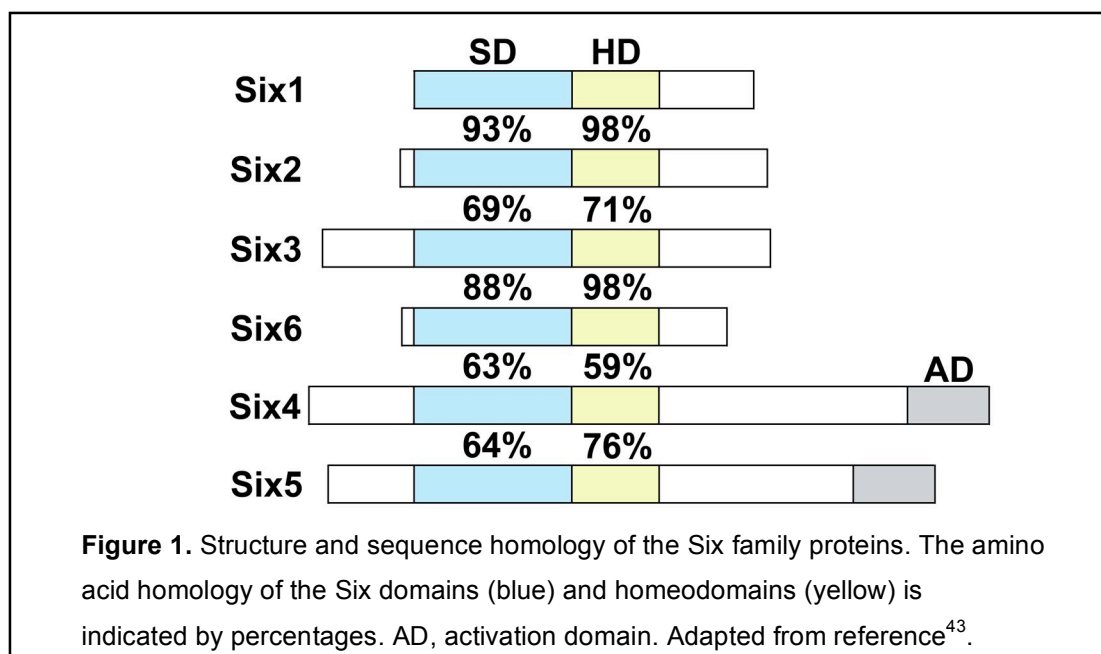
Homeobox genes were first identified in *Drosophila* as proteins that were required for segment identity[2, 10-12]. Since then, homeodomain transcription factors have been found in all bilaterians, and their sequence and functional roles are extremely conserved in evolution[1, 5, 13-15]. Many homeobox-containing genes are clustered; the best example is provided by the Hox genes which, in mammals, are arranged in four separate clusters[2, 5, 13, 16].

In general, homeobox-containing genes participate in the regulation of developmental-related processes such as positional identity and cell patterning, segmentation, anterior-posterior axis determination, dorsal-ventral polarity, cell fate specification, and cell-type differentiation[2, 5, 11, 12, 15, 17-30]. Homeotic genes set up the basic regional layout of an organism, and in most cases, mutations in homeobox-containing genes have drastic phenotypic consequences for the

developing embryo[2, 11, 23, 31]. Therefore, functional inactivation of these genes has facilitated our understanding of the cellular and molecular mechanisms regulating cell type differentiation and organ development in metazoans.
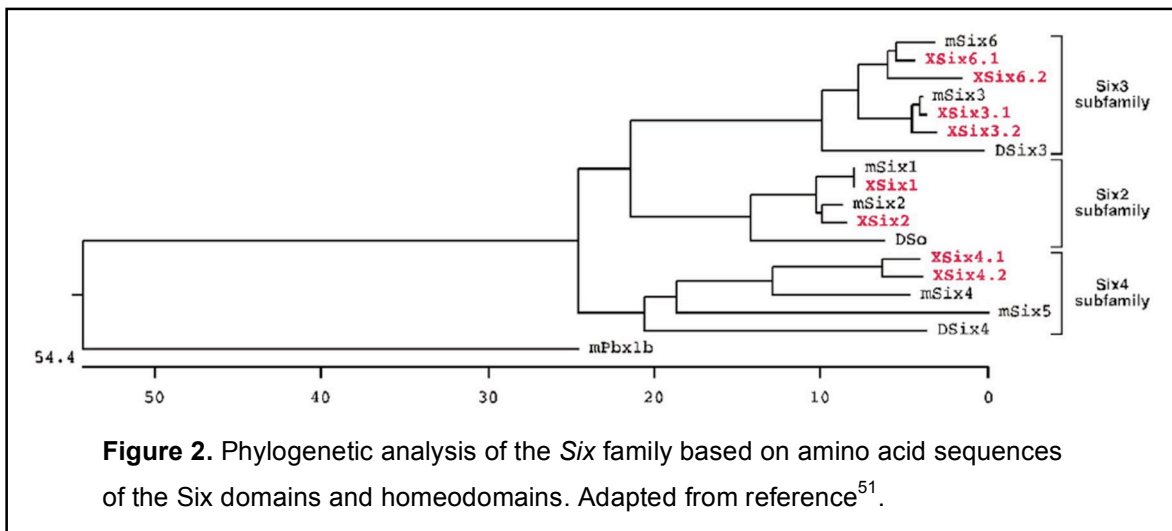
1.1 The Six Family

The mammalian *Six* family of homeobox transcription factors was identified[32] based on its homology to *Drosophila sine oculis* (so), a gene necessary for the development of the complex visual system in the fly[28, 33-35]. In mammals, this family includes six members, *Six1-Six6*, and they all contain a homeodomain and a conserved amino-terminal 110-115 amino acid-long Six domain[32, 36-44] (Figure 1). These conserved regions are necessary for DNA binding activity, and the Six domain is also required for protein-protein interactions[41, 42, 45, 46]. The *Six*-type of homeodomain lacks two typical amino acid residues, arginine at position 5 and glutamine at position 12 of helix 1[43]. These amino acid changes might be responsible for variations in their DNA binding motif as they do not always recognize the typical TAAT core[28, 42, 43, 45, 47, 48].
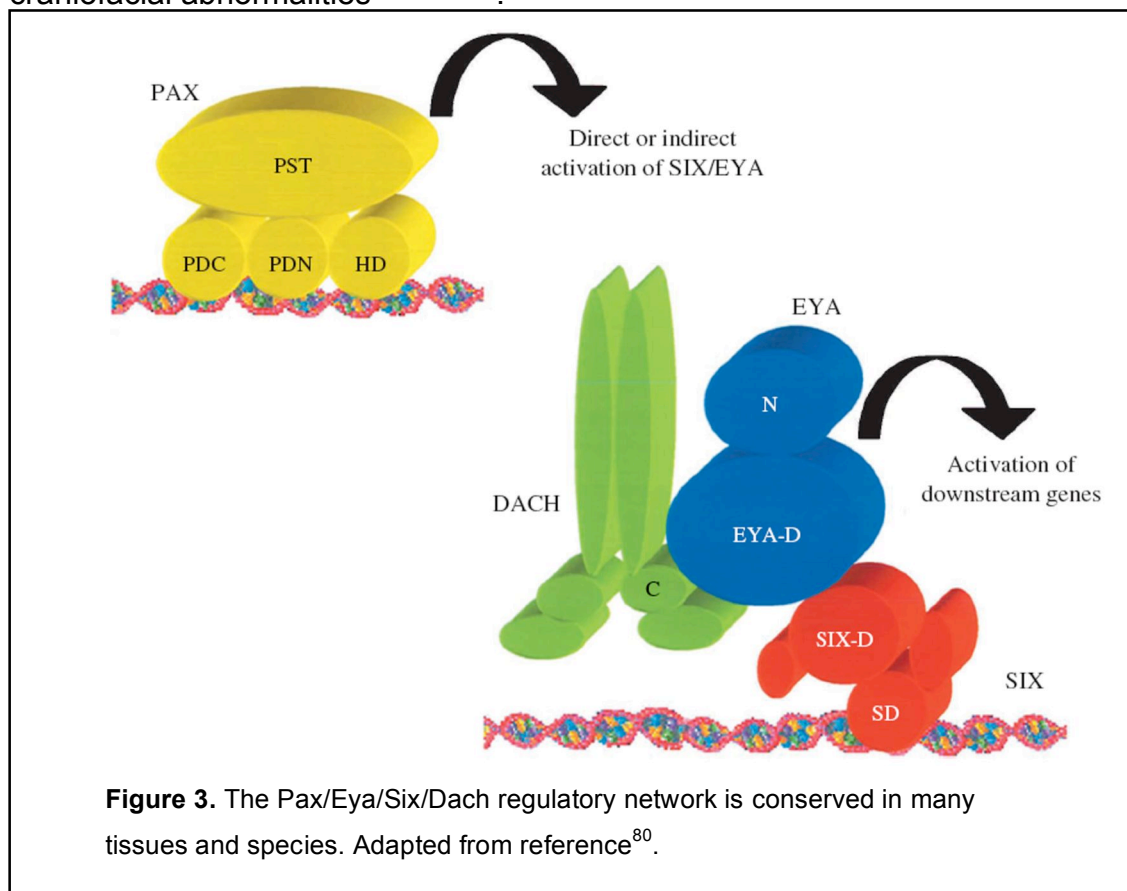

Figure 1. Structure and sequence homology of the Six family proteins. The amino acid homology of the Six domains (blue) and homeodomains (yellow) is indicated by percentages. AD, activation domain. Adapted from reference[43].

Based on their amino acid similarities, the Six proteins can be grouped into the following subfamilies: so/Six1/Six2, D-Six4/Six4/Six5, and Optix/Six3/Six6 (*so, D-Six4,* and *Optix* are the *Drosophila* members of the *so/Six* family)[49] (Figures 1, 2). An interesting attribute of the mammalian *Six* family is their organization in the genome. Human SIX1, SIX4, and SIX6 are located within 230 kb of each other on chromosome 14 with SIX1 and SIX4 on one strand and SIX6 on the opposite strand. SIX2 and SIX3 are located within 70 kb of each other but on opposite strands of chromosome 2, and SIX5 is located on chromosome 19[36-40, 43]. Chromosome 14 contains a member from each subfamily and may represent an amplification event from a single ancestral SIX gene[39]. In mice, the chromosomal localization of the *Six* genes is similar to the human arrangement; *Six1, Six4,* and *Six6* are located on chromosome 12, *Six2* is on chromosome 17 near *Six3*, and *Six5* is on chromosome 7[32, 41-44, 50].

Figure 2. Phylogenetic analysis of the *Six* family based on amino acid sequences of the Six domains and homeodomains. Adapted from reference[51].

Six proteins function as transcription factors that can either activate or repress transcription of target genes and cooperate with various protein partners depending on the cellular context[45, 52-54]. For example, members of the *so/Six1/Six2* and the *D-Six4/Six4/Six5* subfamilies interact with Eya proteins for transcriptional regulation of target genes[45, 46, 53, 55-61] (Figure 3). Members of the *Eya* family of tyrosine phosphatases are mammalian homologues of *Drosophila eyes absent* and are not capable of binding DNA. Coexpression of Six and Eya proteins results in the translocation of Eya proteins to the nucleus[53, 56, 62, 63]. Work

in different cell types, organs, and species suggests that a conserved synergistic regulatory network involving members of the *Pax*, *Eya, Six*, and *Dach* families of proteins (Figure 3) participate in the regulation of a variety of developmental processes in different organisms[20, 35, 46, 57, 61, 64-69]. *Pax* genes are transcription factors possessing two highly conserved DNA binding domains, a paired domain and a homeodomain[70, 71]. *Dach1* and *Dach2* are the mammalian homologues of *Drosophila dachshund* and contain two highly conserved domains, Dachbox-N and Dachbox-C, along with a coil-coil domain[72, 73]. These proteins also cannot bind DNA and, therefore, act as transcriptional cofactors[57, 64]. The Eya phosphatase activity switches the Six1-Dach complex from a transcriptional repressor to an activator[53]. *Eya1* is necessary for murine kidney development and thymus, parathyroid, and thyroid morphogenesis[67, 68, 74]. Human mutations in EYA1, SIX1, and SIX5 that disrupt the binding of EYA1 to SIX proteins result in the Branchio-oto-renal (BOR) syndrome, an autosomal dominant developmental disorder characterized by renal and urinary tract anomalies, deafness, and craniofacial abnormalities[59, 60, 75-79].

Figure 3. The Pax/Eya/Six/Dach regulatory network is conserved in many tissues and species. Adapted from reference[80].
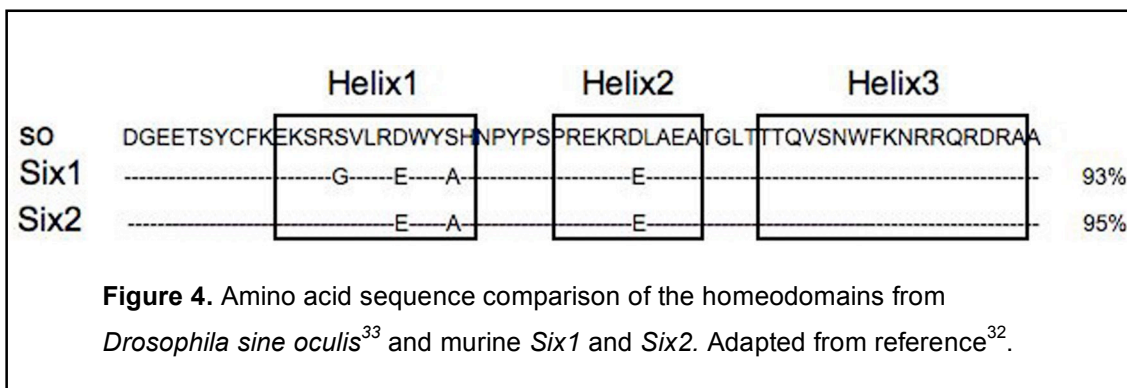
All *Six* genes exhibit characteristic expression patterns during murine development, and recent work has highlighted the functional importance of these genes during embryogenesis. Functional inactivation of *Six1* revealed that this gene is critical for kidney, muscle, ear, and craniofacial development[52, 53, 61, 69, 81-85]. *Six3* is required for forebrain development through direct repression of *Wnt1*[22]. Its activity is also critical for lens placode formation through its direct regulation of Pax6 and Sox2[24]. Mutations in SIX3 cause holoprosencephaly (HPE), the most common forebrain malformation in humans characterized by an incomplete separation of the cerebral hemispheres[86, 87]. Recent work determined that this disorder is caused by the failure of Six3 to activate Sonic hedgehog in the ventral forebrain[88].
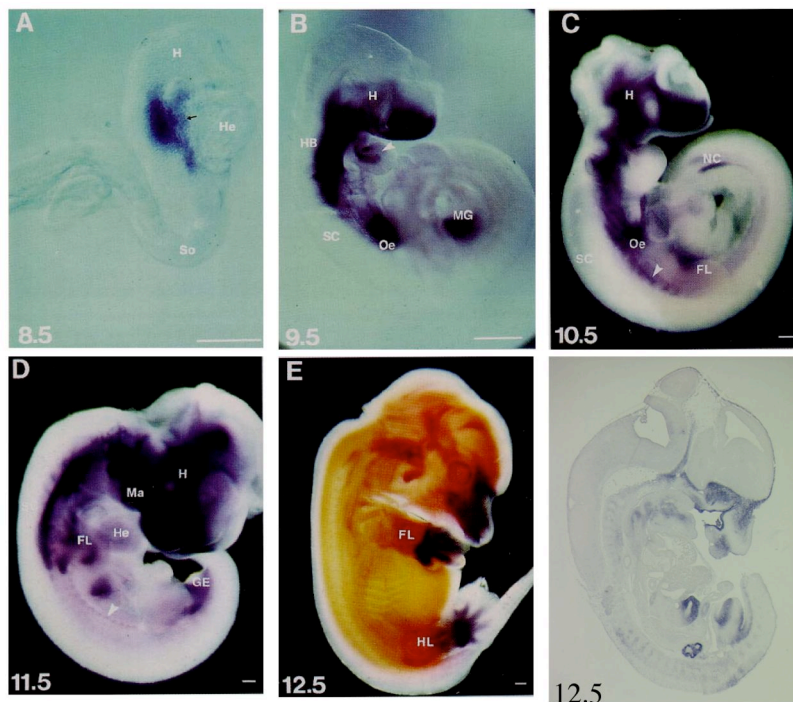
Six4/AREC3, along with Six2 and Six5, are capable of binding the regulatory region of the Na,K-ATPase alpha1 subunit gene[41, 42]. Human SIX5 is adjacent to the myotonic dystrophy protein kinase gene[37]. Myotonic dystrophy (DM1) is a common neuromuscular disease in adults characterized by myotonia, muscle atrophy, cataracts, neurological dysfunction, and cardiac anomalies and is caused by the expansion of a CTG repeat in the 3' untranslated region of the DMPK gene. This CTG repeat suppresses expression of *Six5*, and this decrease in Six5 activity may contribute to DM1 anomalies[89]. *Six5*-null mice exhibit cataracts in adulthood, a phenotype similar to DM1-associated cataracts reported in humans[90, 91]. SIX6 is expressed in the olfactory placodes, the optic stalk, and the retina[92] and is deleted in patients with anophthalmia and pituitary hypoplasia[39, 93]. In mouse, *Six6* is required for proliferation of retinal progenitors and pituitary development[94]. Together, these data argue that the *Six* family of transcriptional regulators play critical roles in health and disease.

1.2 Six2

The coding sequence of *Six2* is 76% similar to that of *sine oculis* and 95% homologous to that of *Six1* (Figure 4). Exclusion of the non-conserved C-terminal region increases the similarity between *Six2* and *sine oculis* to 95%[32]. In the mouse, *Six2* expression begins at around embryonic day (E) 8.5 in the hindbrain

and foregut mesoderm[32] (Figure 5). At E9.5, *Six2* is also detected in the first and second branchial arches, in the ectoderm between the maxillary and mandibular swellings, in pharyngeal-esophageal mesenchyme, and in the splanchnic mesoderm of the gut. *Six2* expression in the nephric cord, mesonephric mesenchyme, and neuroectoderm is also apparent at E10.5. In addition to these tissues, *Six2* expression is found in the genital eminence, metanephric kidney mesenchyme, and limb buds at E11.5[32]. One day later, expression is observed in the smooth muscle and connective tissue of the esophageal region, the posterior region of the stomach, the metanephric mesenchyme, genital tubercle, hindbrain, nasal region, and limb buds. *Six2* expression continues in the bones and muscles of the head, stomach, kidney, and cartilaginous condensations of the digits in later stages of development[32]. In humans, SIX2 is localized to chromosome 2p15-p16 and its expression coincides with many of the tissues affected in Branchio-oto-renal (BOR) syndrome; a result suggesting that some of the defects in BOR syndrome may result from the lack of interaction between EYA1 and SIX2[38].

Figure 4. Amino acid sequence comparison of the homeodomains from *Drosophila sine oculis*[33] and murine *Six1* and *Six2.* Adapted from reference[32].

Figure 5. Expression pattern of *Six2* during mouse development. Adapted from reference[32]. H, head; HB, hindbrain; He, heart; Ma, mandible; SC, spinal cord; HL, hindlimb; Oe, oesophageal-pharyngeal; MG, midgut; FL, forelimb; NC, nephric cord; GE, genital eminence; arrowhead in B, branchial arches; arrowhead in C, nephric cord; arrowhead in D, somites.

Six2 has been shown to be a direct downstream target of Hox genes in several tissues. In the developing kidney, compound null mutations in all three *Hox11* paralogs result in loss of *Six2* expression and complete kidney agenesis[95, 96]. *Six2* expression is also downregulated or lost in several mouse mutant strains exhibiting kidney defects including *Pax2*[97], *Eya1*[68], and *Six1*[53, 61], a result suggesting conservation of the *Pax-Eya-Six* regulatory network during kidney organogenesis. Gong et al.[98] found that a complex of Hox11, Pax2, and Eya1 proteins physically interact and synergistically upregulate the activity of *Six2*. This group also identified a 980 bp region of the *Six2* promoter capable of recapitulating the endogenous pattern of *Six2* expression in the kidney. Mutations in putative Pax2 and Hox binding sites identified in this regulatory region abolished *Six2* expression, a result confirming that the presence of a Hox11-Eya1-Pax2 complex on the *Six2* promoter is necessary for *Six2*

expression during kidney development[98]. In addition, ectopic Hoxd11 activity in the mesonephros also resulted in activation of ectopic *Six2* expression[99]. These data confirmed that *Six2* is downstream of Hox11, Eya1, and Pax2 during kidney development.

During branchial arch development, *Six2* is expressed in the first branchial arch[32, 100]. *Hoxa2* negatively regulates the expression of *Six2* in the second arch as abnormalities caused by ectopic expression of *Six2* in the second arch partially phenocopy the *Hoxa2*-null mutant arch defects[100]. *Hoxa2*-null branchial arches exhibit ectopic expansion of the *Six2* expression domain, and Hoxa2 is sufficient to decrease expression of *Six2* in this mesenchyme. In this case, a 900 bp fragment of the *Six2* promoter is sufficient to recapitulate the endogenous expression pattern of *Six2* in the branchial arches, and Hoxa2 physically interacts with the proximal region of this promoter. These data demonstrate that Hoxa2 function in the second arch is via its direct regulation of *Six2*[100]. The direct binding of Hoxa2 to this region of the Six2 promoter was recently confirmed using in vivo chromatin immunoprecipitation assays[101]. Additional support to these findings was provided by results showing that compound *Hoxa2* and *Six2* mutant embryos exhibit a partial rescue of the *Hoxa2*$^{-/-}$ branchial arch phenotype[101].

2. Kidney Development

The kidney forms a filtration system that functions to maintain water and electrolyte homeostasis in the body and to remove metabolic waste products from the blood and excrete them as urine. The kidney has become a model system in which to investigate fundamental developmental processes such as mesenchymal-to-epithelial transformation, branching morphogenesis, epithelial cell polarization, differentiation, and reciprocal inductive tissue interactions. Since the pioneering work of Grobstein in 1955[102], major advancements have been made towards understanding the mechanisms behind these processes during mammalian kidney development.

In mammals, the first step of kidney development is the formation of the nephric cord within the intermediate mesoderm. The nephric cord includes the

primary nephric duct, an epithelial tube that extends caudally down the anterior-posterior axis of the body, and the mesenchymal population adjacent to it (Figure 6). From this nephric cord, three different kidney anlagen will form. The mesenchymal population in the most anterior region of the nephric cord undergoes mesenchyme-to-epithelia transformation to form the pronephric tubules, rudimentary transient kidney tubules that completely degenerate in mammals. Caudal to the pronephros is the mesonephros, which forms functional mesonephric tubules that act as transient filtration units and later degenerate or become incorporated into the reproductive system[103] (Figure 6).

Figure 6. Excretory system development at E10.5. Adapted from reference[103].
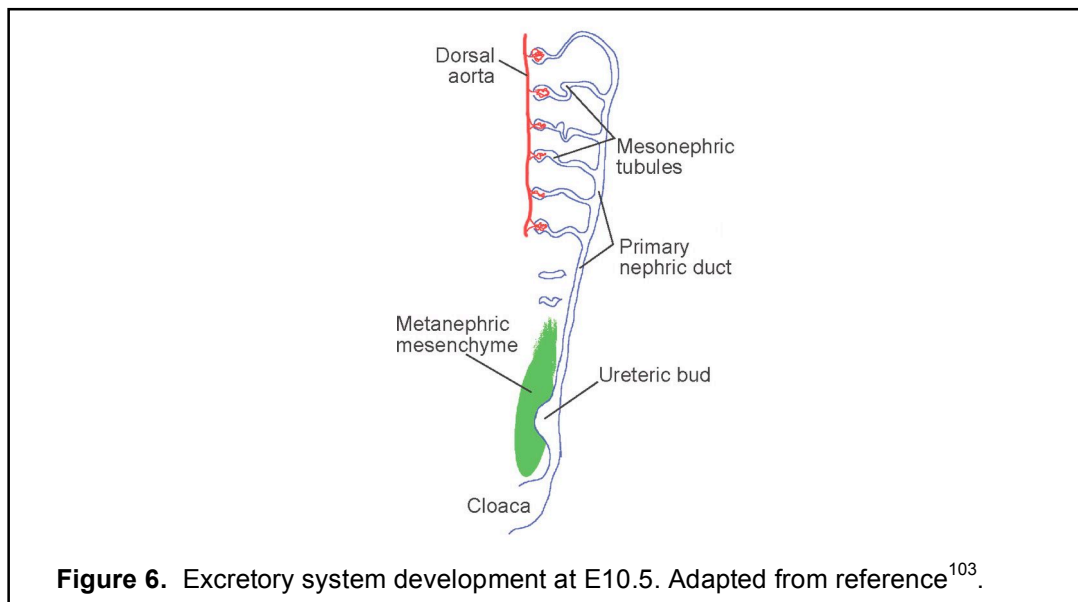
The mammalian definitive kidney, or metanephros, develops in the most caudal region of the nephric cord near the cloaca, a process that occurs in the mouse at around E10.5. The mesenchymal population at this posterior level induces the nephric duct to evaginate and form the ureteric bud (UB) which invades the metanephric blastema[102-105] (Figures 6, 7). Through reciprocal inductive interactions at around E11.0, the UB induces the metanephric mesenchyme (MM) to condense around the UB tip, while the MM induces the UB to undergo branching morphogenesis and grow throughout the MM (Figure 7). At around E12.5, the UB induces the MM on the ventral side of the UB tip to form pretubular aggregates. These aggregates subsequently undergo mesenchymal-

epithelial transition to form the epithelial renal vesicles. Each simple polarized renal vesicle forms a comma-shaped body as endothelial cells invade a cleft in the vesicle (Figure 7). A second cleft forms to generate the structure known as the s-shaped body, and the distal end of the renal tubule becomes continuous with the collecting duct formed by the UB. The proximal end of the tubule forms the glomerulus where the blood capillaries invade the renal filtration system. Specialized segments (proximal tubule, distal convoluted tubule, thick ascending limb, and Henle's loop) continue to differentiate from the s-shaped bodies until mature functional nephrons form (Figure 7). Older nephrons are located in the medullary region of the kidney while newer nephrons form in the cortical nephrogenic zone. This reciprocal inductive process continues at each new branch point until the kidney reaches its final size containing, in the mouse, approximately 12,000 nephrons[102-108].
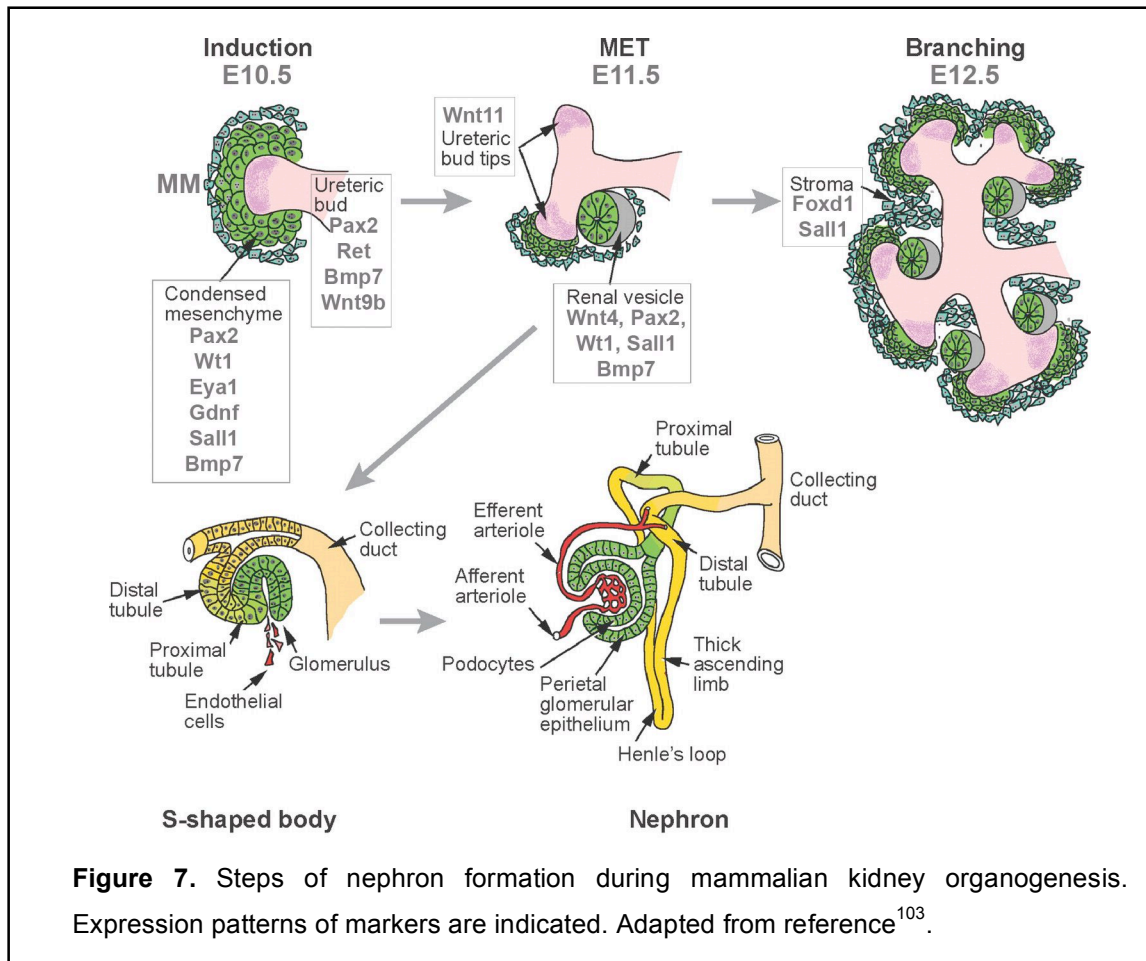
The MM (also called cap mesenchyme) that resides in the periphery of the developing kidney, or on the dorsal side of the UB tips, consists of renal progenitor or stem cells (Figure 7). As nephrogenesis continues throughout kidney development, MM cells are removed from the peripheral renal progenitor pool through the formation of renal vesicles[109-111]. However, not all of the MM cells are induced to differentiate into nephrons during kidney organogenesis. In order for additional rounds of nephrogenesis to take place and for radial growth of the kidney to continue, this MM population must be replenished. The mechanisms behind MM renewal and renal progenitor maintenance are not well characterized. Interstitial stromal cells constitute another population of mesenchymal cells that are not induced to form renal vesicles. These cells reside between the developing nephrons and collecting ducts[108].

Genes such as *Pax2*, *Wt1*, *Eya1*, *Ret*, *Gdnf*, *Wnt11*, *Sall1*, *Foxd1*, *Bmp7*, *Wnt9b*, and *Wnt4* have been shown to be essential for kidney morphogenesis (Figure 7, Table 1). Pax2 is a paired homeodomain protein expressed in the intermediate mesoderm, the nephric duct, the mesonephros, the MM, the ureteric branches, and the developing nephrons[112, 113]. *Pax2* is essential for mesonephric

tubule formation, metanephric kidney development, and genital tract development[97, 114].

The transcription factor Wilms tumor suppressor gene 1 (Wt1) is one of the earliest MM markers. Wt1 continues to be expressed in the epithelial derivatives of the MM after tubulogenesis is initiated and becomes restricted to the podocyte precursors of the glomeruli[115]. Wt1 activity is critical for outgrowth of the UB from the nephric duct and for survival of the metanephric blastema[116-118].

Figure 7. Steps of nephron formation during mammalian kidney organogenesis. Expression patterns of markers are indicated. Adapted from reference[103].

Eya1 is expressed in the MM throughout kidney development, and its activity is necessary for survival of the metanephric blastema[68, 119]. In the absence of *Eya1* function, outgrowth of the UB is disturbed and it does not invade the blastema[68]. In loss-of-function mouse models in which the UB does not invade the MM *(Eya1*, *Wt1*, and *Pax2)*, the resulting phenotype is kidney agenesis[68, 97, 114, 116-118].

UB outgrowth and subsequent branching morphogenesis is controlled by a network of genes including the receptor tyrosine kinase *Ret,* its ligand *Gdnf,* and a member of the noncanonical Wnt pathway *Wnt11.* Expression of *Ret* is confined to the nephric duct and UB branches[120, 121] while *Gdnf* is expressed in the MM adjacent to the tips of the UB[122]. In the absence of *Ret* or *Gdnf* expression, UB outgrowth is defective or completely lost resulting in kidney agenesis[120, 123-127]. Gdnf acts as a chemoattractant and is sufficient to induce ectopic UB outgrowths along the nephric duct[128, 129]. Thus, the Ret/Gdnf pathway determines the localization of UB outgrowth in the nephric duct. Cooperative interactions between Ret, Gdnf, and Wnt11 are important in maintaining UB branching during metanephric development[130]. *Wnt11* expression in the UB tips is upregulated by Gdnf, and its absence results in branching defects and subsequent renal hypoplasia[130-132].

Gene	Expression Pattern	Null Phenotype
Pax2	MM, UB, Nephrons	Complete agenesis
Wt1	MM, Nephrons	Complete agenesis
Eya1	MM	Complete agenesis
Ret	UB	Complete agenesis
Gdnf	MM	Complete agenesis
Wnt11	UB	Branching defects, hypoplasia
Sall1	MM, Nephrons, Stroma	Complete agenesis
Foxd1	Stroma	Few nephrons, reduced branching, hypoplasia
Bmp7	MM, UB, Nephrons	Few nephrons, reduced branching, hypoplasia
Wnt9b	UB	No pretubular aggregates form
Wnt4	MM	No renal vesicles form

Table 1. Summary of the expression patterns and phenotypes of mouse mutants of genes critical for metanephric kidney development

Sall1, a homolog of the Drosophila homeotic gene spalt, is also required for UB invasion and primary induction of the metanephric blastema[133, 134]. Sall1 expression is detected in the MM, comma bodies, and stroma[133, 135]. Another marker of the stromal population is the transcription factor Foxd1, formerly known as Bf2. Foxd1 is expressed in the mesenchymal cells in the periphery of the kidney which are not induced to form renal vesicles and do not express Pax2. This population of cells forms the interstitial stroma that resides between the nephrons and collecting ducts. Foxd1 activity in this population is necessary for differentiation of the mesenchymal aggregates into comma-shaped bodies and for maintaining growth of the kidney after initial UB induction of the MM[136].
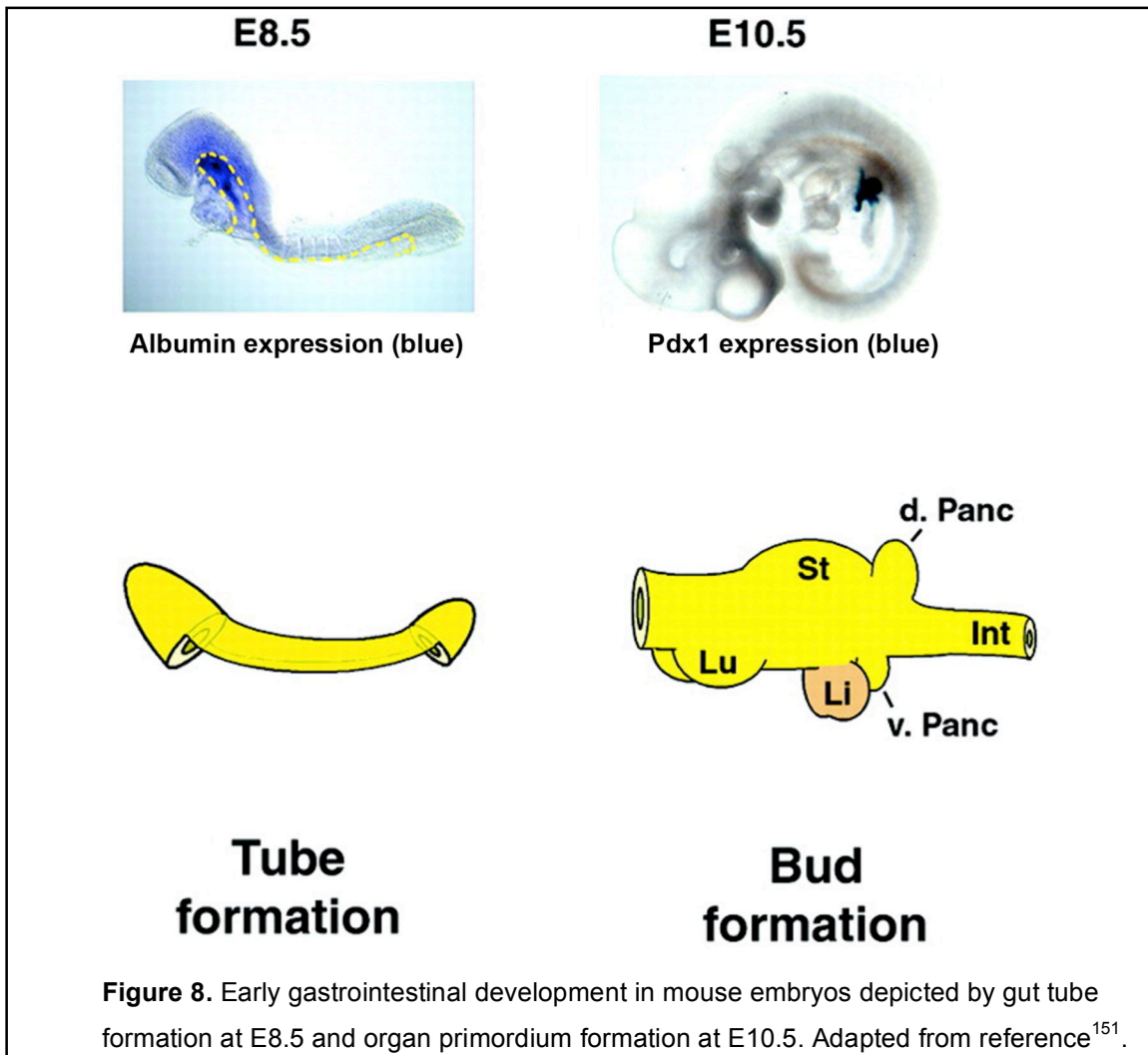
Bone morphogenic protein-7 (Bmp7) is a member of the TGF-β family of secreted growth factors expressed in the UB, MM, and developing nephrons[137-139]. Similar to Foxd1, Bmp7 is also not required for the primary induction of the MM or for initial UB branching. Instead, it inhibits apoptosis and promotes survival of the uninduced MM in the nephrogenic zone of the kidney after E12.5[137, 140, 141].

Two members of the Wnt family have recently been identified as important regulators of nephrogenesis. Canonoical Wnt signaling through Wnt9b expression in the ureteric branches induces the MM to condense and form pretubular aggregates on the ventral sides of the UB tips[142-144]. Wnt9b-null kidneys lack this condensation and aggregation of the MM and subsequent renal vesicle formation[142]. Wnt9b acts upstream of Wnt4, another canonical Wnt signaling member. Expression of Wnt4 in the MM and pretubular aggregates is required for the transition of the induced MM into epithelial renal vesicles[145, 146].

3. Digestive System Development

The organs of the vertebrate digestive system act mechanically and chemically to break down food particles so that they can be absorbed for use in the body or

excreted as waste products. In the mouse, the gut first develops around E8.5 as a simple tube of endoderm surrounded by splanchnic mesoderm. This tube becomes patterned into the various organ primordia of the digestive system between E8.5 and E12.5 (Figure 8) by reciprocal mesenchymal-epithelial interactions[139, 147-152]. Signals derived from the endoderm pattern the gut tube along the A-P axis into the discrete regions of the foregut, midgut, and hindgut. The esophagus, liver, lungs, pancreas, and stomach are derived from the foregut, the duodenum from the midgut, and the large intestine from the hindgut[147, 148, 150-155]. Thick circular muscles called sphincters act as gatekeepers to control the passage of materials into the different compartments of the digestive system.

Figure 8. Early gastrointestinal development in mouse embryos depicted by gut tube formation at E8.5 and organ primordium formation at E10.5. Adapted from reference[151].

Along the length of the gut tube, the splanchnic mesoderm becomes organized into radial layers (Figure 9). Adjacent to the endodermally derived epithelial layer is the lamina propria, a loose interstitial layer of connective tissue rich in lymphatics and blood vessels. Next to the lamina propria lies a layer of smooth muscle, the muscularis mucosa. These three layers (i.e., the epithelial lining, the lamina propria, and the muscularis mucosa) compile the mucosa of the gut tube. The submucosa, adjacent to the mucosa, is another connective tissue layer containing blood vessels, lymphatics, and nerve plexuses of the enteric nervous system. Surrounding the submucosa is an inner circular muscle layer and an outer longitudinal muscle layer. The outer covering of the gut tube is the serosa, a mesothelial layer facing the peritoneal cavity[147, 156].
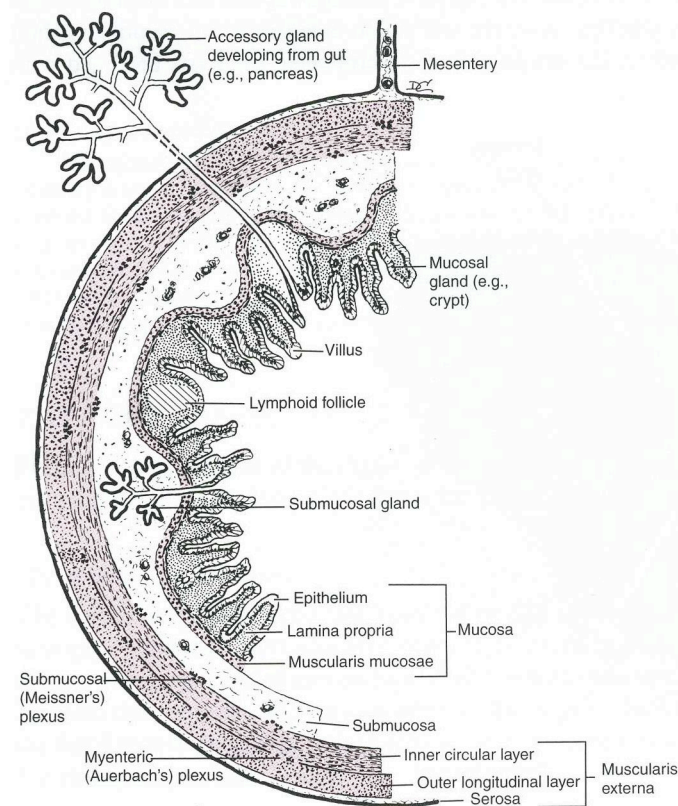
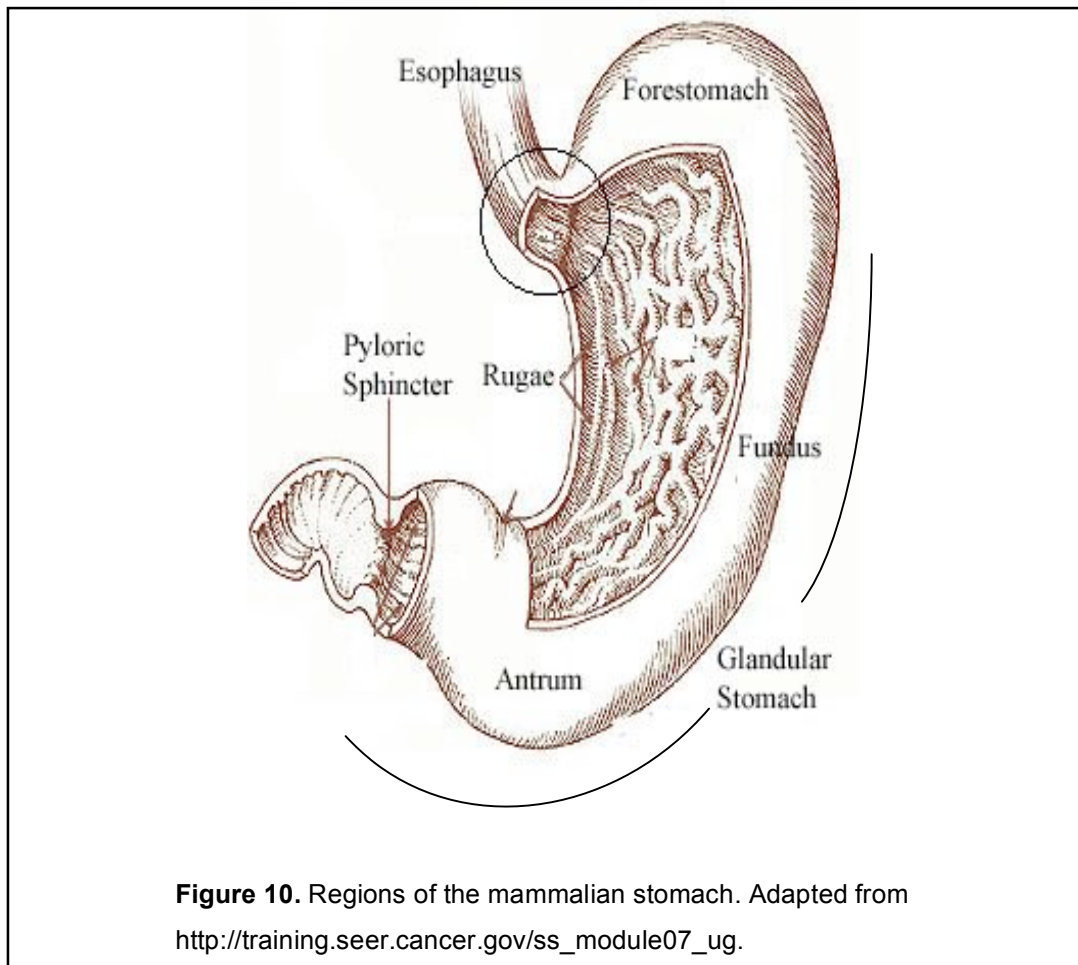**Figure 9.** Cross section depicting radial layers of the digestive tract. Adapted from reference[156].

3.1 Stomach Development

The stomach is a hollow muscular organ with an acidic environment that functions to convert food into chyme which is delivered to the small intestine (SI) through the pyloric sphincter (PS). Peristalsis, ripples of muscular contraction coordinated by the enteric nervous system, aids in grinding and propelling the contents of the stomach towards the SI. The pyloric sphincter reacts to the peristaltic waves by contracting and creating shearing forces that help break up the food particles. The PS acts as a gate to control the quantity of viscous acidic chyme that is released to the duodenum.

In the mouse, the stomach is divided into two main regions based on morphological features (Figure 10). The anterior forestomach (FS) functions as a holding tank for the contents of the stomach during digestion. The posterior glandular stomach (GS) houses cells that produce digestive enzymes and mucous to aid in digestion[147]. These two territories cannot be distinguished until E12.5 when the GS epithelium starts to stratify. At E13.5, differentiation of the FS is initiated and results in a stratified squamous epithelium which lacks glands at birth[157]. The GS can be further subdivided into the fundus, the more anterior region adjacent to the FS, and the most posterior part of the stomach, the antrum. The fundus of the GS is characterized by the presence of numerous pits and glands that contain parietal cells and chief cells, both of which secrete precursors of digestive enzymes, mucous-producing cells, and enteroendocrine cells[157, 158]. The antrum of the GS contains mucous-producing glands that protect the stomach from autodigestion and endocrine cells[159, 160]. The primitive glands of the fundus and antrum are detectable in mouse embryos at E15.5, but at E18.5 only 8% of the cells are differentiated. The rest of the cells are multipotent stem cells and precursors that will form mature glands after birth[158].

The three muscle layers of the stomach, the muscularis mucosa, the inner circular muscle layer, and the outer longitudinal muscle layer (Figure 9), form at different times in the FS and GS[161]. The circular layer forms at E13.5 throughout the stomach at a specific radial distance from the epithelia. The longitudinal

layer appears in the FS at E15.5 and in the GS around birth. The muscularis mucosa forms postnatally adjacent to the epithelium at the same time in both the FS and GS[161].

Figure 10. Regions of the mammalian stomach. Adapted from http://training.seer.cancer.gov/ss_module07_ug.

3.2 Pyloric Sphincter Development
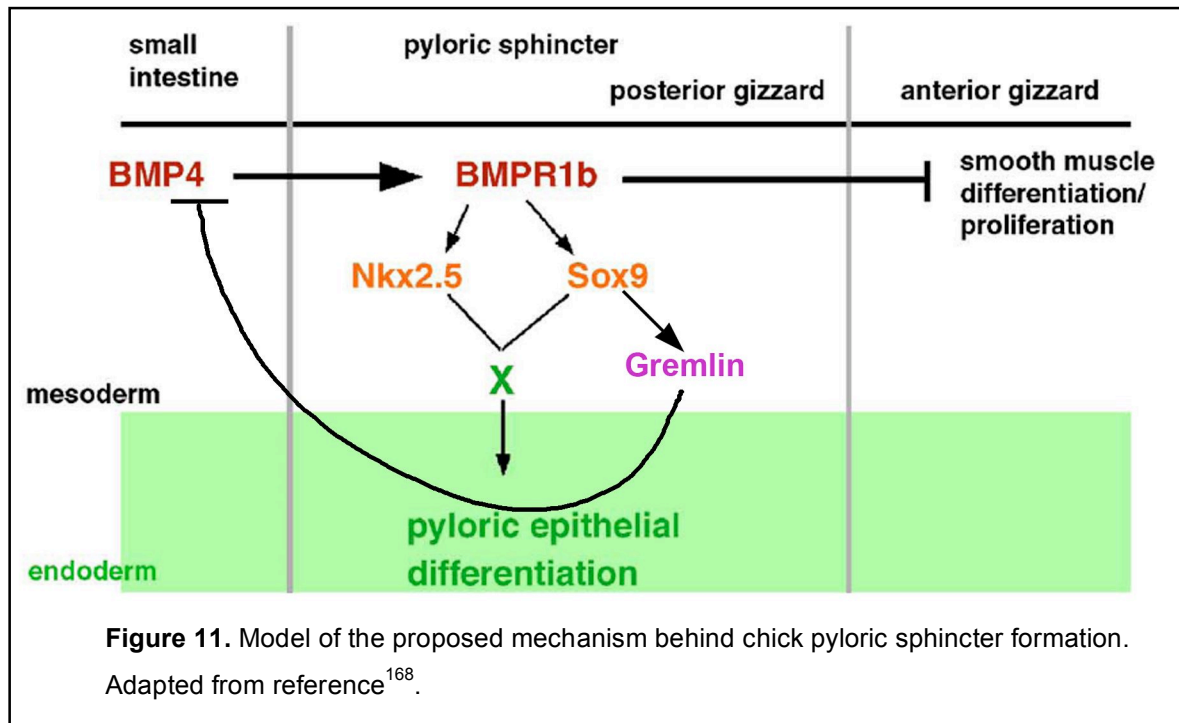
The pyloric sphincter (PS) separates the stomach from the SI and acts as a gate to control the passage of the stomach contents to the duodenum and to prevent retrograde flow. The PS is a thickened region of the inner smooth muscle layer that creates a narrow, constricted region at the posterior boundary of the stomach. The glands of the PS are a continuum of the antral glands and house

mainly mucous-producing cells. The abrupt change in histology from the GS epithelium to the SI epithelium occurs at the posterior boundary of the PS[162].

The mechanisms behind the development of the mammalian PS are not known. However, studies in chick embryos proposed a working model to explain avian PS formation (Figure 11). In chick, *Bmp4* is expressed in the mesoderm of the SI in response to Sonic Hedgehog (Shh) signaling[162-166]. *Bmp receptor 1b* (Bmpr1b) is expressed in the mesoderm of the gizzard, the chick posterior stomach[162, 165, 166]. In the region of mesoderm at the junction of the gizzard and SI, *Bmp4* and *Bmpr1b* expression overlaps and Bmp signaling induces specification of the PS by inducing expression of *Nkx2.5* and *Sox9* in the posterior gizzard mesoderm[165-168]. These two transcription factors are induced by Bmp signaling independently of one another and seem to act in parallel to specify the bleb-like microvilli characteristic of the PS epithelial phenotype[165-168]. Sox9 may function to specify the PS epithelial phenotype by inducing *Gremlin* expression in the PS mesoderm which could in turn antagonize Bmp activity[167].

Figure 11. Model of the proposed mechanism behind chick pyloric sphincter formation. Adapted from reference[168].

Previous studies in chick have also suggested a role for Bmp4 signaling in mediating proliferation and differentiation of the splanchnic mesoderm and, thereby, regulating muscle thickness. In chick, *Bmp4* is expressed throughout the early gut tube except in the stomach where it is expressed only at later stages in the submucosal layer of the gizzard[162, 164-167]. In the gizzard, the muscle layer is much thicker than in the rest of the gut tube where *Bmp4* is expressed at this time. Furthermore, ectopic Bmp4 activity in the gizzard resulted in thinning of the mesoderm and loss of smooth muscle cell differentiation[164-167]. Therefore, *Bmp4* seems to play a key role in limiting growth of the mesodermal layer along the radial axis during gut regionalization[164-168].

Limited analysis of these markers during murine stomach organogenesis has been previously reported. During mouse development, *Bmp4* is expressed in the stomach and SI while *Bmpr1b* is expressed in the posterior stomach[162, 169]. *Nkx2.5* is expressed in the mesoderm of the PS region[165, 170]. Similar expression patterns of these markers in chick and mouse embryos suggest that the mechanisms that underlie PS formation may be conserved in both species. Support for this proposal is provided by the analysis of the stomach phenotype resulting from the lack of Six2 activity in the generated *Six2* mouse mutant strain (Chapter 4).

References

1. McGinnis, W., Garber, R.L., Wirz, J., Kuroiwa, A. & Gehring, W.J. A homologous protein-coding sequence in Drosophila homeotic genes and its conservation in other metazoans. *Cell* **37**, 403-8 (1984).
2. McGinnis, W. & Krumlauf, R. Homeobox genes and axial patterning. *Cell* **68**, 283-302 (1992).
3. McGinnis, W., Levine, M.S., Hafen, E., Kuroiwa, A. & Gehring, W.J. A conserved DNA sequence in homoeotic genes of the Drosophila Antennapedia and bithorax complexes. *Nature* **308**, 428-33 (1984).
4. Muller, M. et al. Isolation and sequence-specific DNA binding of the Antennapedia homeodomain. *EMBO J* **7**, 4299-304 (1988).
5. Scott, M.P., Tamkun, J.W. & Hartzell, G.W., 3rd. The structure and function of the homeodomain. *Biochim Biophys Acta* **989**, 25-48 (1989).
6. Carrasco, A.E., McGinnis, W., Gehring, W.J. & De Robertis, E.M. Cloning of an X. laevis gene expressed during early embryogenesis coding for a peptide region homologous to Drosophila homeotic genes. *Cell* **37**, 409-14 (1984).
7. Otting, G. et al. Protein--DNA contacts in the structure of a homeodomain--DNA complex determined by nuclear magnetic resonance spectroscopy in solution. *EMBO J* **9**, 3085-92 (1990).
8. Otting, G. et al. Secondary structure determination for the Antennapedia homeodomain by nuclear magnetic resonance and evidence for a helix-turn-helix motif. *EMBO J* **7**, 4305-9 (1988).
9. Percival-Smith, A., Muller, M., Affolter, M. & Gehring, W.J. The interaction with DNA of wild-type and mutant fushi tarazu homeodomains. *EMBO J* **9**, 3967-74 (1990).
10. Kaufman, T.C., Lewis, R. & Wakimoto, B. Cytogenetic Analysis of Chromosome 3 in DROSOPHILA MELANOGASTER: The Homoeotic Gene Complex in Polytene Chromosome Interval 84a-B. *Genetics* **94**, 115-133 (1980).
11. Lewis, E.B. A gene complex controlling segmentation in Drosophila. *Nature* **276**, 565-70 (1978).
12. Lewis, R.A., Kaufman, T.C., Denell, R.E. & Tallerico, P. Genetic Analysis of the Antennapedia Gene Complex (Ant-C) and Adjacent Chromosomal Regions of DROSOPHILA MELANOGASTER. I. Polytene Chromosome Segments 84b-D. *Genetics* **95**, 367-381 (1980).
13. Duboule, D. The rise and fall of Hox gene clusters. *Development* **134**, 2549-60 (2007).
14. McGinnis, W. Homeo box sequences of the Antennapedia class are conserved only in higher animal genomes. *Cold Spring Harb Symp Quant Biol* **50**, 263-70 (1985).
15. Muller, M.M., Carrasco, A.E. & DeRobertis, E.M. A homeo-box-containing gene expressed during oogenesis in Xenopus. *Cell* **39**, 157-62 (1984).

16. Deschamps, J. Ancestral and recently recruited global control of the Hox genes in development. *Curr Opin Genet Dev* **17**, 422-7 (2007).

17. Del Bene, F. & Wittbrodt, J. Cell cycle control by homeobox genes in development and disease. *Semin Cell Dev Biol* **16**, 449-60 (2005).

18. Dozier, C., Kagoshima, H., Niklaus, G., Cassata, G. & Burglin, T.R. The Caenorhabditis elegans Six/sine oculis class homeobox gene ceh-32 is required for head morphogenesis. *Dev Biol* **236**, 289-303 (2001).

19. Duverger, O. & Morasso, M.I. Role of homeobox genes in the patterning, specification, and differentiation of ectodermal appendages in mammals. *J Cell Physiol* **216**, 337-46 (2008).

20. Halder, G. et al. Eyeless initiates the expression of both sine oculis and eyes absent during Drosophila compound eye development. *Development* **125**, 2181-91 (1998).

21. Kessel, M. & Gruss, P. Homeotic transformations of murine vertebrae and concomitant alteration of Hox codes induced by retinoic acid. *Cell* **67**, 89-104 (1991).

22. Lagutin, O.V. et al. Six3 repression of Wnt signaling in the anterior neuroectoderm is essential for vertebrate forebrain development. *Genes Dev* **17**, 368-79 (2003).

23. Lewis, D.L. et al. Ectopic gene expression and homeotic transformations in arthropods using recombinant Sindbis viruses. *Curr Biol* **9**, 1279-87 (1999).

24. Liu, W., Lagutin, O.V., Mende, M., Streit, A. & Oliver, G. Six3 activation of Pax6 expression is essential for mammalian lens induction and specification. *EMBO J* **25**, 5383-95 (2006).

25. Mann, R.S. & Hogness, D.S. Functional dissection of Ultrabithorax proteins in D. melanogaster. *Cell* **60**, 597-610 (1990).

26. Morgan, B.A. & Tabin, C.J. The role of Hox genes in limb development. *Prog Clin Biol Res* **383A**, 1-9 (1993).

27. Saint, R., Kalionis, B., Lockett, T.J. & Elizur, A. Pattern formation in the developing eye of Drosophila melanogaster is regulated by the homoeobox gene, rough. *Nature* **334**, 151-4 (1988).

28. Serikaku, M.A. & O'Tousa, J.E. sine oculis is a homeobox gene required for Drosophila visual system development. *Genetics* **138**, 1137-50 (1994).

29. Way, J.C. & Chalfie, M. mec-3, a homeobox-containing gene that specifies differentiation of the touch receptor neurons in C. elegans. *Cell* **54**, 5-16 (1988).

30. Burglin, T.R. & Ruvkun, G. The Caenorhabditis elegans homeobox gene cluster. *Curr Opin Genet Dev* **3**, 615-20 (1993).

31. Sanchez-Herrero, E., Vernos, I., Marco, R. & Morata, G. Genetic organization of Drosophila bithorax complex. *Nature* **313**, 108-13 (1985).

32. Oliver, G. et al. Homeobox genes and connective tissue patterning. *Development* **121**, 693-705 (1995).

33. Cheyette, B.N. et al. The Drosophila sine oculis locus encodes a homeodomain-containing protein required for the development of the entire visual system. *Neuron* **12**, 977-96 (1994).

34. Roederer, K., Cozy, L., Anderson, J. & Kumar, J.P. Novel dominant-negative mutation within the six domain of the conserved eye specification gene sine oculis inhibits eye development in Drosophila. *Dev Dyn* **232**, 753-66 (2005).

35. Wawersik, S. & Maas, R.L. Vertebrate eye development as modeled in Drosophila. *Hum Mol Genet* **9**, 917-25 (2000).

36. Boucher, C.A., Carey, N., Edwards, Y.H., Siciliano, M.J. & Johnson, K.J. Cloning of the human SIX1 gene and its assignment to chromosome 14. *Genomics* **33**, 140-2 (1996).

37. Boucher, C.A. et al. A novel homeodomain-encoding gene is associated with a large CpG island interrupted by the myotonic dystrophy unstable (CTG)n repeat. *Hum Mol Genet* **4**, 1919-25 (1995).

38. Boucher, C.A. et al. Structure, mapping and expression of the human gene encoding the homeodomain protein, SIX2. *Gene* **247**, 145-51 (2000).

39. Gallardo, M.E. et al. Genomic cloning and characterization of the human homeobox gene SIX6 reveals a cluster of SIX genes in chromosome 14 and associates SIX6 hemizygosity with bilateral anophthalmia and pituitary anomalies. *Genomics* **61**, 82-91 (1999).

40. Granadino, B. et al. Genomic cloning, structure, expression pattern, and chromosomal location of the human SIX3 gene. *Genomics* **55**, 100-5 (1999).

41. Kawakami, K., Ohto, H., Ikeda, K. & Roeder, R.G. Structure, function and expression of a murine homeobox protein AREC3, a homologue of Drosophila sine oculis gene product, and implication in development. *Nucleic Acids Res* **24**, 303-10 (1996).

42. Kawakami, K., Ohto, H., Takizawa, T. & Saito, T. Identification and expression of six family genes in mouse retina. *FEBS Lett* **393**, 259-63 (1996).

43. Kawakami, K., Sato, S., Ozaki, H. & Ikeda, K. Six family genes--structure and function as transcription factors and their roles in development. *Bioessays* **22**, 616-26 (2000). Reprinted with permission from Wiley-Liss, Inc. a subsidiary of John Wiley & Sons, Inc.

44. Oliver, G. et al. Six3, a murine homologue of the sine oculis gene, demarcates the most anterior border of the developing neural plate and is expressed during eye development. *Development* **121**, 4045-55 (1995).

45. Ohto, H. et al. Cooperation of six and eya in activation of their target genes through nuclear translocation of Eya. *Mol Cell Biol* **19**, 6815-24 (1999).

46. Pignoni, F. et al. The eye-specification proteins So and Eya form a complex and regulate multiple steps in Drosophila eye development. *Cell* **91**, 881-91 (1997).

47. Brodbeck, S., Besenbeck, B. & Englert, C. The transcription factor Six2 activates expression of the Gdnf gene as well as its own promoter. *Mech Dev* **121**, 1211-22 (2004).

48. Spitz, F. et al. Expression of myogenin during embryogenesis is controlled by Six/sine oculis homeoproteins through a conserved MEF3 binding site. *Proc Natl Acad Sci U S A* **95**, 14220-5 (1998).

49. Seo, H.C., Curtiss, J., Mlodzik, M. & Fjose, A. Six class homeobox genes in drosophila belong to three distinct families and are involved in head development. *Mech Dev* **83**, 127-39 (1999).

50. Jean, D., Bernier, G. & Gruss, P. Six6 (Optx2) is a novel murine Six3-related homeobox gene that demarcates the presumptive pituitary/hypothalamic axis and the ventral optic stalk. *Mech Dev* **84**, 31-40 (1999).

51. Ghanbari, H., Seo, H.C., Fjose, A. & Brandli, A.W. Molecular cloning and embryonic expression of Xenopus Six homeobox genes. *Mech Dev* **101**, 271-7 (2001). Reprinted with permission from Elsevier.

52. Brugmann, S.A., Pandur, P.D., Kenyon, K.L., Pignoni, F. & Moody, S.A. Six1 promotes a placodal fate within the lateral neurogenic ectoderm by functioning as both a transcriptional activator and repressor. *Development* **131**, 5871-81 (2004).

53. Li, X. et al. Eya protein phosphatase activity regulates Six1-Dach-Eya transcriptional effects in mammalian organogenesis. *Nature* **426**, 247-54 (2003).

54. Zhu, C.C. et al. Six3-mediated auto repression and eye development requires its interaction with members of the Groucho-related family of co-repressors. *Development* **129**, 2835-49 (2002).

55. Bonini, N.M., Bui, Q.T., Gray-Board, G.L. & Warrick, J.M. The Drosophila eyes absent gene directs ectopic eye formation in a pathway conserved between flies and vertebrates. *Development* **124**, 4819-26 (1997).

56. Buller, C., Xu, X., Marquis, V., Schwanke, R. & Xu, P.X. Molecular effects of Eya1 domain mutations causing organ defects in BOR syndrome. *Hum Mol Genet* **10**, 2775-81 (2001).

57. Heanue, T.A. et al. Synergistic regulation of vertebrate muscle development by Dach2, Eya2, and Six1, homologs of genes required for Drosophila eye formation. *Genes Dev* **13**, 3231-43 (1999).

58. Ikeda, K., Watanabe, Y., Ohto, H. & Kawakami, K. Molecular interaction and synergistic activation of a promoter by Six, Eya, and Dach proteins mediated through CREB binding protein. *Mol Cell Biol* **22**, 6759-66 (2002).

59. Ozaki, H., Watanabe, Y., Ikeda, K. & Kawakami, K. Impaired interactions between mouse Eyal harboring mutations found in patients with branchio-oto-renal syndrome and Six, Dach, and G proteins. *J Hum Genet* **47**, 107-16 (2002).

60. Ruf, R.G. et al. SIX1 mutations cause branchio-oto-renal syndrome by disruption of EYA1-SIX1-DNA complexes. *Proc Natl Acad Sci U S A* **101**, 8090-5 (2004).

61. Xu, P.X. et al. Six1 is required for the early organogenesis of mammalian kidney. *Development* **130**, 3085-94 (2003).

62. Rayapureddi, J.P. et al. Eyes absent represents a class of protein tyrosine phosphatases. *Nature* **426**, 295-8 (2003).

63. Tootle, T.L. et al. The transcription factor Eyes absent is a protein tyrosine phosphatase. *Nature* **426**, 299-302 (2003).

64. Chen, R., Amoui, M., Zhang, Z. & Mardon, G. Dachshund and eyes absent proteins form a complex and function synergistically to induce ectopic eye development in Drosophila. *Cell* **91**, 893-903 (1997).

65. Fabrizio, J.J., Boyle, M. & DiNardo, S. A somatic role for eyes absent (eya) and sine oculis (so) in Drosophila spermatocyte development. *Dev Biol* **258**, 117-28 (2003).

66. Niimi, T., Seimiya, M., Kloter, U., Flister, S. & Gehring, W.J. Direct regulatory interaction of the eyeless protein with an eye-specific enhancer in the sine oculis gene during eye induction in Drosophila. *Development* **126**, 2253-60 (1999).

67. Sajithlal, G., Zou, D., Silvius, D. & Xu, P.X. Eya 1 acts as a critical regulator for specifying the metanephric mesenchyme. *Dev Biol* **284**, 323-36 (2005).

68. Xu, P.X. et al. Eya1-deficient mice lack ears and kidneys and show abnormal apoptosis of organ primordia. *Nat Genet* **23**, 113-7 (1999).

69. Zheng, W. et al. The role of Six1 in mammalian auditory system development. *Development* **130**, 3989-4000 (2003).

70. Quiring, R., Walldorf, U., Kloter, U. & Gehring, W.J. Homology of the eyeless gene of Drosophila to the Small eye gene in mice and Aniridia in humans. *Science* **265**, 785-9 (1994).

71. Treisman, J., Harris, E. & Desplan, C. The paired box encodes a second DNA-binding domain in the paired homeo domain protein. *Genes Dev* **5**, 594-604 (1991).

72. Hammond, K.L., Hanson, I.M., Brown, A.G., Lettice, L.A. & Hill, R.E. Mammalian and Drosophila dachshund genes are related to the Ski proto-oncogene and are expressed in eye and limb. *Mech Dev* **74**, 121-31 (1998).

73. Kozmik, Z. et al. Molecular cloning and expression of the human and mouse homologues of the Drosophila dachshund gene. *Dev Genes Evol* **209**, 537-45 (1999).

74. Xu, P.X. et al. Eya1 is required for the morphogenesis of mammalian thymus, parathyroid and thyroid. *Development* **129**, 3033-44 (2002).

75. Abdelhak, S. et al. Clustering of mutations responsible for branchio-oto-renal (BOR) syndrome in the eyes absent homologous region (eyaHR) of EYA1. *Hum Mol Genet* **6**, 2247-55 (1997).

76. Abdelhak, S. et al. A human homologue of the Drosophila eyes absent gene underlies branchio-oto-renal (BOR) syndrome and identifies a novel gene family. *Nat Genet* **15**, 157-64 (1997).

77. Hoskins, B.E. et al. Transcription factor SIX5 is mutated in patients with branchio-oto-renal syndrome. *Am J Hum Genet* **80**, 800-4 (2007).

78. Kumar, S. et al. Identification of three novel mutations in human EYA1 protein associated with branchio-oto-renal syndrome. *Hum Mutat* **11**, 443-9 (1998).

79.   Vincent, C. et al. BOR and BO syndromes are allelic defects of EYA1. *Eur J Hum Genet* **5**, 242-6 (1997).

80.   Hanson, I.M. Mammalian homologues of the Drosophila eye specification genes. *Semin Cell Dev Biol* **12**, 475-84 (2001). Reprinted with permission from Elsevier.

81.   Laclef, C. et al. Altered myogenesis in Six1-deficient mice. *Development* **130**, 2239-52 (2003).

82.   Laclef, C., Souil, E., Demignon, J. & Maire, P. Thymus, kidney and craniofacial abnormalities in Six 1 deficient mice. *Mech Dev* **120**, 669-79 (2003).

83.   Kobayashi, H., Kawakami, K., Asashima, M. & Nishinakamura, R. Six1 and Six4 are essential for Gdnf expression in the metanephric mesenchyme and ureteric bud formation, while Six1 deficiency alone causes mesonephric-tubule defects. *Mech Dev* **124**, 290-303 (2007).

84.   Ozaki, H. et al. Six1 controls patterning of the mouse otic vesicle. *Development* **131**, 551-62 (2004).

85.   Zou, D., Silvius, D., Fritzsch, B. & Xu, P.X. Eya1 and Six1 are essential for early steps of sensory neurogenesis in mammalian cranial placodes. *Development* **131**, 5561-72 (2004).

86.   Pasquier, L. et al. A new mutation in the six-domain of SIX3 gene causes holoprosencephaly. *Eur J Hum Genet* **8**, 797-800 (2000).

87.   Wallis, D.E. et al. Mutations in the homeodomain of the human SIX3 gene cause holoprosencephaly. *Nat Genet* **22**, 196-8 (1999).

88.   Geng X, S.C., Lagutin O, Inbal A, Liu W, Solnica-Krezel L, Jeong Y, Epstein D, Oliver G. Haploinsufficiency of Six3 fails to activate Sonic hedgehog expression in the ventral forebrain and causes holoprosencephaly. *Dev Cell* **15**, 1-12 (2008) In press.

89.   Sato, S. et al. Identification of transcriptional targets for Six5: implication for the pathogenesis of myotonic dystrophy type 1. *Hum Mol Genet* **11**, 1045-58 (2002).

90.   Klesert, T.R. et al. Mice deficient in Six5 develop cataracts: implications for myotonic dystrophy. *Nat Genet* **25**, 105-9 (2000).

91.   Sarkar, P.S. et al. Heterozygous loss of Six5 in mice is sufficient to cause ocular cataracts. *Nat Genet* **25**, 110-4 (2000).

92.   Lopez-Rios, J., Gallardo, M.E., Rodriguez de Cordoba, S. & Bovolenta, P. Six9 (Optx2), a new member of the six gene family of transcription factors, is expressed at early stages of vertebrate ocular and pituitary development. *Mech Dev* **83**, 155-9 (1999).

93.   Toy, J., Yang, J.M., Leppert, G.S. & Sundin, O.H. The optx2 homeobox gene is expressed in early precursors of the eye and activates retina-specific genes. *Proc Natl Acad Sci U S A* **95**, 10643-8 (1998).

94.   Li, X., Perissi, V., Liu, F., Rose, D.W. & Rosenfeld, M.G. Tissue-specific regulation of retinal and pituitary precursor cell proliferation. *Science* **297**, 1180-3 (2002).

95. Davis, A.P., Witte, D.P., Hsieh-Li, H.M., Potter, S.S. & Capecchi, M.R. Absence of radius and ulna in mice lacking hoxa-11 and hoxd-11. *Nature* **375**, 791-5 (1995).

96. Wellik, D.M., Hawkes, P.J. & Capecchi, M.R. Hox11 paralogous genes are essential for metanephric kidney induction. *Genes Dev* **16**, 1423-32 (2002).

97. Torres, M., Gomez-Pardo, E., Dressler, G.R. & Gruss, P. Pax-2 controls multiple steps of urogenital development. *Development* **121**, 4057-65 (1995).

98. Gong, K.Q., Yallowitz, A.R., Sun, H., Dressler, G.R. & Wellik, D.M. A Hox-Eya-Pax complex regulates early kidney developmental gene expression. *Mol Cell Biol* **27**, 7661-8 (2007).

99. Mugford, J.W., Sipila, P., Kobayashi, A., Behringer, R.R. & McMahon, A.P. Hoxd11 specifies a program of metanephric kidney development within the intermediate mesoderm of the mouse embryo. *Dev Biol* **319**, 396-405 (2008).

100. Kutejova, E., Engist, B., Mallo, M., Kanzler, B. & Bobola, N. Hoxa2 downregulates Six2 in the neural crest-derived mesenchyme. *Development* **132**, 469-78 (2005).

101. Kutejova, E. et al. Six2 functions redundantly immediately downstream of Hoxa2. *Development* **135**, 1463-70 (2008).

102. Grobstein, C. Inductive interactions in the development of the mouse metanephros. *J Exp Zool* **130**, 319-340 (1955).

103. Dressler, G.R. The cellular basis of kidney development. *Annu Rev Cell Dev Biol* **22**, 509-29 (2006). Reprinted with permission by Annual Reviews www.annualreviews.org.

104. Gruenwald, P. Stimulations of nephrogenic tissues by normal and abnormal inductors. *Anat Rec* **86**, 321-335 (1943).

105. Saxen, L. & Sariola, H. Early organogenesis of the kidney. *Pediatr Nephrol* **1**, 385-92 (1987).

106. Cullen-McEwen, L.A., Kett, M.M., Dowling, J., Anderson, W.P. & Bertram, J.F. Nephron number, renal function, and arterial pressure in aged GDNF heterozygous mice. *Hypertension* **41**, 335-40 (2003).

107. He, C. et al. Dissociation of glomerular hypertrophy, cell proliferation, and glomerulosclerosis in mouse strains heterozygous for a mutation (Os) which induces a 50% reduction in nephron number. *J Clin Invest* **97**, 1242-9 (1996).

108. Vainio, S. & Lin, Y. Coordinating early kidney development: lessons from gene targeting. *Nat Rev Genet* **3**, 533-43 (2002).

109. Herzlinger, D., Koseki, C., Mikawa, T. & al-Awqati, Q. Metanephric mesenchyme contains multipotent stem cells whose fate is restricted after induction. *Development* **114**, 565-72 (1992).

110. Nishinakamura, R. & Osafune, K. Essential roles of sall family genes in kidney development. *J Physiol Sci* **56**, 131-6 (2006).

111. Osafune, K., Takasato, M., Kispert, A., Asashima, M. & Nishinakamura, R. Identification of multipotent progenitors in the embryonic mouse kidney by a novel colony-forming assay. *Development* **133**, 151-61 (2006).

112. Dressler, G.R., Deutsch, U., Chowdhury, K., Nornes, H.O. & Gruss, P. Pax2, a new murine paired-box-containing gene and its expression in the developing excretory system. *Development* **109**, 787-95 (1990).

113. Dressler, G.R. & Douglass, E.C. Pax-2 is a DNA-binding protein expressed in embryonic kidney and Wilms tumor. *Proc Natl Acad Sci U S A* **89**, 1179-83 (1992).

114. Favor, J. et al. The mouse Pax2(1Neu) mutation is identical to a human PAX2 mutation in a family with renal-coloboma syndrome and results in developmental defects of the brain, ear, eye, and kidney. *Proc Natl Acad Sci U S A* **93**, 13870-5 (1996).

115. Armstrong, J.F., Pritchard-Jones, K., Bickmore, W.A., Hastie, N.D. & Bard, J.B. The expression of the Wilms' tumour gene, WT1, in the developing mammalian embryo. *Mech Dev* **40**, 85-97 (1993).

116. Donovan, M.J. et al. Initial differentiation of the metanephric mesenchyme is independent of WT1 and the ureteric bud. *Dev Genet* **24**, 252-62 (1999).

117. Kreidberg, J.A. et al. WT-1 is required for early kidney development. *Cell* **74**, 679-91 (1993).

118. Moore, A.W., McInnes, L., Kreidberg, J., Hastie, N.D. & Schedl, A. YAC complementation shows a requirement for Wt1 in the development of epicardium, adrenal gland and throughout nephrogenesis. *Development* **126**, 1845-57 (1999).

119. Kalatzis, V., Sahly, I., El-Amraoui, A. & Petit, C. Eya1 expression in the developing ear and kidney: towards the understanding of the pathogenesis of Branchio-Oto-Renal (BOR) syndrome. *Dev Dyn* **213**, 486-99 (1998).

120. Schuchardt, A., D'Agati, V., Pachnis, V. & Costantini, F. Renal agenesis and hypodysplasia in ret-k- mutant mice result from defects in ureteric bud development. *Development* **122**, 1919-29 (1996).

121. Pachnis, V., Mankoo, B. & Costantini, F. Expression of the c-ret proto-oncogene during mouse embryogenesis. *Development* **119**, 1005-17 (1993).

122. Hellmich, H.L., Kos, L., Cho, E.S., Mahon, K.A. & Zimmer, A. Embryonic expression of glial cell-line derived neurotrophic factor (GDNF) suggests multiple developmental roles in neural differentiation and epithelial-mesenchymal interactions. *Mech Dev* **54**, 95-105 (1996).

123. Moore, M.W. et al. Renal and neuronal abnormalities in mice lacking GDNF. *Nature* **382**, 76-9 (1996).

124. Pichel, J.G. et al. GDNF is required for kidney development and enteric innervation. *Cold Spring Harb Symp Quant Biol* **61**, 445-57 (1996).

125. Sanchez, M.P. et al. Renal agenesis and the absence of enteric neurons in mice lacking GDNF. *Nature* **382**, 70-3 (1996).

126. Sariola, H. & Saarma, M. GDNF and its receptors in the regulation of the ureteric branching. *Int J Dev Biol* **43**, 413-8 (1999).

127. Vega, Q.C., Worby, C.A., Lechner, M.S., Dixon, J.E. & Dressler, G.R. Glial cell line-derived neurotrophic factor activates the receptor tyrosine kinase RET and promotes kidney morphogenesis. *Proc Natl Acad Sci U S A* **93**, 10657-61 (1996).

128. Sainio, K. et al. Glial-cell-line-derived neurotrophic factor is required for bud initiation from ureteric epithelium. *Development* **124**, 4077-87 (1997).

129. Tang, M.J., Worley, D., Sanicola, M. & Dressler, G.R. The RET-glial cell-derived neurotrophic factor (GDNF) pathway stimulates migration and chemoattraction of epithelial cells. *J Cell Biol* **142**, 1337-45 (1998).

130. Majumdar, A., Vainio, S., Kispert, A., McMahon, J. & McMahon, A.P. Wnt11 and Ret/Gdnf pathways cooperate in regulating ureteric branching during metanephric kidney development. *Development* **130**, 3175-85 (2003).

131. Kispert, A., Vainio, S., Shen, L., Rowitch, D.H. & McMahon, A.P. Proteoglycans are required for maintenance of Wnt-11 expression in the ureter tips. *Development* **122**, 3627-37 (1996).

132. Pepicelli, C.V., Kispert, A., Rowitch, D.H. & McMahon, A.P. GDNF induces branching and increased cell proliferation in the ureter of the mouse. *Dev Biol* **192**, 193-8 (1997).

133. Nishinakamura, R. et al. Murine homolog of SALL1 is essential for ureteric bud invasion in kidney development. *Development* **128**, 3105-15 (2001).

134. Nishinakamura, R. & Takasato, M. Essential roles of Sall1 in kidney development. *Kidney Int* **68**, 1948-50 (2005).

135. Self, M. et al. Six2 is required for suppression of nephrogenesis and progenitor renewal in the developing kidney. *EMBO J* **25**, 5214-28 (2006).

136. Hatini, V., Huh, S.O., Herzlinger, D., Soares, V.C. & Lai, E. Essential role of stromal mesenchyme in kidney morphogenesis revealed by targeted disruption of Winged Helix transcription factor BF-2. *Genes Dev* **10**, 1467-78 (1996).

137. Dudley, A.T., Lyons, K.M. & Robertson, E.J. A requirement for bone morphogenetic protein-7 during development of the mammalian kidney and eye. *Genes Dev* **9**, 2795-807 (1995).

138. Dudley, A.T. & Robertson, E.J. Overlapping expression domains of bone morphogenetic protein family members potentially account for limited tissue defects in BMP7 deficient embryos. *Dev Dyn* **208**, 349-62 (1997).

139. Lyons, K.M., Hogan, B.L. & Robertson, E.J. Colocalization of BMP 7 and BMP 2 RNAs suggests that these factors cooperatively mediate tissue interactions during murine development. *Mech Dev* **50**, 71-83 (1995).

140. Dudley, A.T., Godin, R.E. & Robertson, E.J. Interaction between FGF and BMP signaling pathways regulates development of metanephric mesenchyme. *Genes Dev* **13**, 1601-13 (1999).

141. Luo, G. et al. BMP-7 is an inducer of nephrogenesis, and is also required for eye development and skeletal patterning. *Genes Dev* **9**, 2808-20 (1995).

142. Carroll, T.J., Park, J.S., Hayashi, S., Majumdar, A. & McMahon, A.P. Wnt9b plays a central role in the regulation of mesenchymal to epithelial transitions underlying organogenesis of the mammalian urogenital system. *Dev Cell* **9**, 283-92 (2005).

143. Park, J.S., Valerius, M.T. & McMahon, A.P. Wnt/beta-catenin signaling regulates nephron induction during mouse kidney development. *Development* **134**, 2533-9 (2007).

144. Qian, J. et al. Mouse Wnt9b transforming activity, tissue-specific expression, and evolution. *Genomics* **81**, 34-46 (2003).

145. Stark, K., Vainio, S., Vassileva, G. & McMahon, A.P. Epithelial transformation of metanephric mesenchyme in the developing kidney regulated by Wnt-4. *Nature* **372**, 679-83 (1994).

146. Vainio, S.J. & Uusitalo, M.S. A road to kidney tubules via the Wnt pathway. *Pediatr Nephrol* **15**, 151-6 (2000).

147. Hogan, B.L.M., Zaret K. S. in Mouse Development: Patterning, Morphogenesis, and Organogenesis (ed. Rossant, J., Tam, P. P. L.) 301-330 (Academic Press, San Diego, 2002).

148. Aufderheide, E. & Ekblom, P. Tenascin during gut development: appearance in the mesenchyme, shift in molecular forms, and dependence on epithelial-mesenchymal interactions. *J Cell Biol* **107**, 2341-9 (1988).

149. Kedinger, M. et al. Smooth muscle actin expression during rat gut development and induction in fetal skin fibroblastic cells associated with intestinal embryonic epithelium. *Differentiation* **43**, 87-97 (1990).

150. Roberts, D.J. Molecular mechanisms of development of the gastrointestinal tract. *Dev Dyn* **219**, 109-20 (2000).

151. Wells, J.M. & Melton, D.A. Vertebrate endoderm development. *Annu Rev Cell Dev Biol* **15**, 393-410 (1999). Reprinted, with permission, from the Annual Review of Cell and Developmental Biology, Volume 15 ©1999 by Annual Reviews www.annualreviews.org

152. Yasugi, S. Role of Epithelial-Mesenchymal Interactions in Differentiation of Epithelium of Vertebrate Digestive Organs. *Develop. Growth & Differ.* **35**, 1-9 (1993).

153. Duluc, I., Freund, J.N., Leberquier, C. & Kedinger, M. Fetal endoderm primarily holds the temporal and positional information required for mammalian intestinal development. *J Cell Biol* **126**, 211-21 (1994).

154. Haffen, K., Kedinger, M. & Simon-Assmann, P. Mesenchyme-dependent differentiation of epithelial progenitor cells in the gut. *J Pediatr Gastroenterol Nutr* **6**, 14-23 (1987).

155. Lawson, K.A., Meneses, J.J. & Pedersen, R.A. Cell fate and cell lineage in the endoderm of the presomite mouse embryo, studied with an intracellular tracer. *Dev Biol* **115**, 325-39 (1986).

156. Cormack, D. in Essential Histology (ed. Anthony, R.) 299-334 (Lippincott Williams & Wilkins, Philadelphia, 2001).

157. Fukamachi, H., Mizuno, T. & Takayama, S. Epithelial-mesenchymal interactions in differentiation of stomach epithelium in fetal mice. *Anat Embryol (Berl)* **157**, 151-60 (1979).

158. Karam, S.M., Li, Q. & Gordon, J.I. Gastric epithelial morphogenesis in normal and transgenic mice. *Am J Physiol* **272**, G1209-20 (1997).

159. Lee, E.R. Dynamic histology of the antral epithelium in the mouse stomach: I. Architecture of antral units. *Am J Anat* **172**, 187-204 (1985).

160. Wright, N.A. Epithelial stem cell repertoire in the gut: clues to the origin of cell lineages, proliferative units and cancer. *Int J Exp Pathol* **81**, 117-43 (2000).

161. Takahashi, Y., Imanaka, T. & Takano, T. Spatial pattern of smooth muscle differentiation is specified by the epithelium in the stomach of mouse embryo. *Dev Dyn* **212**, 448-60 (1998).

162. Smith, D.M., Grasty, R.C., Theodosiou, N.A., Tabin, C.J. & Nascone-Yoder, N.M. Evolutionary relationships between the amphibian, avian, and mammalian stomachs. *Evol Dev* **2**, 348-59 (2000).

163. Roberts, D.J. et al. Sonic hedgehog is an endodermal signal inducing Bmp-4 and Hox genes during induction and regionalization of the chick hindgut. *Development* **121**, 3163-74 (1995).

164. Roberts, D.J., Smith, D.M., Goff, D.J. & Tabin, C.J. Epithelial-mesenchymal signaling during the regionalization of the chick gut. *Development* **125**, 2791-801 (1998).

165. Smith, D.M., Nielsen, C., Tabin, C.J. & Roberts, D.J. Roles of BMP signaling and Nkx2.5 in patterning at the chick midgut-foregut boundary. *Development* **127**, 3671-81 (2000).

166. Smith, D.M. & Tabin, C.J. BMP signalling specifies the pyloric sphincter. *Nature* **402**, 748-9 (1999).

167. Moniot, B. et al. SOX9 specifies the pyloric sphincter epithelium through mesenchymal-epithelial signals. *Development* **131**, 3795-804 (2004).

168. Theodosiou, N.A. & Tabin, C.J. Sox9 and Nkx2.5 determine the pyloric sphincter epithelium under the control of BMP signaling. *Dev Biol* **279**, 481-90 (2005). Reprinted with permission from Elsevier.

169. Bitgood, M.J. & McMahon, A.P. Hedgehog and Bmp genes are coexpressed at many diverse sites of cell-cell interaction in the mouse embryo. *Dev Biol* **172**, 126-38 (1995).

170. Chi, X. et al. Complex cardiac Nkx2-5 gene expression activated by noggin-sensitive enhancers followed by chamber-specific modules. *Proc Natl Acad Sci U S A* **102**, 13490-5 (2005).

Chapter 2

Six2 is required for suppression of nephrogenesis and progenitor renewal in the developing kidney

Self M, Lagutin O, Bowling B, Hendrix J, Cai Y,

Dressler G, and Oliver G.

THE
EMBO
JOURNAL

Six2 is required for suppression of nephrogenesis and progenitor renewal in the developing kidney

Michelle Self[1], Oleg V Lagutin[1], Beth Bowling[1], Jaime Hendrix[1], Yi Cai[2], Gregory R Dressler[2] and Guillermo Oliver[1,*]

[1]Department of Genetics and Tumor Cell Biology, St Jude Children's Research Hospital, Memphis, TN, USA and [2]Department of Pathology, University of Michigan, Ann Arbor, MI, USA

During kidney development and in response to inductive signals, the metanephric mesenchyme aggregates, becomes polarized, and generates much of the epithelia of the nephron. As such, the metanephric mesenchyme is a renal progenitor cell population that must be replenished as epithelial derivatives are continuously generated. The molecular mechanisms that maintain the undifferentiated state of the metanephric mesenchymal precursor cells have not yet been identified. In this paper, we report that functional inactivation of the homeobox gene *Six2* results in premature and ectopic differentiation of mesenchymal cells into epithelia and depletion of the progenitor cell population within the metanephric mesenchyme. Failure to renew the mesenchymal cells results in severe renal hypoplasia. Gain of Six2 function in cortical metanephric mesenchymal cells was sufficient to prevent their epithelial differentiation in an organ culture assay. We propose that in the developing kidney, Six2 activity is required for maintaining the mesenchymal progenitor population in an undifferentiated state by opposing the inductive signals emanating from the ureteric bud.

Introduction

The development of the mammalian kidney is a paradigm for the reciprocal inductive interactions that control branching morphogenesis and the transition of mesenchyme into epithelia. In mice, the metanephric kidney begins to develop at embryonic day (E) 10.5. Signals from the metanephric blastema, a population of mesenchymal cells in the caudal portion of the intermediate mesoderm, induce the ureteric bud (UB) to evaginate from the Wolffian duct (Gruenwald, 1943; Grobstein, 1955). At around E11.0, the ingrowth of the UB into the metanephric blastema induces the metanephric mesenchyme (MM) at the bud tips to condense around the UB tips. On the ventral side of the UB tips, the condensed

*Corresponding author. Department of Genetics and Tumor Cell Biology, St Jude Children's Research Hospital, 332 North Lauderdale Street, Memphis, TN 38105-2794, USA. Tel.: +1 901 495 2697; Fax: +1 901 526 2907; E-mail: guillermo.oliver@stjude.org

cells cluster into pretubular aggregates. Subsequently, these aggregates undergo a mesenchymal–epithelial transition that leads to the formation of epithelial vesicles, which sequentially differentiate into comma-shaped bodies, S-shaped bodies, and eventually functional nephrons (Saxen and Sariola, 1987; Dressler, 2002; Vainio and Lin, 2002; Vize *et al*, 2003).

As the MM cells condense and differentiate, they also reciprocally induce the UB to continue growing toward the periphery of the kidney and branching repeatedly to form the collecting duct system. The tips of each new UB branch go on to induce additional mesenchymal cells and generate new nephrons. Thus, the pattern of the developing kidney is established along a radial axis, with the oldest nephrons located near the medulla and distributed among interstitial stromal cells, and the youngest nephrons located in the peripheral nephrogenic zone (Saxen, 1987). This reciprocal inductive interaction between mesenchyme and UB epithelia is crucial for kidney development and must be maintained during kidney organogenesis.

Mesenchymal cell progenitors generate the different epithelial cell types of the nephron in response to induction (Herzlinger *et al*, 1992; Nishinakamura and Osafune, 2006). These mesenchymal stem/progenitor cells must be constantly renewed so that the kidney can continue to grow and induce additional generations of nephrons. Signals from the MM are likely necessary to oppose nephrogenesis and, therefore, maintain an available pool of undifferentiated progenitors within the peripheral nephrogenic zone. However, the identity of the genes and mechanisms required to maintain this mesenchymal stem/progenitor cell population in an undifferentiated condition is not yet known.

Here we investigated the role of the homeobox gene *Six2* in kidney nephrogenesis. Our data indicate that *Six2* is part of a genetic mechanism that opposes epithelial polarization and regulates renal epithelial precursor cell renewal by maintaining the undifferentiated state of MM progenitors.

Results and discussion

Six2 is expressed in the metanephric mesenchyme

We have previously shown that *Six2* is expressed throughout the development of the excretory system, including the nephrogenic cords and metanephroi (Oliver *et al*, 1995). At around E10.0, *Six2* expression was detected in the metanephric blastema before UB invasion (Oliver *et al*, 1995). Half a day later, *Six2* expression was localized in the MM surrounding the UB (Figure 1A). At E11.5, the expression was detected in the induced MM surrounding the UB epithelium (Figure 1B). High levels of *Six2* were observed on the dorsal side of the UB, and lower levels were found on the ventral side near the ureteric stalk where the pretubular aggregates will form (arrows in Figure 1B). Later during development (E14.5), *Six2* mRNA (Figure 1C and Supplementary Figure
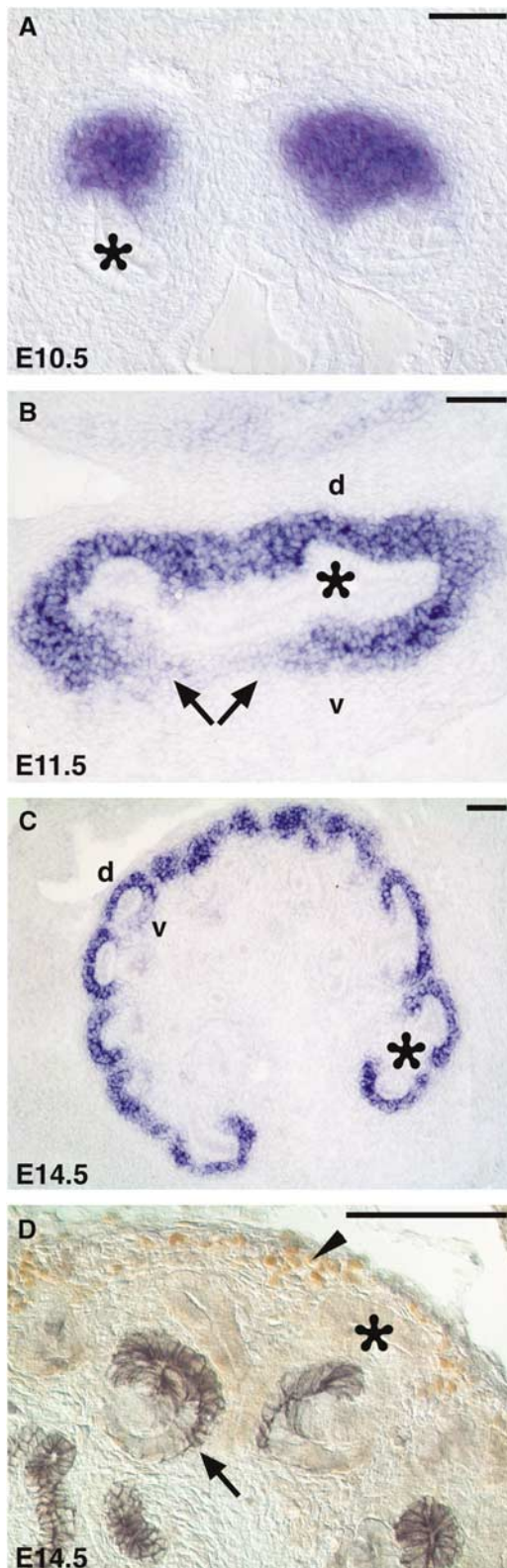
Figure 1 Six2 expression during renal development. (**A**) At E10.5, Six2 (blue) was expressed in the metanephric blastema, which signals the UB (asterisk) to evaginate from the Wolffian duct. (**B**) Six2 is expressed at high levels in the dorsal MM (d) at E11.5 and is downregulated where pretubular aggregates will form (arrows) on the ventral side (v) of the UB. (**C**) At E14.5, Six2 expression persists in the peripheral mesenchyme of the renal cortex. (**D**) Six2 protein (brown; arrowhead) is localized in the nephrogenic zone but is absent from the epithelial derivatives of the MM, which express Cadherin-6 (gray; arrow). Scale bar, 100 μm.

S2B) and Six2 protein (arrowhead, Figures 1D and 5O) remained in the Pax2-expressing condensing mesenchyme on the dorsal side of the UB tips (MM progenitor pool; Supplementary Figure S2A) but were downregulated in cells that, following aggregation and subsequent mesenchymal-to-epithelial transition, formed Cadherin-6-, Pax2-, and Wnt4-expressing comma bodies (arrows in Figures 1D and 5O, and Supplementary Figure S2A and C). This expression pattern suggested that, similar to Six1 (Xu et al, 2003), Six2 controls some aspects of early MM development. To directly address this question, we functionally inactivated Six2 in mice by deleting most of the Six2-coding sequence, including the two DNA-binding domains, the homeobox domain and the Six domain (Supplementary Figure S1).

Six2 activity is required for the normal development of the mammalian kidney

Six2-heterozygous mice did not exhibit any obvious abnormalities. However, Six2-nullizygous mice died soon after birth. An initial morphologic characterization of the mutant mice indicated major defects in the development of the kidney. Isolation of the E14.5 urogenital tract showed that the $Six2^{-/-}$ kidney was approximately 50% smaller than that of the wild-type littermate (Figure 2A); at E16.5, the reduction was even more dramatic at approximately 65% (Figure 2B). These results suggested that Six2 activity is required for the normal development of the mammalian kidney. No obvious alterations were observed in the genital tract or in the mesonephroi.

Histologic analysis of the Six2-null kidneys revealed some intriguing morphologic defects. At E11.5, the wild-type UB is surrounded by condensing mesenchyme (arrowhead, Figure 2C); however, formation of epithelial vesicles is not yet observed at this stage. Instead, the E11.5 $Six2^{-/-}$ kidney displayed ectopic and premature mesenchymal–epithelial transition that lead to the formation of precocious epithelial renal vesicles surrounding the UB (arrows, Figure 2D). At E12.5, the wild-type UB had begun its second round of branching, and the pretubular aggregates on the ventral side of the ureteric branches had undergone mesenchymal–epithelial transition to form renal vesicles (arrows, Figure 2E). In $Six2^{-/-}$ littermates, the UB had not branched beyond the initial 'T' stage of development (asterisk, Figure 2F), the ectopic renal vesicles surrounding the UB continued to develop further (arrows), and absence of condensing MM was apparent (arrowhead). At E14.5, the wild-type kidney exhibited condensing MM (arrowhead, Figure 2G) and growing UB branches (asterisk) in the cortical nephrogenic zone and interstitial stromal cells dispersed throughout the kidney. In contrast, the Six2-null kidney exhibited abnormal, unorganized masses of nephric epithelia (arrows, Figure 2H) and lacked condensing mesenchyme in the peripheral nephrogenic zone (arrowheads) and UB branches throughout the kidney (asterisk). The interstitial stromal cell population appeared to be normally distributed among the epithelial structures of the Six2-null kidney (Figure 2H).

Six2-null kidneys exhibit premature and ectopic renal vesicles

The presence of precocious ectopic supernumerary renal vesicles in the Six2-null kidney is a rather unique and
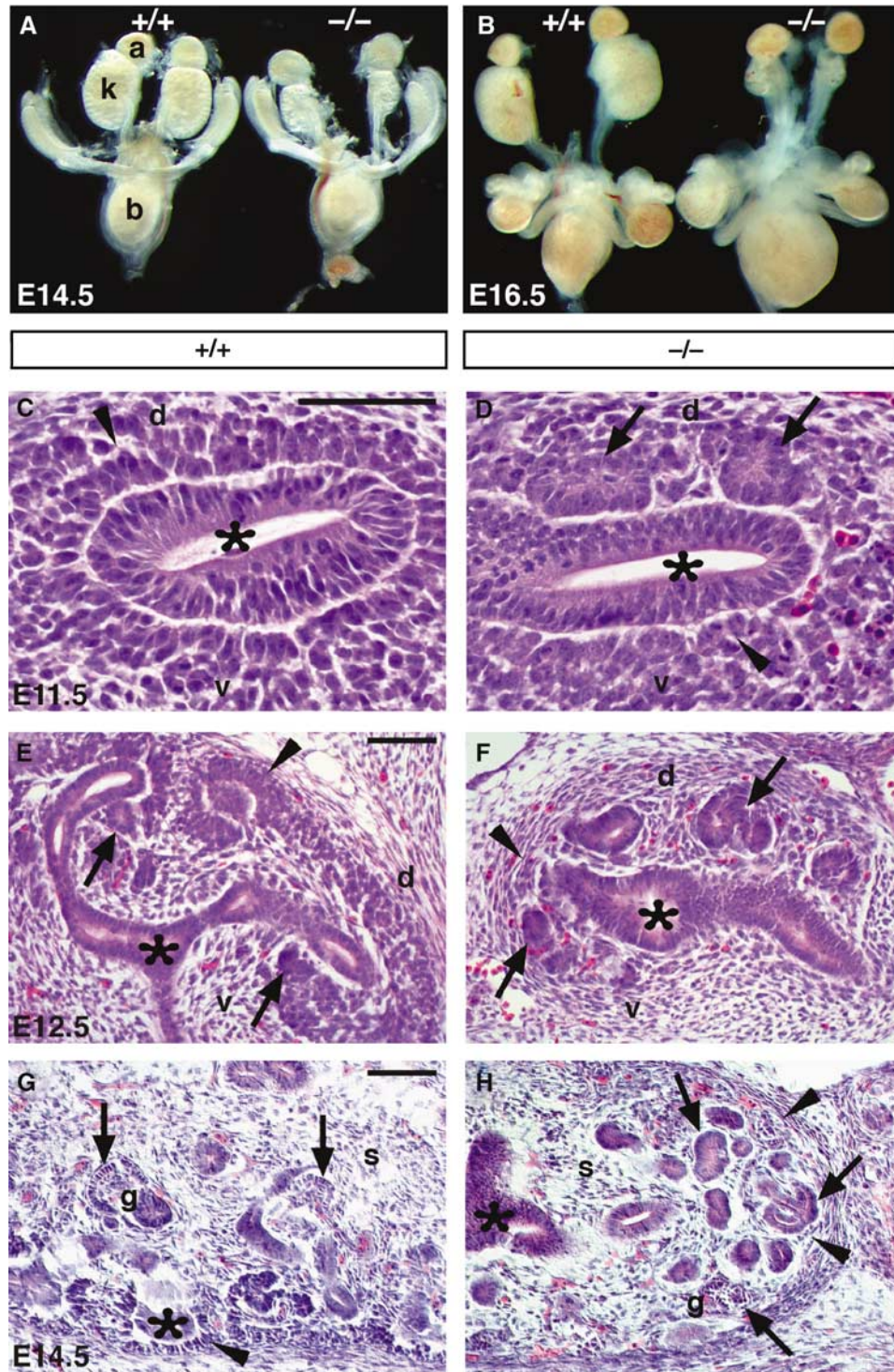
Figure 2 Six2 is crucial for kidney development. Analysis of urogenital tracts dissected at E14.5 (**A**) and E16.5 (**B**) revealed that *Six2*-null kidneys (k) were approximately 50% smaller than those of wild-type (+/+) littermates at E14.5 and 65% smaller at E16.5. The adrenal glands (a) and bladder (b) appeared normal. (C–H) Hematoxylin and eosin staining showed that at E11.5 in the wild-type kidney (**C**) the UB (asterisk) has induced the MM (arrowhead) to condense, but no pretubular aggregates or epithelia were present at this stage. (**D**) In *Six2*-null littermates, the MM has formed ectopic and premature epithelial vesicles (arrows) on the dorsal (d) side of the UB. (**E**) At E12.5, the wild-type MM on the ventral side of the UB tips has begun to transform into the epithelia of the renal vesicle (arrows). Condensing mesenchyme (arrowhead) was also detected on the dorsal side of the UB tips. (**F**) In *Six2*$^{-/-}$ littermates, the MM on the ventral and dorsal sides of the UB transitioned from mesenchyme to epithelia and formed precocious and ectopic renal vesicles (arrows). Note the lack of condensing MM (arrowhead) at the bud tips. (**G**) At E14.5, the wild-type kidney exhibited its typical uninduced and condensing mesenchyme (arrowhead) and growing branch tips (asterisk) in the cortex, maturing glomeruli (g; arrow) in the medulla, and interstitial stromal cells (s) dispersed throughout. (**H**) The *Six2*-null kidney revealed an absence of condensing mesenchyme in the cortex (arrowheads), unorganized epithelial structures (arrows) throughout the kidney including a few glomerular structures (g), and a normal distribution of stromal cells (s). Scale bar, 100 μm.

intriguing phenotype that has not been previously described. In an effort to confirm and better characterize these morphologic alterations, *Six2*-null kidneys were dissected at E11.5, cultured for 24, 48, and 96 h, and then stained with the following antibodies: anti-pan-cytokeratin to label the UB (Fleming and Symes, 1987), anti-E-cadherin to label the UB and distal tubules (Cho *et al*, 1998), anti-laminin-A to label all the polarized epithelial structures (Ekblom *et al*, 1980, 1991), anti-Cadherin-6 to label proximal tubule precursors (Cho *et al*, 1998), and anti-Wt1 to label podocyte precursors/ glomeruli (Buckler *et al*, 1991; Armstrong *et al*, 1993; Miner and Li, 2000).

In wild-type explants maintained in culture for 24 h, new epithelial renal vesicles formed on the ventral side of the UB tips and were beginning to express Cadherin-6 in a few cells (arrow, Figure 3A). Instead, *Six2*-null kidney explants displayed an abundance of Cadherin-6 expression in the precocious renal vesicles that formed on the ventral and dorsal sides of the UB (arrows, Figure 3B). This result confirmed that in the *Six2*-mutant kidney, developing nephrons form and differentiate prematurely. As expected, in wild-type explants maintained in culture for 48 h, laminin-A-expressing epithelial renal vesicles continued to differentiate into comma- and S-shaped bodies, only on the ventral side of the UB tips (arrows, Figure 3C). In the *Six2*-null kidney, the UB showed very limited branching (asterisk, Figure 3D) and was completely surrounded on both the ventral and dorsal sides by laminin-A-expressing epithelial vesicles (arrows). The expression of laminin-A and the absence of pan-cytokeratin indicated that the vesicles were polarized epithelia derived from the mesenchyme that formed ectopically on the dorsal side of the UB branch tips.

To determine whether *Six2*-null kidneys produce morphologically normal nephrons, we maintained explants in culture for 96 h. As indicated by the nuclear labeling of Wt1, the *Six2*-null kidney formed glomeruli (arrows, Figure 3F; nephron quantification included in Supplementary Figure S3A), but in contrast to the wild-type kidney, it lacked a reserve of MM in the cortex (white arrowhead, Figure 3F). In the wild-type kidney, Cadherin-6 and E-cadherin were coexpressed at the boundary of the proximal and distal tubules (yellow arrowheads in Figure 3G); in the *Six2*-null kidney, their expression domains were abnormally expanded and overlapped to a much greater extent (yellow arrowheads, Figure 3F and H). The expression of additional markers of tubule segments including *Slc34a1* (Collins and Ghishan, 1994; Murer *et al*, 2004), *Slc12a1* (Gamba *et al*, 1994), *Slc12a3* (Gamba *et al*, 1994; Hebert *et al*, 2004), and *Calbindin-3* (Shamley *et al*, 1992) was also detected in the E15.5 *Six2*-mutant kidney (Supplementary Figure S3).

Wild-type nephrons normally contain a single glomerular structure connected to the UB via the distal tubule ('c' in Figure 3E and G). In contrast, despite the presence of numerous glomeruli, only a few (1–3) connections between the nephric structures and the UB were identified in the *Six2*-null explants ('c' in Figure 3F and H). Together, these results indicate that the *Six2*-null kidney forms glomeruli and expresses markers for distinct tubule segments; however, the lack of Six2 activity leads to defects in patterning and regionalization of nephric tubules and defects in the connections of nephrons to the UB. These defects are likely secondary to the lack of UB branching.

The metanephric kidney forms through reciprocal interactions between the MM and the UB epithelium, and these interactions lead to the formation of functional nephrons (Grobstein, 1955). During this process, a number of well-characterized genes, including *Wt1*, *Eya1*, *Bmp7*, *Pax2*, *Six1*, *Lim1*, *Sall1*, *Wnt4*, *Sfrp2*, *Wnt11*, *Gdnf*, *Ret*, and *Foxd1*, are essential for normal kidney morphogenesis (Vainio and Lin, 2002; Yu *et al*, 2004). To identify the cause of the phenotypic alterations observed in *Six2*-null kidneys, we analyzed the expression of these genes at different developmental stages.

The Wilms' tumor suppressor *Wt1* encodes a zinc-finger transcription factor necessary for UB outgrowth and survival of the metanephric blastema (Kreidberg *et al*, 1993; Donovan *et al*, 1999; Moore *et al*, 1999). Wt1 is expressed weakly in the metanephric blastema at E10.5 (arrowhead, Figure 4A) but as development progresses, its expression increases in MM (arrowhead, Figure 4G), aggregates, comma bodies, and S-shaped bodies and persists in podoctye precursors and epithelia of the Bowman's capsule (arrows, Figure 4M). The *eyes absent 1* (*Eya1*) gene encodes a protein tyrosine phosphatase that acts as a transcriptional coactivator (Li *et al*, 2003), is expressed in the MM (Figure 4C, I, and O) (Kalatzis *et al*, 1998), and is required for UB invasion of the MM (Xu *et al*, 1999). In *Eya1*-null embryos, the UB fails to invade the kidney mesenchyme, and the kidneys do not develop (Xu *et al*, 1999). Bone morphogenetic protein-7 (*Bmp7*), a member of the TGF-β family of secreted growth factors, is expressed initially in the UB, the MM, and in the early tubules derived from the mesenchyme (Figure 4E, K, and Q) (Dudley *et al*, 1995; Lyons *et al*, 1995; Dudley and Robertson, 1997). In *Bmp7*-null embryos, the condensed MM cells are gradually lost after E12.5, which leads to hypoplastic kidneys with few glomeruli at birth. This result suggests that Bmp7 acts as a survival factor for the nephrogenic progenitor pool during kidney development (Dudley *et al*, 1995; Luo *et al*, 1995).

Expression of all the above-mentioned molecular markers was normal in the E10.5 *Six2*-null blastema (Figure 4A–F). In the wild-type kidney, epithelial vesicles were first detected exclusively on the ventral side of the branched UBs at around E12.5 (Figure 4M). In agreement with the earliest morphological indications of developmental defects in *Six2*-null kidney, premature and ectopic Wt1-expressing (arrow, Figure 4H) and *Bmp7*-expressing (Figure 4L) epithelial vesicles were detected at around E11.5 in the mutant kidney. In addition, we observed a reduction in the size of the mesenchymal population that expresses Wt1, *Eya1*, and *Bmp7* (arrowheads, Figure 4H, J, and L). At E12.5, the presence of ectopic Wt1-, Cadherin-6-, and *Bmp7*-expressing epithelial vesicles surrounding the whole UB of the *Six2*-null kidney (arrows, Figure 4N and R) most likely contributed to the abnormal depletion of the *Eya1*-expressing MM (Figure 4P) that is normally present in the wild-type kidney at this stage (Figure 4M, O, and Q).

Pax2, a paired-domain protein expressed in the UB, MM, and in epithelial derivatives of the MM (Figure 5A, G, and M), is a key player in kidney morphogenesis (Dressler *et al*, 1990; Dressler and Douglass, 1992). In *Pax2*-deficient embryos, the kidney and genital tract never develop (Torres *et al*, 1995; Favor *et al*, 1996). *Sall1*, the murine homologue of the *Drosophila* homeotic *spalt* gene, which is necessary for UB invasion of the MM (Nishinakamura *et al*, 2001; Nishinakamura and Takasato, 2005), is expressed in the
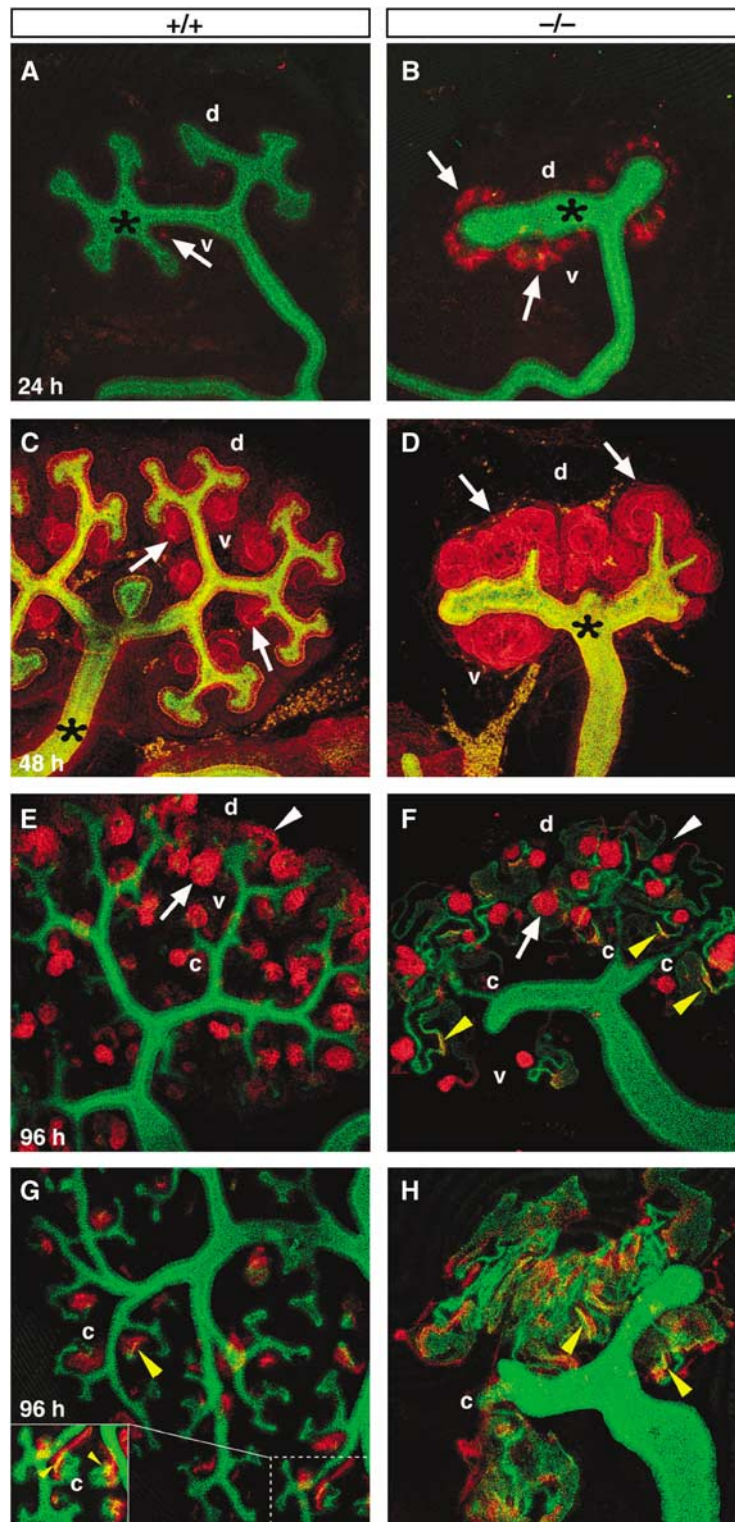
Figure 3 *Six2*-null kidneys exhibit precocious nephrogenesis. (**A, B**) Wild-type and *Six2*-null kidney explants maintained in culture and costained with E-cadherin to label the UB (green; asterisk) and Cadherin-6 to label developing nephrons (red; arrows). After 24 h culture, few cells expressed Cadherin-6 in the wild-type renal vesicles (A); instead, more advanced epithelial structures (arrows) on the dorsal and ventral sides of the UB tips were seen in the *Six2*$^{-/-}$ explant (B). (**C, D**) After 48 h, immunohistochemistry was performed using anti-pan-cytokeratin (green) to label the UB (asterisk) and anti-laminin-A (red) to label epithelial structures. (C) Normal developing comma and S-shaped bodies (arrows) were seen on the ventral sides (v) of the bud tips of the wild-type kidney. (D) Numerous ectopic renal epithelial structures (arrows) and decreased branching of the UB were identified in the *Six2*-null explant. (**E, F**) Explants cultured for 96 h were labeled with Wt1 (red), Cadherin-6 (red), and E-cadherin (green). (E) A normal reserve of mesenchymal progenitors (arrowhead) at the tips of the UB (green) and normal developing glomeruli (arrow) throughout the kidney were observed in the wild-type explant. (F) *Six2*$^{-/-}$ explants lacked MM in the periphery (white arrowhead) but formed glomeruli (arrow). (**G, H**) Explants cultured for 96 h were labeled with only Cadherin-6 (red) and E-cadherin (green) to identify any overlap in their expression at the boundary of the proximal and distal tubules (yellow arrowheads). The *Six2*-null explant (H) displayed abnormally extensive coexpression of these markers in mispatterned masses of developing tubules and rare connections of the tubules to the UB (c).
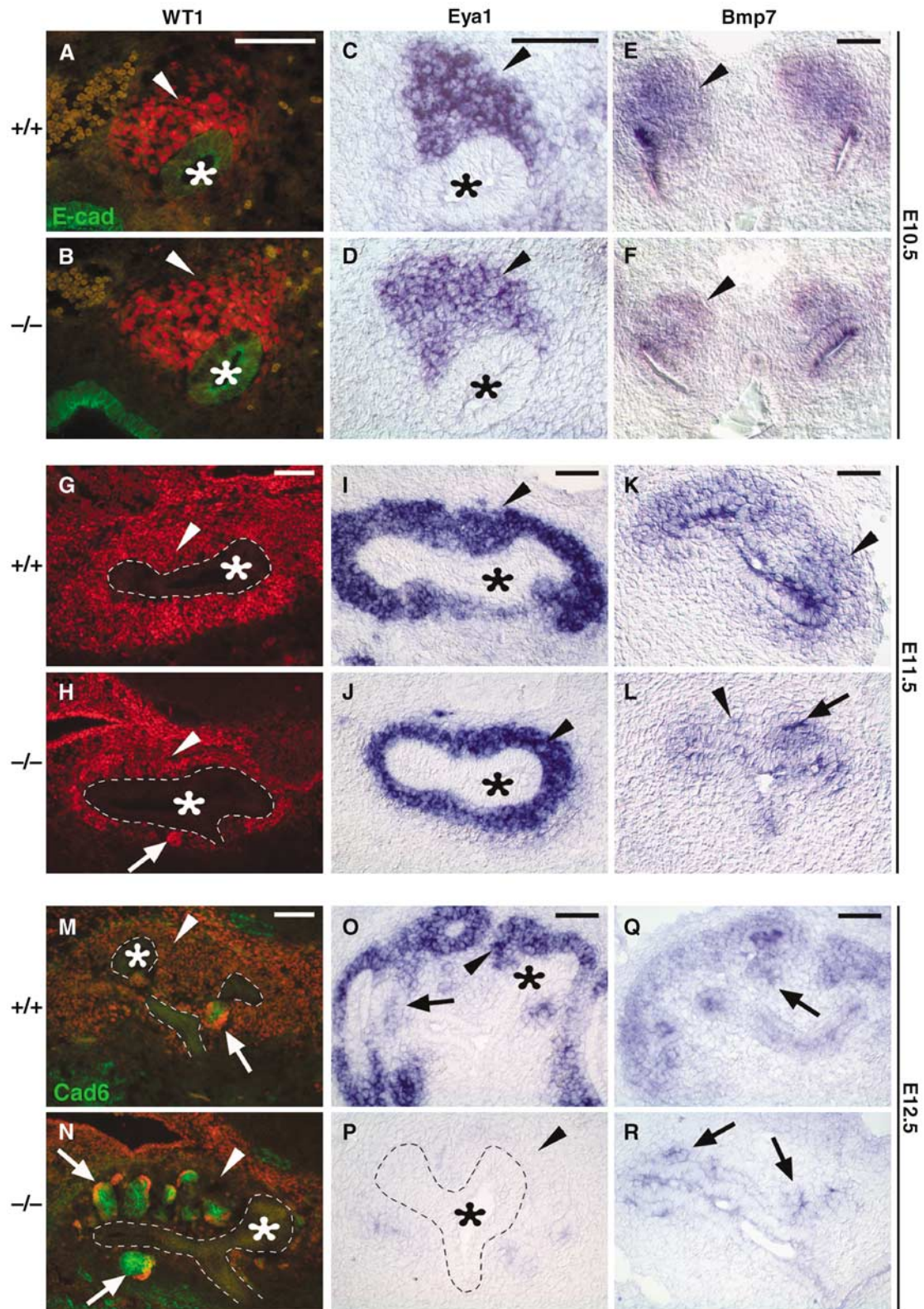
Figure 4 Molecular characterization of the *Six2*-null kidney. At E10.5, no obvious differences in the levels of expression of Wt1 (**A, B**; red), *Eya1* (**C, D**), or *Bmp7* (**E, F**) were detected in the MM (arrowheads) localized at the tip of the UB (asterisk) in *Six2*-null kidneys. No changes in their expression levels were also detected at E11.5 (**G–L**), although the size of the MM (arrowheads) surrounding the UB (asterisk and outlined) was reduced and premature and ectopic renal vesicles were already present (arrows) in *Six2⁻/⁻*. At E12.5, epithelial vesicles (arrows) with MM progenitors residing in the cortex (arrowheads) are seen in control kidneys (**M, O, Q**). *Six2*-null kidney (**N**) displayed Wt1 (red)- and Cadherin-6 (green)-expressing ectopic renal vesicles (arrows) on the dorsal and ventral sides of the UB and an absence of MM in the cortex (arrowhead). (**P**) In agreement with the depletion of the MM surrounding the UB (asterisk; outlined with dashes), expression of *Eya1* was lost in E12.5 *Six2*-null kidneys. (**R**) *Bmp7* was expressed at normal levels in the ectopic renal vesicles and UB at this stage. Scale bar, 100 μm.

mesenchymal population of the E10.5 blastema (Figure 5A) and in the MM, comma bodies, and faintly in a population of cells excluded from the expression domain of Pax2 at later stages (green arrowhead, Figure 5M). At around E10.5, before (data not shown) and after UB invasion (Figure 5B), expression of Pax2 and Sall1 was normal in the uninduced MM of *Six2*-null embryos. At E11.5, the expression level of *Pax2* was also normal in the MM and UB of *Six2*$^{-/-}$ kidneys; however, the number of *Pax2*-positive MM cells surrounding the ingrown UB was reduced (Figure 5H). As indicated by the expression of Sall1 and Pax2, ectopic comma bodies were detected in the mutant kidney at E12.5 (arrow, Figure 5N). As already demonstrated by the markers used in Figure 4, depletion of MM precursors in the periphery of the *Six2*-null kidney was further supported by the absence of Pax2 expression; however, cells faintly expressing Sall1 remained in the cortical stromal population (Figure 5N).

Wnt4 and Sfrp2 are ectopically expressed in the Six2-null metanephric mesenchyme

The *Wnt* signaling pathways regulate various key morphogenetic steps during embryogenesis, including the conversion of renal mesenchyme into epithelia. *Wnt4* encodes an essential mesenchyme-derived signal required for the transition of pretubular aggregates into epithelial renal vesicles, and its activity is necessary for nephron formation (Stark *et al*, 1994; Vainio and Uusitalo, 2000). In *Wnt4*-null kidneys, the mesenchyme initially condenses around the UB outgrowth, but aggregates of cells that would normally form nephrons fail to epithelialize, and few renal vesicles form (Stark *et al*, 1994). In addition, Wnt4 is sufficient to trigger tubulogenesis in isolated MM (Kispert *et al*, 1998). However, Wnt4 is unlikely to be the primary UB-derived inductive signal, as it is expressed first in the mesenchymal aggregates on the ventral side of the UB tips (Stark *et al*, 1994).

It has been previously shown that *Wnt* activity is modulated by the secreted frizzled-related proteins (*Sfrp*). The stroma expresses Sfrp1, a factor that blocks epithelialization of the mesenchyme presumably by competing with the frizzled receptor for Wnt4 binding (Yoshino *et al*, 2001). The inhibitory activity of Sfrp1 is suppressed by Sfrp2, another member of this family whose expression pattern is similar to that of *Wnt4* (Leimeister *et al*, 1998; Lescher *et al*, 1998). Thus, the ability of Sfrp2 to antagonize the suppres-

sive function of Sfrp1 could promote epithelial polarization (Yoshino *et al*, 2001).

The precocious nephrogenesis observed in the *Six2*$^{-/-}$ kidney suggests that *Wnt* signaling may be altered in the mutant MM. At E10.5, *Wnt4* expression was detected only in the ventral-most MM (that closest to the Wolffian duct) of the wild-type kidney (arrow, Figure 5C), whereas in *Six2*-null littermates, *Wnt4* expression ectopically extended into the MM dorsal to the UB (arrowhead, Figure 5D). As shown in Figure 5E, *Sfrp2* expression was detected at low levels in the wild-type MM surrounding the Wolffian duct. Similar to *Wnt4*, *Sfrp2* expression was also ectopically expanded and strongly upregulated in the *Six2*$^{-/-}$ MM (Figure 5F). These results determined that as early as E10.5, the lack of Six2 activity promoted ectopic expansion of the mesenchymal territory permissive to inductive signals.

Interestingly, at around E11.5, the expression pattern of Six2 was mostly complementary to those of *Wnt4* and *Sfrp2* in the wild-type MM, with minimal overlap in their expression domains; Six2 expression was mostly localized on the dorsal side of the UB (brown, Figure 5I), whereas *Wnt4* and *Sfrp2* expression remained restricted to pretubular aggregates on the ventral side of the UB (arrows, Figure 5I and K). In the *Six2*$^{-/-}$ kidney, *Wnt4* expression remained ectopically expanded into the dorsal MM (arrowhead, Figure 5J), colocalizing with strong ectopic *Sfrp2* expression (Figure 5L). The presence of ectopic premature nephrogenesis and the depletion of the MM in the *Six2*$^{-/-}$ kidney were confirmed by analysis of the expression of these same signaling molecules at E12.5. At this stage in a normal kidney, *Wnt4* and *Sfrp2* were expressed in pretubular aggregates, comma bodies, and S-shaped bodies (arrows, Figure 5O and Q), all of which were derived from the Six2-expressing mesenchymal population. As shown previously in the E12.5 *Six2*-null kidney, the MM population has already been depleted owing to the premature formation of supernumerary ectopic renal vesicles dorsal and ventral to the UB tips (Figure 4N, P, and R), which continue to express these molecular markers (Figure 5P and R).

Recently, *Wnt9b* has also been reported to be expressed in the Wolffian duct and UB branches during kidney development (Qian *et al*, 2003). Furthermore, this gene acts upstream of Wnt4 in the induction of nephrogenesis and is essential for induction of MM and subsequent formation of epithelial renal tubules (Carroll *et al*, 2005). At E11.5 and E12.5, *Wnt9b*

Figure 5 Expression of members of the *Wnt* pathway is ectopically and prematurely detected in *Six2*-null kidneys. (**A, B**) Pax2 (red) and Sall1 (green) were used to identify the E10.5 MM. At this stage, expression of both these markers was normal in *Six2*$^{-/-}$ (**B**). (**C**) *Wnt4* expression was localized in the ventral-most mesenchyme (arrow) of an E10.5 wild-type kidney; instead, it was ectopically expanded into the dorsal-most mesenchyme (arrowheads) of the *Six2*-null littermate (**D**). (**E**) At this stage, normal low levels of *Sfrp2* were present in the wild-type mesenchyme surrounding the Wolffian duct (arrow). *Sfrp2* expression was also ectopically expanded into the dorsal side of the UB (arrowheads) and its expression was highly upregulated in the mutant littermate (**F**). (**G, H**) At E11.5, *Pax2* expression in the UB and MM of the *Six2*-null kidney was similar to that of the wild type, although the size of the MM was reduced. (**I**) At this stage, the expression of Six2 (brown) and that of *Wnt4* (blue) in the MM were complementary, that is, Six2 was expressed predominantly on the dorsal side of the UB and *Wnt4* (arrow) only on the ventral side. (**J**) In the *Six2*$^{-/-}$ kidney, *Wnt4* expression ectopically expanded to the dorsal MM (arrowhead). (**K**) At E11.5, *Sfrp2* expression in the wild-type MM was similar to that of *Wnt4;* dotted line indicates UB epithelium. (**L**) In the *Six2*$^{-/-}$ kidney, the level of *Sfrp2* was upregulated and ectopically expanded to the dorsal side (arrowhead). (**M**) At E12.5, Pax2 and Sall1 expression remained in the MM (white arrowhead) and was also detected in renal vesicles (arrows). Sall1 was also expressed by the stromal population (green arrowhead). (**N**) At E12.5, Pax2 expression in the *Six2*$^{-/-}$ kidney highlighted the presence of ectopic supernumerary renal vesicles (arrows) surrounding the UB. Pax2 expression was normal in the UB and renal vesicles, but mesenchymal cells (white arrowhead) expressing Pax2 were absent. However, Sall1-expressing stromal cells (green arrowhead) were still present in the *Six2*-null kidney at this stage. (**P, R**) *Wnt4* and *Sfrp2* were expressed in the ectopic renal vesicles (arrows) of the E12.5 *Six2*$^{-/-}$ kidney at levels comparable to those of wild-type (**O, Q**) kidney. Scale bar, 100 μm.

expression was normal in the *Six2*-null Wolffian duct and its derivative, the UB (Supplementary Figure S4). The finding that the expression of *Wnt4* is ectopically expanded and that of *Wnt9b* remains normal in the *Six2*-mutant kidney suggests that Six2 is a MM regulator of the Wnt-promoted nephrogenesis cascade (downstream of Wnt9b but upstream of Wnt4). In this scenario, Six2 activity will be normally required to repress this inductive signal in the dorsal mesenchyme and thus suppress nephrogenesis in the mesenchymal progenitor pool.

Reciprocal inductive interactions are defective in *Six2*-null kidneys

Next, we analyzed whether in addition to the identified changes in the expression of some genes regulating MM differentiation, expression of other genes whose activities
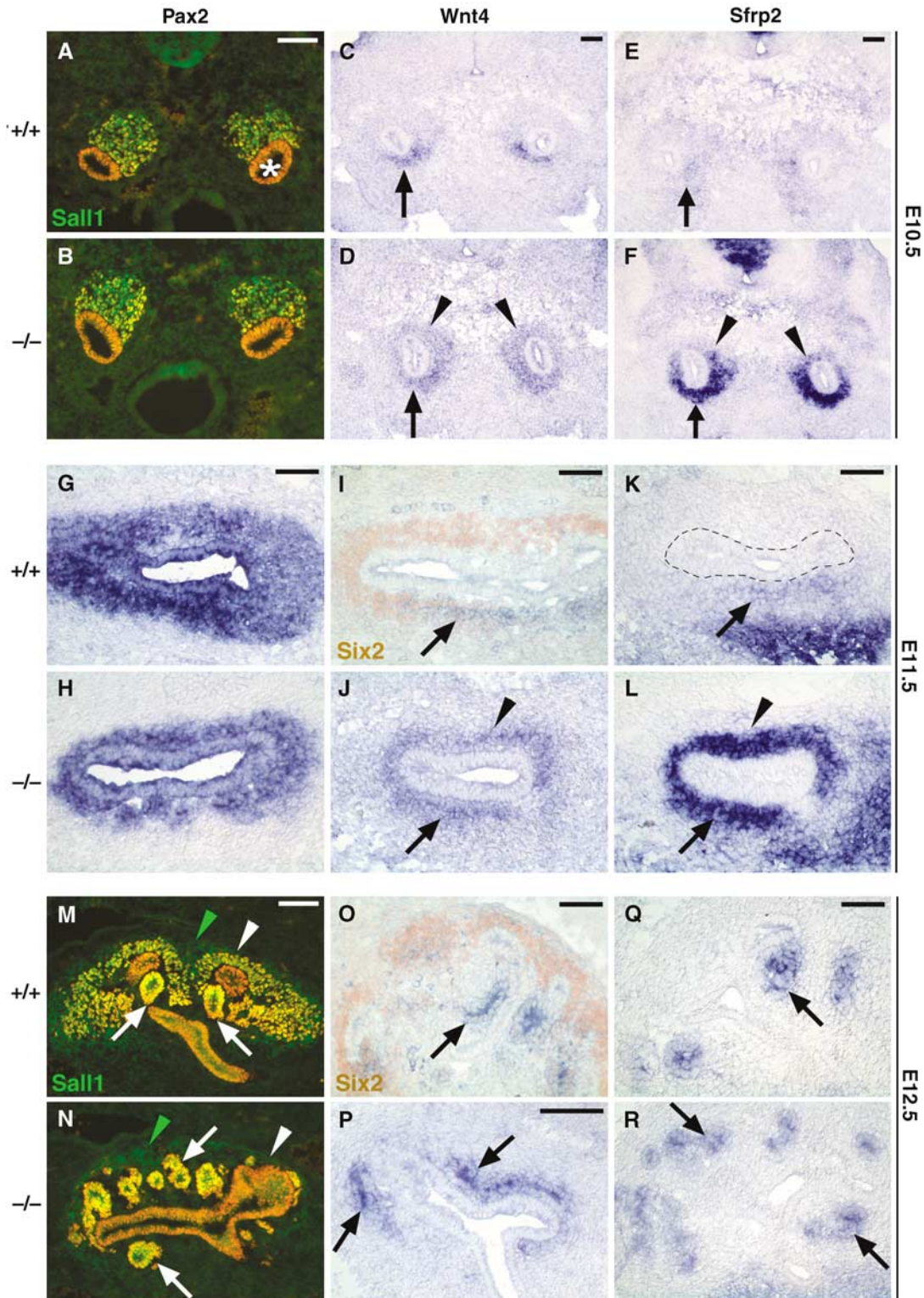
are necessary for UB branching was also affected in the *Six2*-null kidney. UB branching requires cooperative interactions between Wnt11, Gdnf, and Ret (Majumdar *et al*, 2003). Expression of *Wnt11* is normally detected in the branching UB tips (Figure 6A, G, and M; Kispert *et al*, 1996). Functional inactivation of *Wnt11* results in mild renal hypoplasia caused by subtle defects in branching morphogenesis of the UB (Majumdar *et al*, 2003). The glial-derived neurotrophic factor (*Gdnf*), which is expressed in the mesenchyme (Figure 6E, K, and Q), and its receptor tyrosine kinase *Ret*, which is expressed by the UB (Figure 6C, I, and O), are essential to promote UB outgrowth from the nephric duct (Pachnis *et al*, 1993; Durbec *et al*, 1996; Hellmich *et al*, 1996; Moore *et al*, 1996; Pichel *et al*, 1996; Sanchez *et al*, 1996; Trupp *et al*, 1996; Vega *et al*, 1996; Schuchardt *et al*, 1996; Sariola and Saarma, 1999). As the UB invaded the metanephric blastema at E10.5, *Wnt11* expression in the UB tips of the *Six2$^{-/-}$* kidney appeared normal (Figure 6B), confirming that initial UB induction was not affected. By E11.5, the invading UB has branched into a T-shaped structure with two expanding ampullae at both tips that express *Wnt11* (Figure 6G). At this stage, *Wnt11* was reduced in the UB tips of the *Six2$^{-/-}$* kidney (Figure 6H). This reduced expression of *Wnt11* was the earliest indication that the reciprocal interactions between the MM and UB were affected in the *Six2*-null kidney. At E12.5, *Wnt11* expression was extinguished in the *Six2*-null UB (Figure 6N), a result suggesting that the inductive mechanisms for UB branching morphogenesis had been prematurely disrupted in the mutant kidney. The levels of expression of *Gdnf* and *Ret* were normal in *Six2*-null kidneys at E10.5, E11.5, and E12.5 (Figure 6D, F, J, L, P, and R); therefore, this downregulation in the expression of *Wnt11* might be due to defects in some other alternative mechanism such as changes in the proteoglycan environment (Kispert *et al*, 1996).

In addition to the genes analyzed in Figures 4–6, we also characterized the expression of other well-known regulators of kidney development such as *Six1* (Oliver *et al*, 1995; Xu *et al*, 2003), *Pax8* (Plachov *et al*, 1990), *Fgf8* (Crossley and Martin, 1995), and *Lim1* (Fujii *et al*, 1994). Changes in the expression pattern of *Six1*, *Pax8*, *Fgf8* (data not shown), and *Lim1* (Supplementary Figure S4) were in agreement with those we previously observed when using other markers (e.g., Pax2, Eya1, Wnt4) that recognize similar cell populations. Those results, together with the kidney phenotypes resulting from the functional inactivation of these genes (Shawlot and Behringer, 1995; Mansouri *et al*, 1998; Tsang *et al*, 2000; Bouchard *et al*, 2002; Laclef *et al*, 2003; Li *et al*, 2003; Xu *et al*, 2003; Grieshammer *et al*, 2005; Perantoni *et al*, 2005), indicated that most likely they did not contribute to the *Six2*-null phenotype. Also, no obvious changes were identified in the stromal cell population that expresses *Foxd1* (Hatini *et al*, 1996), although this cell population was reduced owing to the smaller size of the *Six2*-null kidney (Supplementary Figure S4). Together, these results indicated that the primary reciprocal induction between the UB and the E10.5 metanephric blastema was largely unaffected in *Six2*-null kidney and suggested that UB invasion and MM induction do not require *Six2* activity. However, the precocious and ectopic nephrogenesis promoted by removal of Six2 activity caused the depletion of the mesenchymal progenitor/stem cell population and loss of reciprocal inductive interactions

required for continued kidney growth. Later during development (E14.5), most of the essential mesenchymal and ureteric genes (e.g., *Eya1*, *Pax2*, *Ret*) were downregulated or absent in the mutant kidney, whereas expression of Wnt4 remained in the developing nephrons and that of stromal markers (e.g., *Foxd1*, *Sfrp1*, *Raldh2*) remained unchanged (Supplementary Figure S5, and data not shown).

### *Apoptosis contributes to the loss of the mesenchymal progenitor pool in Six2-null kidneys*

The detection of precocious ectopic epithelial vesicles suggested that MM lacking Six2 undergoes premature nephrogenesis, resulting in a rapid reduction in the size of the uninduced mesenchymal cell population. A reduction in the size of the E11.5 MM population before the appearance of renal vesicles was also revealed by the analysis of the MM markers *Eya1*, *Pax2*, *Bmp7*, and *Gdnf* (Figures 4–6). To confirm the reduction of the E11.5 MM population and to analyze proliferation in the *Six2*-null kidney, we used antibodies against phosphohistone H3 and Pax2 on adjacent sections. Quantification of the number of PH3-positive cells in the Pax2-positive population revealed that the rate of proliferation and size of the MM were unaltered in E10.5 *Six2*-null kidney (Figure 7A and B). However, although the rate of proliferation was similar in the E11.5 wild-type and mutant kidneys, the size of the MM population was reduced by approximately 40% in the *Six2*-null kidney (Figure 7C and D). In addition, the amount of cell death detected by TUNEL assay increased significantly in the MM and stroma of the E11.5 *Six2*-null kidney (Figure 7H); this increase of apoptosis in the progenitor pool is also likely to contribute to the observed reduction in the size of both populations throughout kidney development. No significant changes in apoptosis were detected at E10.5 or E12.5 (Figure 7E, F and I, J); however, cell death increased from E14.5 to E17.5 (Figure 7K and L, and data not shown). The result of these phenotypic alterations is a severely hypoplastic and nonfunctional kidney at birth.

Together, these results indicated that in the *Six2*-null kidney, the MM aggregated rapidly and the renal vesicles formed ectopically and prematurely. These events, along with the presence of abnormal apoptosis, depleted the mesenchymal progenitor/stem cell population, which was not replenished. Thus, Six2 activity is required to repress epithelial polarization, at least in a portion of MM, thus allowing for the renewal of undifferentiated mesenchymal progenitors as the organ grows. Six2 opposes tubulogenesis promoted by the UB-derived inductive signal and thus reserve a subset of mesenchymal progenitor/stem cells in an undifferentiated state for future rounds of nephrogenesis.

Six2 ectopic expression repressed the differentiation of mesenchymal cells into epithelia in an organ culture system

To further test this working model, we expressed Six2 ectopically under the control of the chicken β-actin promoter in mouse kidney organ cultures. Plasmids expressing either EGFP or FLAG-tagged Six2 were introduced into wild-type E12.5 kidneys grown on Transwell filters using a modified version of a previously published electroporation protocol (Gao *et al*, 2005). Expression of EGFP was robust after 24 h in culture and could be maintained for several days. After 48 h
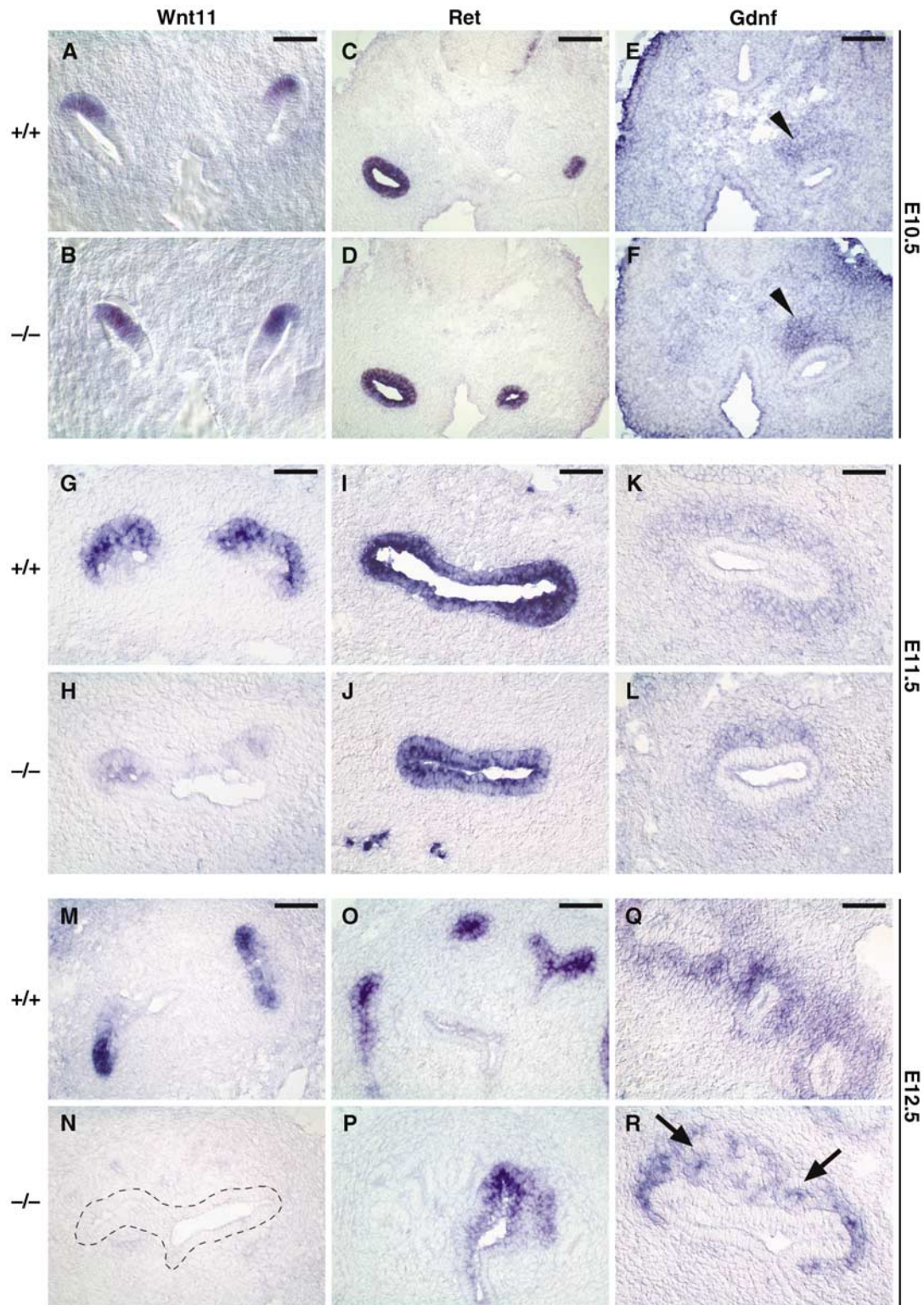
Figure 6 Reciprocal inductive interactions are lost in *Six2*-null kidney. *Wnt11* (**A, B**), *Ret* (**C, D**), and *Gdnf* (**E, F**) expression was normal in *Six2*$^{-/-}$ kidney at E10.5, indicating that the initial inductive mechanism of the UB was unaffected. (**G, H**) At E11.5, *Wnt11* expression was downregulated in the UB tips of the *Six2*$^{-/-}$ kidney as compared to wild-type littermates but that of *Ret* (**I, J**) and *Gdnf* (**K, L**) was normal. (**M, N**) At E12.5, reciprocal inductive interactions were lost in the *Six2*$^{-/-}$ kidney as indicated by the lack of *Wnt11* expression in the UB (dashed outline). (**O, P**) *Ret* expression remained at normal levels in the *Six2*-null UB at E12.5. (**Q, R**) *Gdnf* expression confirmed the abnormal reduction in the size of the MM population and the presence of ectopic developing nephrons (arrows). Scale bar, 100 μm.

in culture, the electroporated kidneys were fixed and sectioned to identify the distribution of EGFP and FLAG-Six2 expression. In the control cultures ($n = 8$), EGFP-labeled

cells were found in both the mesenchymal and epithelial components of the developing kidney at near equal proportions (Figure 8A, B and E, F, and Table I). In agreement with
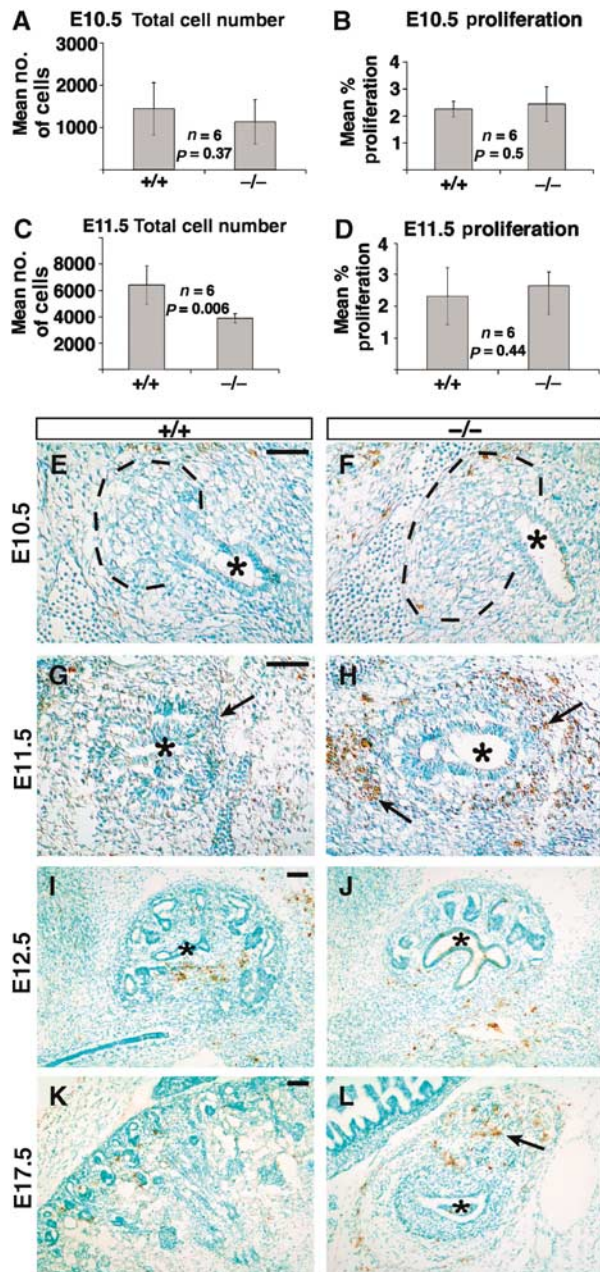
Figure 7 *Six2*$^{-/-}$ kidneys exhibit increased apoptosis at E11.5. (**A**, **B**) No differences in the mean total number of cells (A) or in the mean percentage of proliferating cells (B) were measured in the E10.5 *Six2*-null MM. (**C**, **D**) At E11.5, *Six2*$^{-/-}$ kidneys were significantly smaller than wild type (C; $P = 0.006$); however, the number of proliferating cells was comparable. (**E**, **F**) Similar to its wild-type littermate, no apoptotic cells were detected at E10.5 in *Six2*-mutant kidneys. The UB (asterisk) and the area of the metanephric blastema (dashed line) are indicated. (**G**, **H**) An abnormal increase in the number of apoptotic cells was identified in the *Six2*-null MM (arrows) surrounding the UB at this stage. (**I**, **J**) At E12.5, there was no significance difference in the number of apoptotic cells between wild-type and *Six2*$^{-/-}$ kidneys. (**K**, **L**) An increase in the number of apoptotic cells was again detected at E17.5 in the mutant kidney (arrow) as compared to wild-type controls. Scale bar, 100 μm.

previous results indicating that MM cells can be incorporated into the UB epithelia (Qiao *et al*, 1995), we observed EGFP-positive cells in branching epithelial tubules and developing nephrons; both these epithelial structures were Pax2-positive

(Figure 8A and B) and were surrounded by a laminin-containing basement membrane (Figure 8E and F). In contrast, electroporation of the *Six2* expression vector ($n = 8$) resulted in high levels of FLAG-Six2 labeling almost exclusively in the mesenchymal population (Figure 8C, D and G, H, and Table I). The FLAG-Six2-positive cells were localized along the peripheral mesenchyme and in the interstitial cells, as shown by *Foxd1* expression (Figure 8I and J). FLAG-Six2 was rarely detected in epithelial structures derived from MM or UB epithelia. Thus, ectopic expression of Six2 repressed the differentiation of mesenchymal cells into epithelia in the organ culture system. These results support the hypothesis that Six2 opposes epithelial polarization and helps maintain an undifferentiated population of renal blastemal cells.

Six2 activity maintains kidney blastemal cells in an undifferentiated state

Before induction, the MM is a small aggregate of a few thousand cells. In response to inductive signals, these cells coordinate a precise program of proliferation and differentiation to generate most of the epithelial cells in the nephrons. Because of the sequential nature of kidney patterning, new nephrons are induced in the periphery as the kidney grows. Thus, some of the MM cells aggregate and become polarized early, whereas others proliferate and remain mesenchymal to generate nephrons at subsequent stages. Our results identify an essential role of Six2 in maintaining and renewing this undifferentiated population of MM progenitor cells. Although mutations in genes such as *Pax2, Wt1, Eya1, Six1*, and *Sall1* (Kreidberg *et al*, 1993; Torres *et al*, 1995; Xu *et al*, 1999, 2003; Nishinakamura *et al*, 2001) affect the response to inductive signaling resulting in complete developmental arrest and kidney agenesis, the *Six2*-mutant phenotype is unique in that it exhibits premature and ectopic epithelial differentiation. Most likely, these events and the ectopic apoptosis detected during early stages of MM development deplete the peripheral mesenchymal progenitor population so that no new nephrons are generated. In addition, the defective maintenance of reciprocal inductive interactions we identified in the mutant kidneys most likely leads to the arrest in UB branching and mispatterning of nephrons observed at later stages. Furthermore, gain-of-function experiments in kidney organ culture demonstrated that persistent Six2 expression inhibits conversion of mesenchyme to epithelia. Therefore, Six2 must be downregulated in mesenchyme cells for epithelialization of mesenchymal pretubular aggregates to proceed. As previously mentioned, it has been suggested that Bmp7 acts as a survival factor for the nephrogenic progenitor pool during kidney development (Dudley *et al*, 1995; Luo *et al*, 1995); therefore, the Bmp7 signaling pathway may mediate Six2 function. However, no obvious phenotypic alterations were observed in the *Bmp7*-null kidneys before E12.5 (Dudley *et al*, 1995; Luo *et al*, 1995; Dudley and Robertson, 1997), and we did not detect obvious changes in the expression level of *Bmp7* in the E11.5 *Six2*$^{-/-}$ MM (Figure 4L). Together, these results indicated that most likely Bmp7 does not play a significant role in the *Six2*$^{-/-}$ phenotype and, therefore, is not a key player in the maintenance of the mesenchymal progenitor pool at the earliest stages of kidney development (i.e., E10.5–E11.5).

It is important to stress that although premature tubulogenesis resulted from a lack of Six2 activity, none of the
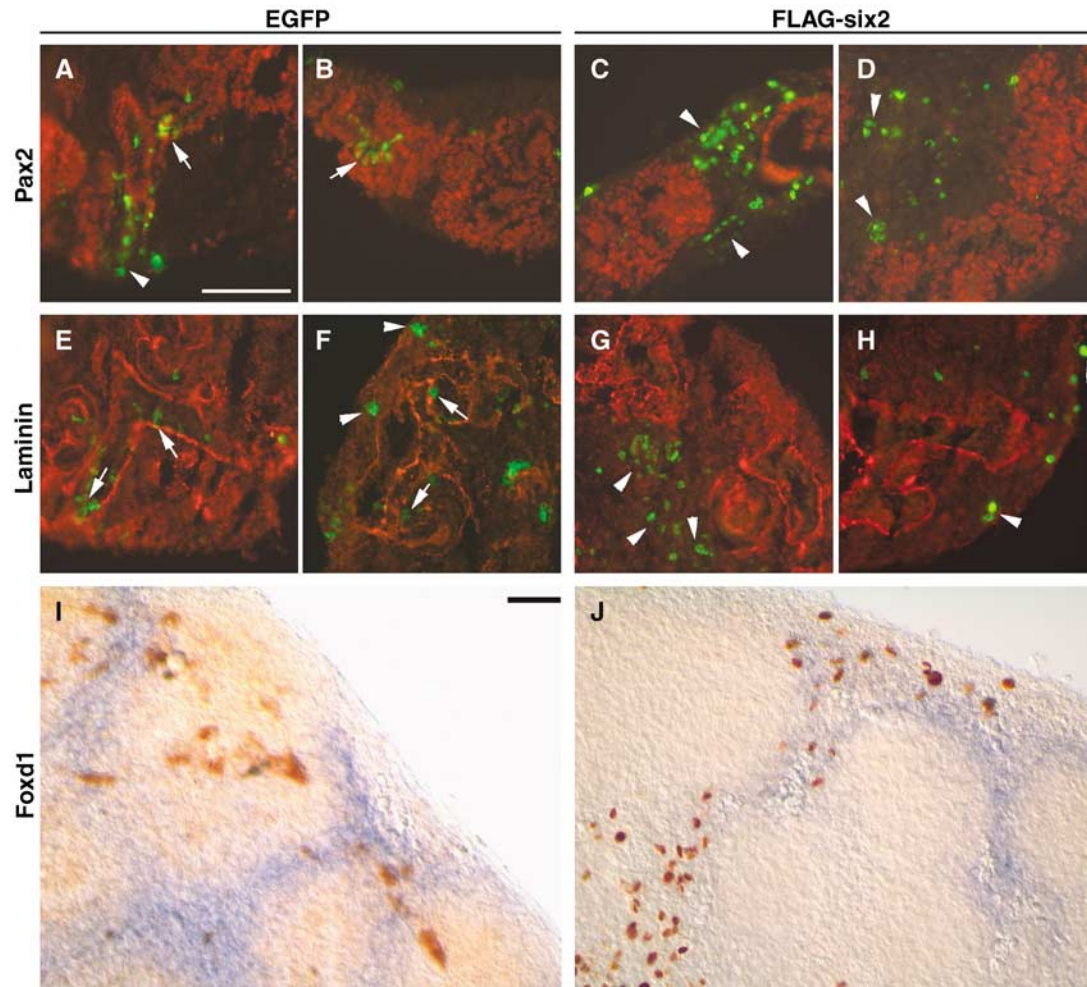
Figure 8 Overexpression of Six2 in wild-type kidney organ cultures. Forty-eight hours after microinjection and electroporation of EGFP or FLAG-Six2 expression plasmids, sections of E12.5 kidney organ cultures were labeled with antibodies specific for Pax2 (red; A–D), laminin (red; E–H), EGFP (green), or FLAG-Six2 (green). (**A, B**) EGFP and Pax2 were coexpressed in epithelial structures (arrows), and EGFP was also expressed in peripheral mesenchyme (arrowhead). (**C, D**) Cells expressing FLAG-Six2 were almost exclusively found in peripheral and interstitial mesenchyme (arrowheads), separated from Pax2-positive cells. (**E, F**) EGFP-positive cells were located within the developing tubules (arrows), as demarcated by laminin-containing basement membranes, and in the peripheral mesenchyme (arrowheads). (**G, H**) FLAG-Six2-expressing cells (arrowheads) were not surrounded by laminin-containing basement membranes and exhibited a mesenchymal phenotype. (**I, J**) *In situ* hybridization for *Foxd1* followed by immunohistochemistry using anti-GFP (I) or anti-FLAG (J) antibodies indicated that the cells expressing FLAG-Six2 resided mainly in the interstitial stroma, whereas cells expressing the EGFP control vector resided in all cell populations. Scale bar, 100 μm.

Table I Electroporation of E12.5 kidney organ cultures

Vector	Laminin ($+$)	Laminin ($-$)	Pax2 ($+$)	Pax2 ($-$)	Cells/section
EGFP	7.6 ± 4.0	13.8 ± 7.9	9.7 ± 5.2	11.3 ± 6.4	21.2 ± 7.6 $(n = 24)$[a]
Fl-Six2	0.44 ± 0.89	18.8 ± 12.4	1.2 ± 1.4	20.4 ± 4.5	20.6 ± 12.6 $(n = 32)$[a]

[a]Number of sections from eight electroporated cultures.

genetic markers for the stromal population were significantly changed. This finding indicates that Six2 differentially controls the fate of progenitor cells that are committed toward the epithelial lineage. This is consistent with the hypothesis that stromal and nephric lineages are specified separately at an early stage during kidney development (Hatini *et al*, 1996).

As suggested by our expression data, Six2 opposes tubulogenesis by directly or indirectly repressing the expression of *Wnt4* and *Sfrp2* within the MM. Importantly, although

Six2 and its closely related family member Six1 are expressed in the same population of the embryonic MM, their loss-of-function phenotypes suggest that they are functionally nonredundant and control different aspects of kidney development. On the basis of these results, we propose that Six2 controls the fate of the renal epithelial progenitor/ stem cell population by suppressing the inductive signals that promote epithelial differentiation and maintaining available pools of blastemal cells in an undifferentiated state.

Materials and methods

Functional inactivation of Six2

$Six2^{-/-}$ mice were generated by replacing the *Nco*I–*Eco*RI fragment of the *Six2* gene containing exon 1, the transcriptional initiation site, the *Six* domain, and the homeodomain with a 1.6-kb fragment containing the pGK-Neo cassette (Supplementary Figure S1). The vector pKO Scrambler NTKV-1901 (Stratagene) was used as a backbone. The *Hin*dIII site upstream of exon 2 was deleted during the cloning of the 3′ arm for genotyping purposes. Electroporation and selection of embryonic stem cells was performed using standard methods. Positive clones were identified and injected into blastocysts to generate chimeras. The mutated *Six2* allele was identified by Southern blot analysis and amplified by PCR.

In situ hybridization

Embryos were fixed in 4% paraformaldehyde and either processed for whole-mount *in situ* hybridization (Wilkinson, 1995) or cryo-preserved for cryosectioning. Whole-mount tissue was sectioned on a vibratome. Nonradioactive *in situ* hybridization was performed on sections as described previously (Schaeren-Wiemers and Gerfin-Moser, 1993).

Microinjection, electroporation, and culture of metanephric explants

E11.5 kidneys were dissected in L-15 medium (Gibco) and maintained in culture on Costar Transwell filters (0.4-μm pore size). The culture medium consisted of DMEM/F12 (1:1 mix), 10% fetal calf serum, and penicillin and streptomycin (Cellgro). Explants were maintained in culture for 24, 48, and 96 h at 37°C with 5% CO_2 for immunohistochemical analysis.

For transfection experiments, E12.5 kidneys were microdissected at room temperature in Dulbecco's PBS and placed on Transwell plates (24-mm diameter, 8-μm pore size, polycarbonate membrane; Corning) with 1 ml of DMEM. Using a glass capillary microelectrode controlled by an Eppendorf FemtoJet microinjection system, we injected 0.02–0.03 μl of PBS containing purified plasmid DNA (1.5 μg/μl) into different regions of the kidney. Immediately after

injection, we delivered five square electrical pulses of 40 V for 50 ms each at 100 ms intervals through platinum electrodes (7-mm diameter, 1-cm distance) by using a BTX ECM 830 (San Diego) electroporator. The kidneys were then maintained in culture for 48 h at 37°C with 5% CO_2. The kidneys were fixed in 4% paraformaldehyde at 4°C for 20 min, rinsed in PBS, cryoprotected in 0.5 M sucrose for 4 h, embedded in OCT medium, and stored at −80°C. Sections of kidney (14-μm thick) were cut on a cryostat and immunolabeled with anti-GFP (1:50, Invitrogen), anti-Flag (1:200, Sigma), anti-Pax2 (1:200), and anti-laminin (1:200, Sigma) antibodies. Whole-mount *in situ* hybridization was performed as described previously (Wilkinson, 1995) to detect *Foxd1* mRNA expression followed by whole-mount immunohistochemistry for either anti-GFP or anti-Flag antibodies using diaminobenzidine as a substrate.

Immunohistochemistry, TUNEL, and proliferation studies

See Supplementary data.

Supplementary data

Supplementary data are available at *The EMBO Journal* Online (http://www.embojournal.org).

References

Armstrong JF, Pritchard-Jones K, Bickmore WA, Hastie ND, Bard JB (1993) The expression of the Wilms' tumour gene, WT1, in the developing mammalian embryo. *Mech Dev* **40:** 85–97

Bouchard M, Souabni A, Mandler M, Neubuser A, Busslinger M (2002) Nephric lineage specification by Pax2 and Pax8. *Genes Dev* **16:** 2958–2970

Buckler AJ, Pelletier J, Haber DA, Glaser T, Housman DE (1991) Isolation, characterization, and expression of the murine Wilms' tumor gene (WT1) during kidney development. *Mol Cell Biol* **11:** 1707–1712

Carroll TJ, Park JS, Hayashi S, Majumdar A, McMahon AP (2005) Wnt9b plays a central role in the regulation of mesenchymal to epithelial transitions underlying organogenesis of the mammalian urogenital system. *Dev Cell* **9:** 283–292

Cho EA, Patterson LT, Brookhiser WT, Mah S, Kintner C, Dressler GR (1998) Differential expression and function of cadherin-6 during renal epithelium development. *Development* **125:** 803–812

Collins JF, Ghishan FK (1994) Molecular cloning, functional expression, tissue distribution, and *in situ* hybridization of the renal sodium phosphate (Na+/P(i)) transporter in the control and hypophosphatemic mouse. *FASEB J* **8:** 862–868

Crossley PH, Martin GR (1995) The mouse Fgf8 gene encodes a family of polypeptides and is expressed in regions that direct outgrowth and patterning in the developing embryo. *Development* **121:** 439–451

Donovan MJ, Natoli TA, Sainio K, Amstutz A, Jaenisch R, Sariola H, Kreidberg JA (1999) Initial differentiation of the metanephric mesenchyme is independent of WT1 and the ureteric bud. *Dev Genet* **24:** 252–262

Dressler GR (2002) Development of the excretory system. In *Mouse Development: Patterning, Morphogenesis, and Organogenesis*, Rossant J, Tam PPL (eds) pp 395–420. San Diego, CA: Academic Press

Dressler GR, Deutsch U, Chowdhury K, Nornes HO, Gruss P (1990) Pax2, a new murine paired-box-containing gene and its expression in the developing excretory system. *Development* **109:** 787–795

Dressler GR, Douglass EC (1992) Pax-2 is a DNA-binding protein expressed in embryonic kidney and Wilms tumor. *Proc Natl Acad Sci USA* **89:** 1179–1183

Dudley AT, Lyons KM, Robertson EJ (1995) A requirement for bone morphogenetic protein-7 during development of the mammalian kidney and eye. *Genes Dev* **9:** 2795–2807

Dudley AT, Robertson EJ (1997) Overlapping expression domains of bone morphogenetic protein family members potentially account for limited tissue defects in BMP7 deficient embryos. *Dev Dyn* **208:** 349–362

Durbec P, Marcos-Gutierrez CV, Kilkenny C, Grigoriou M, Wartiowaara K, Suvanto P, Smith D, Ponder B, Costantini F, Saarma M, Sariola H, Pachnis V (1996) GDNF signalling through the Ret receptor tyrosine kinase. *Nature* **381:** 789–793

Ekblom P, Alitalo K, Vaheri A, Timpl R, Saxen L (1980) Induction of a basement membrane glycoprotein in embryonic kidney: possible role of laminin in morphogenesis. *Proc Natl Acad Sci USA* **77:** 485–489

Ekblom P, Klein G, Ekblom M, Sorokin L (1991) Laminin isoforms and their receptors in the developing kidney. *Am J Kidney Dis* **17:** 603–605

Favor J, Sandulache R, Neuhauser-Klaus A, Pretsch W, Chatterjee B, Senft E, Wurst W, Blanquet V, Grimes P, Sporle R, Schughart K (1996) The mouse Pax2(1Neu) mutation is identical to a human PAX2 mutation in a family with renal-coloboma syndrome and results in developmental defects of the brain, ear, eye, and kidney. *Proc Natl Acad Sci USA* **93:** 13870–13875

Fleming S, Symes CE (1987) The distribution of cytokeratin antigens in the kidney and in renal tumours. *Histopathology* **11:** 157–170

Fujii T, Pichel JG, Taira M, Toyama R, Dawid IB, Westphal H (1994) Expression patterns of the murine LIM class homeobox gene lim1 in the developing brain and excretory system. *Dev Dyn* **199:** 73–83

Gamba G, Miyanoshita A, Lombardi M, Lytton J, Lee WS, Hediger MA, Hebert SC (1994) Molecular cloning, primary structure, and characterization of two members of the mammalian electroneutral sodium–(potassium)–chloride cotransporter family expressed in kidney. *J Biol Chem* **269:** 17713–17722

Gao X, Chen X, Taglienti M, Rumballe B, Little MH, Kreidberg JA (2005) Angioblast-mesenchyme induction of early kidney development is mediated by Wt1 and Vegfa. *Development* **132:** 5437–5449

Grieshammer U, Cebrian C, Ilagan R, Meyers E, Herzlinger D, Martin GR (2005) FGF8 is required for cell survival at distinct stages of nephrogenesis and for regulation of gene expression in nascent nephrons. *Development* **132:** 3847–3857

Grobstein C (1955) Inductive interactions in the development of the mouse metanephros. *J Exp Zool* **130:** 319–340

Gruenwald P (1943) Stimulations of nephrogenic tissues by normal and abnormal inductors. *Anat Rec* **86:** 321–335

Hatini V, Huh SO, Herzlinger D, Soares VC, Lai E (1996) Essential role of stromal mesenchyme in kidney morphogenesis revealed by targeted disruption of Winged Helix transcription factor BF-2. *Genes Dev* **10:** 1467–1478

Hebert SC, Mount DB, Gamba G (2004) Molecular physiology of cation-coupled Cl⁻ cotransport: the SLC12 family. *Pflugers Arch* **447:** 580–593

Hellmich HL, Kos L, Cho ES, Mahon KA, Zimmer A (1996) Embryonic expression of glial cell-line derived neurotrophic factor (GDNF) suggests multiple developmental roles in neural differentiation and epithelial–mesenchymal interactions. *Mech Dev* **54:** 95–105

Herzlinger D, Koseki C, Mikawa T, al-Awqati Q (1992) Metanephric mesenchyme contains multipotent stem cells whose fate is restricted after induction. *Development* **114:** 565–572

Kalatzis V, Sahly I, El-Amraoui A, Petit C (1998) Eya1 expression in the developing ear and kidney: towards the understanding of the pathogenesis of Branchio-Oto-Renal (BOR) syndrome. *Dev Dyn* **213:** 486–499

Kispert A, Vainio S, McMahon AP (1998) Wnt-4 is a mesenchymal signal for epithelial transformation of metanephric mesenchyme in the developing kidney. *Development* **125:** 4225–4234

Kispert A, Vainio S, Shen L, Rowitch DH, McMahon AP (1996) Proteoglycans are required for maintenance of Wnt-11 expression in the ureter tips. *Development* **122:** 3627–3637

Kreidberg JA, Sariola H, Loring JM, Maeda M, Pelletier J, Housman D, Jaenisch R (1993) WT-1 is required for early kidney development. *Cell* **74:** 679–691

Laclef C, Souil E, Demignon J, Maire P (2003) Thymus, kidney and craniofacial abnormalities in Six 1 deficient mice. *Mech Dev* **120:** 669–679

Leimeister C, Bach A, Gessler M (1998) Developmental expression patterns of mouse sFRP genes encoding members of the secreted frizzled related protein family. *Mech Dev* **75:** 29–42

Lescher B, Haenig B, Kispert A (1998) sFRP-2 is a target of the Wnt-4 signaling pathway in the developing metanephric kidney. *Dev Dyn* **213:** 440–451

Li X, Oghi KA, Zhang J, Krones A, Bush KT, Glass CK, Nigam SK, Aggarwal AK, Maas R, Rose DW, Rosenfeld MG (2003) Eya protein phosphatase activity regulates Six1–Dach–Eya transcriptional effects in mammalian organogenesis. *Nature* **426:** 247–254

Luo G, Hofmann C, Bronckers AL, Sohocki M, Bradley A, Karsenty G (1995) BMP-7 is an inducer of nephrogenesis, and is also required for eye development and skeletal patterning. *Genes Dev* **9:** 2808–2820

Lyons KM, Hogan BL, Robertson EJ (1995) Colocalization of BMP 7 and BMP 2 RNAs suggests that these factors cooperatively mediate tissue interactions during murine development. *Mech Dev* **50:** 71–83

Majumdar A, Vainio S, Kispert A, McMahon J, McMahon AP (2003) Wnt11 and Ret/Gdnf pathways cooperate in regulating ureteric branching during metanephric kidney development. *Development* **130:** 3175–3185

Mansouri A, Chowdhury K, Gruss P (1998) Follicular cells of the thyroid gland require Pax8 gene function. *Nat Genet* **19:** 87–90

Miner JH, Li C (2000) Defective glomerulogenesis in the absence of laminin alpha5 demonstrates a developmental role for the kidney glomerular basement membrane. *Dev Biol* **217:** 278–289

Moore AW, McInnes L, Kreidberg J, Hastie ND, Schedl A (1999) YAC complementation shows a requirement for Wt1 in the development of epicardium, adrenal gland and throughout nephrogenesis. *Development* **126:** 1845–1857

Moore MW, Klein RD, Farinas I, Sauer H, Armanini M, Phillips H, Reichardt LF, Ryan AM, Carver-Moore K, Rosenthal A (1996) Renal and neuronal abnormalities in mice lacking GDNF. *Nature* **382:** 76–79

Murer H, Forster I, Biber J (2004) The sodium phosphate cotransporter family SLC34. *Pflugers Arch* **447:** 763–767

Nishinakamura R, Matsumoto Y, Nakao K, Nakamura K, Sato A, Copeland NG, Gilbert DJ, Jenkins NA, Scully S, Lacey DL, Katsuki M, Asashima M, Yokota T (2001) Murine homolog of SALL1 is essential for ureteric bud invasion in kidney development. *Development* **128:** 3105–3115

Nishinakamura R, Osafune K (2006) Essential roles of sall family genes in kidney development. *J Physiol Sci* **56:** 131–136

Nishinakamura R, Takasato M (2005) Essential roles of Sall1 in kidney development. *Kidney Int* **68:** 1948–1950

Oliver G, Wehr R, Jenkins NA, Copeland NG, Cheyette BN, Hartenstein V, Zipursky SL, Gruss P (1995) Homeobox genes and connective tissue patterning. *Development* **121:** 693–705

Pachnis V, Mankoo B, Costantini F (1993) Expression of the c-ret proto-oncogene during mouse embryogenesis. *Development* **119:** 1005–1017

Perantoni AO, Timofeeva O, Naillat F, Richman C, Pajni-Underwood S, Wilson C, Vainio S, Dove LF, Lewandoski M (2005) Inactivation of FGF8 in early mesoderm reveals an essential role in kidney development. *Development* **132:** 3859–3871

Pichel JG, Shen L, Sheng HZ, Granholm AC, Drago J, Grinberg A, Lee EJ, Huang SP, Saarma M, Hoffer BJ, Sariola H, Westphal H (1996) Defects in enteric innervation and kidney development in mice lacking GDNF. *Nature* **382:** 73–76

Plachov D, Chowdhury K, Walther C, Simon D, Guenet JL, Gruss P (1990) Pax8, a murine paired box gene expressed in the developing excretory system and thyroid gland. *Development* **110:** 643–651

Qian J, Jiang Z, Li M, Heaphy P, Liu YH, Shackleford GM (2003) Mouse Wnt9b transforming activity, tissue-specific expression, and evolution. *Genomics* **81:** 34–46

Qiao J, Cohen D, Herzlinger D (1995) The metanephric blastema differentiates into collecting system and nephron epithelia *in vitro*. *Development* **121:** 3207–3214

Sanchez MP, Silos-Santiago I, Frisen J, He B, Lira SA, Barbacid M (1996) Renal agenesis and the absence of enteric neurons in mice lacking GDNF. *Nature* **382:** 70–73

Sariola H, Saarma M (1999) GDNF and its receptors in the regulation of the ureteric branching. *Int J Dev Biol* **43:** 413–418

Saxen L (1987) Organogenesis of the kidney. In *Developmental and Cell Biology Series 19*, Bard JBL, Barlow PW, Kirk DL (eds) Cambridge: Cambridge University Press

Saxen L, Sariola H (1987) Early organogenesis of the kidney. *Pediatr Nephrol* **1:** 385–392

Schaeren-Wiemers N, Gerfin-Moser A (1993) A single protocol to detect transcripts of various types and expression levels in neural tissue and cultured cells: *in situ* hybridization using digoxigenin-labelled cRNA probes. *Histochemistry* **100:** 431–440

Schuchardt A, D'Agati V, Pachnis V, Costantini F (1996) Renal agenesis and hypodysplasia in ret-k- mutant mice result from defects in ureteric bud development. *Development* **122:** 1919–1929

Shamley DR, Opperman LA, Buffenstein R, Ross FP (1992) Ontogeny of calbindin-D28K and calbindin-D9K in the mouse kidney, duodenum, cerebellum and placenta. *Development* **116:** 491–496

Shawlot W, Behringer RR (1995) Requirement for Lim1 in head-organizer function. *Nature* **374:** 425–430

Stark K, Vainio S, Vassileva G, McMahon AP (1994) Epithelial transformation of metanephric mesenchyme in the developing kidney regulated by Wnt-4. *Nature* **372:** 679–683

Torres M, Gomez-Pardo E, Dressler GR, Gruss P (1995) Pax-2 controls multiple steps of urogenital development. *Development* **121:** 4057–4065

Trupp M, Arenas E, Fainzilber M, Nilsson AS, Sieber BA, Grigoriou M, Kilkenny C, Salazar-Grueso E, Pachnis V, Arumae U (1996) Functional receptor for GDNF encoded by the c-ret proto-oncogene. *Nature* **381:** 785–789

Tsang TE, Shawlot W, Kinder SJ, Kobayashi A, Kwan KM, Schughart K, Kania A, Jessell TM, Behringer RR, Tam PP (2000) Lim1 activity is required for intermediate mesoderm differentiation in the mouse embryo. *Dev Biol* **223:** 77–90

Vainio S, Lin Y (2002) Coordinating early kidney development: lessons from gene targeting. *Nat Rev Genet* **3:** 533–543

Vainio SJ, Uusitalo MS (2000) A road to kidney tubules via the Wnt pathway. *Pediatr Nephrol* **15:** 151–156

Vega QC, Worby CA, Lechner MS, Dixon JE, Dressler GR (1996) Glial cell line-derived neurotrophic factor activates the receptor tyrosine kinase RET and promotes kidney morphogenesis. *Proc Natl Acad Sci USA* **93:** 10657–10661

Vize PD, Woolf AS, Bard JBL (2003) *The Kidney, from Normal Development to Congenital Disease.* London: Academic Press

Wilkinson DG (1995) RNA detection using non-radioactive *in situ* hybridization. *Curr Opin Biotechnol* **6:** 20–23

Xu PX, Adams J, Peters H, Brown MC, Heaney S, Maas R (1999) Eya1-deficient mice lack ears and kidneys and show abnormal apoptosis of organ primordia. *Nat Genet* **23:** 113–117

Xu PX, Zheng W, Huang L, Maire P, Laclef C, Silvius D (2003) Six1 is required for the early organogenesis of mammalian kidney. *Development* **130:** 3085–3094

Yoshino K, Rubin JS, Higinbotham KG, Uren A, Anest V, Plisov SY, Perantoni AO (2001) Secreted Frizzled-related proteins can regulate metanephric development. *Mech Dev* **102:** 45–55

Yu J, McMahon AP, Valerius MT (2004) Recent genetic studies of mouse kidney development. *Curr Opin Genet Dev* **14:** 550–557

Chapter 3

Six2 defines and regulates a multipotent self-renewing nephron progenitor population throughout mammalian kidney development

Kobayashi A, Valerius MT, Mugford J, Carroll T,

Self M, Oliver G, and McMahon A.

Six2 Defines and Regulates a Multipotent Self-Renewing Nephron Progenitor Population throughout Mammalian Kidney Development

Akio Kobayashi,[1] M. Todd Valerius,[1] Joshua W. Mugford,[1] Thomas J. Carroll,[1,3] Michelle Self,[2] Guillermo Oliver,[2] and Andrew P. McMahon[1,*]

[1]Department of Molecular and Cellular Biology, Harvard University, 16 Divinity Avenue, Cambridge, MA 02138, USA
[2]Department of Genetics and Tumor Cell Biology, St. Jude Children's Hospital, 262 Danny Thomas Place, Memphis, TN 38105, USA
[3]Present address: Departments of Internal Medicine (Nephrology) and Molecular Biology, University of Texas Southwestern Medical Center, 5323 Harry Hines Boulevard, Dallas, TX 75390, USA
*Correspondence: mcmahon@mcb.harvard.edu

SUMMARY

Nephrons, the basic functional units of the kidney, are generated repetitively during kidney organogenesis from a mesenchymal progenitor population. Which cells within this pool give rise to nephrons and how multiple nephron lineages form during this protracted developmental process are unclear. We demonstrate that the *Six2*-expressing cap mesenchyme represents a multipotent nephron progenitor population. *Six2*-expressing cells give rise to all cell types of the main body of the nephron during all stages of nephrogenesis. Pulse labeling of *Six2*-expressing nephron progenitors at the onset of kidney development suggests that the *Six2*-expressing population is maintained by self-renewal. Clonal analysis indicates that at least some *Six2*-expressing cells are multipotent, contributing to multiple domains of the nephron. Furthermore, *Six2* functions cell autonomously to maintain a progenitor cell status, as cap mesenchyme cells lacking *Six2* activity contribute to ectopic nephron tubules, a mechanism dependent on a *Wnt9b* inductive signal. Taken together, our observations suggest that *Six2* activity cell-autonomously regulates a multipotent nephron progenitor population.

INTRODUCTION

The metanephric kidney of the mouse initiates development at 10.5 days postcoitum (10.5 dpc). Reciprocal interactions between the Wolffian duct-derived ureteric bud and the adjacent metanephric mesenchyme population drive the process of kidney development (Costantini, 2006; Dressler, 2006; Saxen, 1987; Schedl, 2007). The mesenchymal population supports branching growth of the ureteric bud. Conversely, Wnt9b from the ureteric bud is required for a subset of cells within the adjacent mesenchyme to epithelialize, establishing the renal vesicle, the precursor for the glomerular and renal tubule compartment of the main body of the nephron (Carroll et al., 2005). The ureteric

epithelium generates the collecting duct network of the mature kidney while other cell populations, notably the renal interstitium (stroma), are likely generated from the mesenchymal pool. Reciprocal interactions over weeks or months, depending upon the mammalian species, generate the full complement of nephrons.

Recently, the homeodomain transcriptional regulator Six2 has emerged as a key factor within the kidney mesenchyme. *Six2* is expressed in a subset of metanephric mesenchyme, where its expression is maintained throughout kidney development (Oliver et al., 1995); no expression is detected in adult mouse kidneys (Humphreys et al., 2008). In *Six2* null mice, ectopic renal vesicles form on the dorsal (cortical) side of the ureteric bud at the onset of nephrogenesis, the progenitor pool is rapidly lost, and nephrogenesis terminates after induction of only a few nephrons (Self et al., 2006). Thus, *Six2* is required to maintain a nephron progenitor population.

We have addressed the tubule-forming lineage of the nephron and the cellular processes that underlie nephrogenesis. Our data suggest that *Six2*-expressing (*Six2*+) cells represent a self-renewing, multipotent nephron progenitor population throughout kidney organogenesis. *Six2* acts cell-autonomously within this population to maintain a progenitor state. In this, *Six2* may act, at least in part, to block *Wnt9b* action, thereby permitting renewal of uncommitted nephron progenitors. Thus, *Six2* ensures the development of a full complement of nephrons and, consequently, a functional organ system.

RESULTS

Six2+ Mesenchymal Cells Are Progenitors for the Main Body of the Nephron

The mesenchymal cell populations that surround the ureteric bud during nephrogenesis are a mosaic of molecularly distinct cell types. Among these, *Six2*+ cells lie in close proximity to the inductive ureteric epithelium. To determine the fate map of this population of the cap mesenchyme in vivo, we generated four *Six2-Cre* alleles in the mouse: a BAC transgenic allele with a *Tet-off-eGFPCre* (*Six2-TGC^{tg/+}*) cassette; and knockin alleles with *TGC* (*Six2^{TGC/+}*), *CreER^{T2}* (*Six2^{CE/+}*), and *eGFPCreER^{T2}* (*Six2^{GCE/+}*) cassettes introduced into the *Six2* locus at the position of the *Six2* initiation codon (see Figure S1 available online).
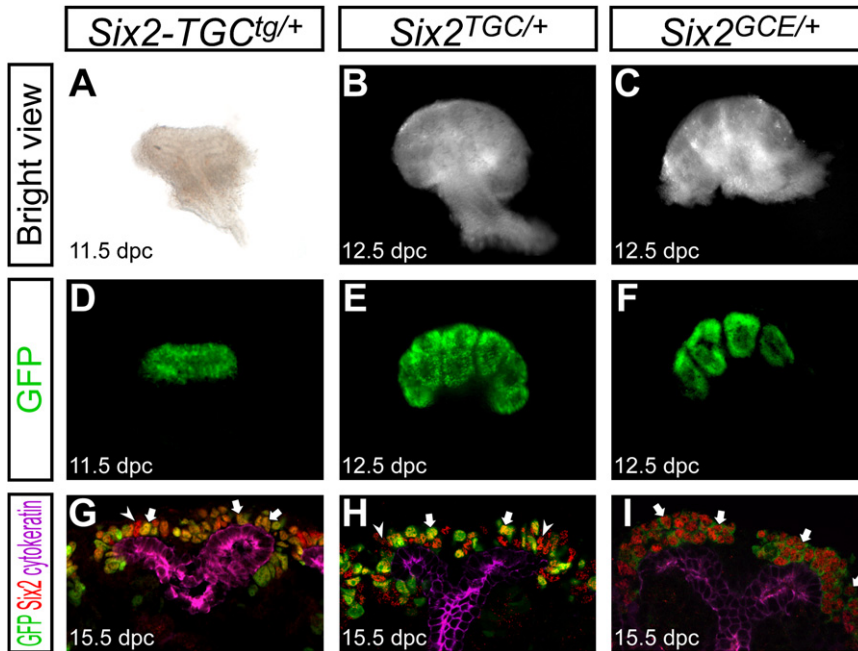
Figure 1. *Six2-eGFPCre* Transgenes Are Expressed in the Cap Mesenchyme

Kidneys from *Six2-TGC^{tg/+}* BAC transgenic (A, D, and G) and *Six2^{TGC/+}* (B, E, and H) and *Six2^{GCE/+}* (C, F, and I) knockin alleles at 11.5 dpc (A and D), 12.5 dpc (B, C, E, and F) and 15.5 dpc (G–I). (A–F) Whole-mount kidneys. (A–C) Bright view. (D–F) GFP expression. Backgrounds from nontissue regions were subtracted from images in (D) and (F). (G–I) Confocal immunofluorescence images of GFP (green), Six2 (red), and cytokeratin (purple). Cytokeratin is expressed in the ureteric tip and collecting duct. Arrow and arrowheads indicate Six2⁺ GFP⁺ and Six2⁺ GFP⁻ cells, respectively.

The knockin alleles remove *Six2* function; however, *Six2* heterozygous mice are phenotypically normal (data not shown and Self et al. [2006]). The *TGC* alleles were designed to enable doxycycline-regulated control of an *eGFPCre* transgene within the *Six2* expression domain (Bond et al., 2000; Rodda and McMahon, 2006). However, doxycycline addition did not silence Cre activity in the *TGC* BAC transgenic allele but disabled Cre activity in most cells in the *TGC* knockin allele (data not shown). The *CE* and *GCE* alleles enable tamoxifen-dependent regulation of Cre activity.

To validate expression patterns of transgenes, we examined GFP expression of the *TGC* and *GCE* alleles. In all lines, GFP expression was restricted to the cap mesenchyme from the onset of metanephric development (Figure 1 and data not shown). As expected, GFP+ cells were also Six2+, and no GFP+ cells were Six2−, though some Six2+ cells did not show detectable GFP expression in *Six2-TGC^{tg/+}* and *Six2^{TGC/+}* kidneys (Figures 1G–1I). As this slight mosaicism is observed in the *TGC* alleles, but not in the *GCE* allele, this likely reflects a component of the Tet regulatory system. In conclusion, GFP expression of all alleles was restricted to most or all Six2+ cells of the cap mesenchyme from the onset of nephrogenesis (Figures 1 and 2F–2I and data not shown).

The fate of *Six2*+ cells was examined during kidney development. *Six2-TGC^{tg/+}* mice were intercrossed with mice carrying a *R26R-lacZ* reporter allele (*R26R^{lacZ/+}*) (Soriano, 1999) to permanently label descendant cells from the *Six2*+ population. In addition to the kidney, we observed β-galactosidase (β-gal) activity from the *R26R-lacZ* allele in the developing head, ear, and limb, where *Six2* is also expressed (Figure 2A) (Oliver et al., 1995).

During early stages of kidney development, at the onset of nephron induction, β-gal activity was observed in the cap mesenchyme surrounding the ureteric bud epithelium (Figures 2B–2E). By 15.5 dpc, the ureteric bud has developed numerous branches and nephrogenesis is well advanced. At this time, GFP, like endogenous Six2, was restricted to the cap mesenchyme and early pretubular aggregates; no GFP activity was observed within the renal vesicle or its later derivatives (Figures 2F–2I and data not shown). All cells in the cap mesenchyme were β-gal+, indicating that all cap mesenchyme cells are derived from GFPCre-expressing cells. β-gal was also detected in early developing nephron tubules undergoing nephrogenesis and patterning (Figures 2G–2I) and in fully formed nephrons from the most proximal (renal corpuscle, Figure 2J) to the most distal (junction with the collecting duct, yellow arrow in Figure 2M) structures.

We further determined which cell types were populated by the *Six2*+ descendant lineage. Proteins assayed included Wt1 (cap mesenchyme, podocytes), PECAM-1 and Flk1 (endothelial cells), PDGFRb (glomerular mesangium, pericytes), uromodulin (loop of Henle), SMA (smooth muscle) and cytokeratin (collecting duct) (Figures 2J–2O and data not shown). In the maturing renal corpuscle, both parietal (Bowman's capsule) and visceral (podocyte) cells were Wt1+ and β-gal+ (Figure 2J), confirming that the *Six2*+ cap mesenchyme is the source of these nephron components. In contrast, the glomerular capillary system marked by PECAM-1 and Flk1 (Figure 2K and data not shown) and the glomerular mesangium marked by PDGFRb (Figure 2L) are β-gal−, indicating that these cells originate outside of *Six2*+ population. Interestingly, at the collecting duct-nephron junction in the cortex, no double-positive, β-gal+ cytokeratin+ cells were detected (Figure 2M), suggesting that the connecting segment derives from the main body of the nephron and not the collecting duct and that the *Six2*+ cap mesenchyme does not contribute to the ureteric tip. In the medullary region, adjacent epithelial tubules were identified using uromodulin (loop of Henle of the nephron) and cytokeratin (collecting duct). We detected β-gal+ uromodulin+ cell types, but no β-gal+ cytokeratin+ cells (Figure 2N and data not shown), indicating that these cell lineages are distinct. All SMA+ cells were β-gal−, suggesting that the smooth muscle is not derived from the cap mesenchyme. Overall, β-gal activity was observed specifically within the epithelial body of the nephron.
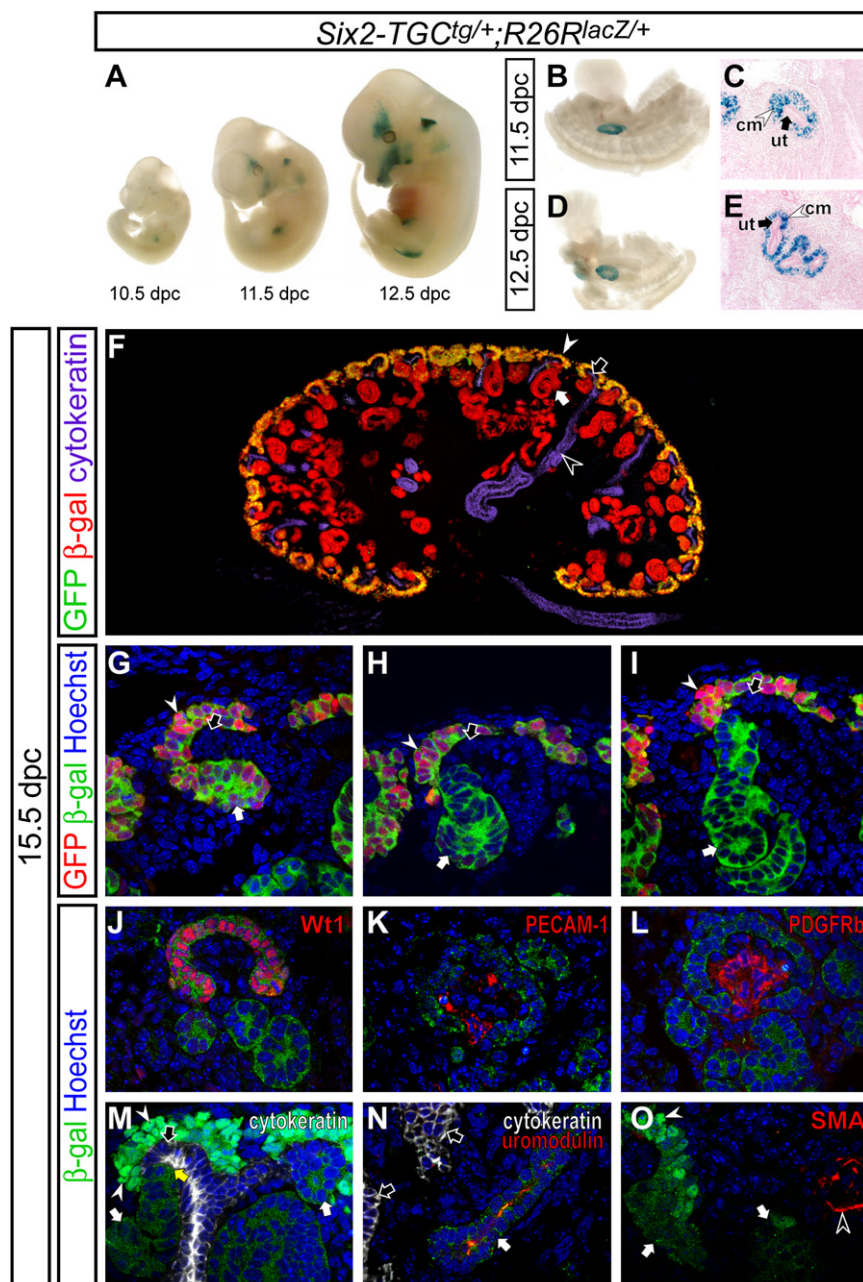
Figure 2. The *Six2*+ Population Contributes to All Cells of the Nephron Tubule

Fate mapping of the *Six2*+ population in *Six2-TGC^{tg/+}* ; *R26R^{lacZ/+}* embryos.

(A–E) β-gal staining. (A) Whole-mount embryos at 10.5, 11.5, and 12.5 dpc. (B and D) Dissected whole-mount posterior region of embryos at 11.5 and 12.5 dpc, respectively. (C and E) Sections counterstained with nuclear fast red of (B) and (D), respectively.

(F) Epi-immunofluorescence imaging of the kidney with anti-GFP (green), anti-β-gal (red), and anti-cytokeratin (purple) staining.

(G–I) Confocal immunofluorescence imaging of the cortical region of kidneys with anti-GFP (green), anti-β-gal (red), and Hoechst (blue) staining. (G) Early pretubular aggregate. (H) Comma-shaped body. (I) S-shaped body.

(J–O) Confocal immunofluorescence imaging of kidneys with anti-β-gal (green) and Hoechst (blue) staining. (J–L) The glomerulus stained with Wt1, PECAM-1, and PDGFRb in red, respectively. (M) Cytokeratin (white) staining in the cortical region of the kidney. Endogenous GFP is also visible in the cap mesenchyme localized to the nucleus (white arrowheads). The yellow arrow indicates the collecting duct-nephron junction. (N) Cytokeratin (white) and uromodulin (red) immunofluorescence in the medullary regions of kidneys. (O) Smooth muscle actin (SMA, red) immunofluorescence. White arrows, white arrowheads, black arrows, and black arrowheads indicate the developing nephron tubule, cap mesenchyme, ureteric tip, and collecting duct, respectively.

Six2+ cells were labeled in *Six2^{GCE/+}* ; *R26R^{lacZ/+}* embryos by tamoxifen induction at 16.5 dpc, and the distribution of β-gal-labeled cells was determined in the kidney at 18.5 dpc (Figures 3A–3D). β-gal activity was observed in the cap mesenchyme and developing nephron tubules of embryos from dams injected with tamoxifen (Figures 3B and 3D). No β-gal activity was observed in oil-injected controls, demonstrating that Cre recombinase activity is absolutely dependent on drug administration (Figures 3A and 3C). Thus, *Six2*+ cells continuously contribute to nephron formation throughout kidney development.

**Six2+ Cap Mesenchyme Cells Continuously Contribute to Nephron Tubule Formation throughout Kidney Development**

To determine whether *Six2*+ cells similarly contribute to nephron formation at later stages in kidney development, we used the *GCE* allele for tamoxifen-dependent labeling of *Six2*+ cells. In this allele, fusion of GFP with Cre does not alter Cre activity (Le et al., 1999). Further, analysis of the recombinase activity of the eGFPCreER^{T2} protein confirmed drug-dependent regulation of this fusion protein; no background recombination was observed in the absence of drug administration (Figure S2).

Self-Maintenance of the Nephron Progenitor Population from an Early Pool of Six2+ Cap Mesenchyme Cells

To obtain a more quantitative understanding of nephron formation, we used FACS of GFP+ cells in kidneys from *Six2^{GCE/+}* embryos to determine the increase in *Six2*+ cells from early to late stages of nephrogenesis. On average, the *Six2*+ compartment of a single kidney undergoes a 15.6-fold increase from 11,751 ± 3,133 cells at 11.5 dpc (n = 12) to 183,102 ± 41,382 cells at
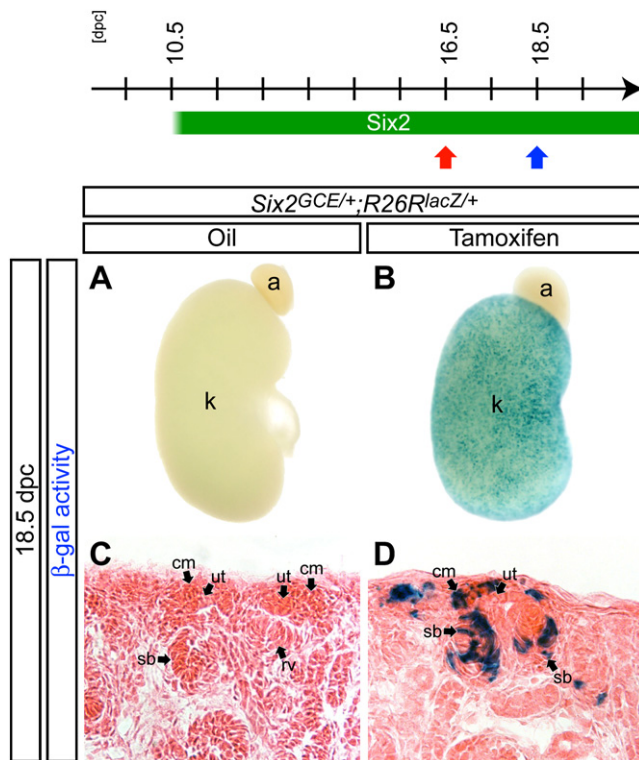
Figure 3. *Six2*+ Cells in the Cap Mesenchyme Contribute to the Nephron Tubule throughout Kidney Organogenesis

β-gal-stained kidneys from *Six2*$^{GCE/+}$; *R26R*$^{lacZ/+}$ embryos at 18.5 dpc after injection of oil only (A and C) or 6 mg tamoxifen (B and D) at 16.5 dpc. (A and B) Whole-mount view. (C and D) Sections counterstained with eosin. a, adrenal gland; cm, cap mesenchyme; k, kidney; rv, renal vesicle; sb, S-shaped body; ut, ureteric tip.

19.5 dpc (n = 8), a substantial increase, given the continued commitment of *Six2*+ cells to *Six2*− nephron structures.

The expansion of the *Six2*+ nephron progenitor population may reflect two distinct mechanisms. In the first, *Six2*+ cells may generate more *Six2*+ cells; that is self-maintenance of the progenitor pool. Alternatively, a *Six2*− progenitor population may exist outside of the *Six2*+ cap mesenchyme and continuously repopulate the *Six2*+ cap mesenchyme component. To distinguish between these possibilities, we labeled *Six2*+ cells at the onset of nephrogenesis with a transient pulse of tamoxifen activity and then examined the fate of labeled cells toward the end of kidney development at 19.5 dpc (Figures 4A and 4B). If the *Six2*+ cell population is a self-renewing population, β-gal+ cells should be retained in the cap mesenchyme in similar proportion to that observed immediately after transient labeling (Figure 4A). In contrast, if *Six2*− cells give rise to additional *Six2*+ cells after the onset of kidney development, these β-gal− cells would be expected to dilute out the initial β-gal+ cap mesenchyme population over time (Figure 4B).

The dynamics of Cre enzymatic activity are critical in drawing a conclusion. *Six2* expression commences in the mouse metanephros around 10.5 dpc prior to ingrowth of the ureteric bud (Oliver et al., 1995; Self et al., 2006). When 2 mg of tamoxifen was injected at 9.5 dpc, we rarely detected β-gal-labeled cells

in the kidney (Figures 4C, 4H, and 4M and data not shown), whereas injection at 10.5 dpc led to extensive labeling (Figure 4E). These results are consistent with tamoxifen induction of CreER^{T2} activity being confined to a window of less than 24 hr. Labeling from 10.5 to 11.5 dpc correlates with ingrowth and branching of the ureteric bud epithelium and the first induction of *Six2*+ progenitors to nephron precursors (Carroll et al., 2005). Consistent with a self-maintenance mechanism, we observed extensive contribution of β-gal+ cells within both the cortical cap mesenchyme and developing nephron structures at 19.5 dpc (Figures 4D, 4E, 4 I, 4J, 4N, and 4O). In contrast, when we labeled cells within the nonepithelial pretubular aggregate by transient activation of a *Wnt4*$^{GCE/+}$ allele (Figure S3) by tamoxifen induction at 12.5 dpc, β-gal+ cells were predominantly in mature nephron tubule structures outside of the cortical region at 19.5 dpc (Figures 4F, 4G, 4K, 4L, 4P, and 4Q). Thus, *Wnt4*+ cells derived from the *Six2*+ cap mesenchyme form a transient population that rapidly converts to nephron fates. In contrast, self-renewal by a *Six2*+ population plays a major role in maintaining the nephron progenitor pool.
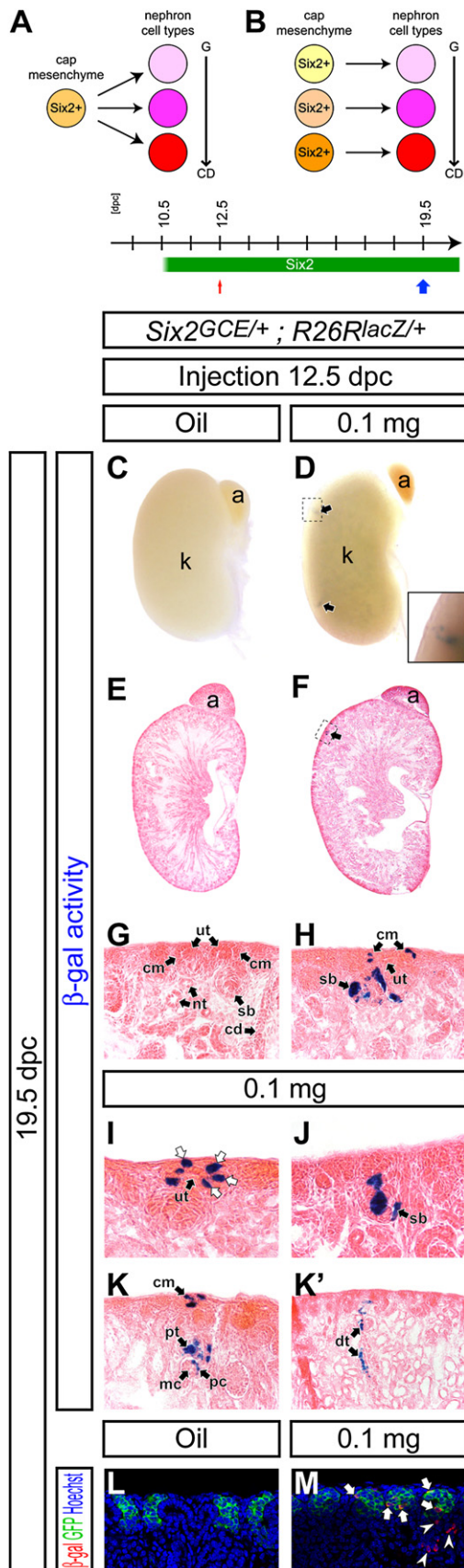
A *Six2*+ Cell Can Give Rise to Multiple Cell Types of the Nephron Tubule

The nephron tubule contains many specialized cell types along its proximodistal (glomerular-collecting duct) axis (Reggiani et al., 2007; Wingert et al., 2007), all of which derive from the *Six2*+ progenitor pool. To address whether this pool contains cells with extensive nephron-forming capability or a population of cells with narrowly restricted nephron fates, we performed a clonal analysis of *Six2*+ cells. If a single *Six2*+ cell is multipotent, its clonal descendants would contribute to different cell types along the axis of the nephron tubule (Figure 5A). In contrast, if a *Six2*+ population is a mosaic of cells already committed to generating regionally restricted cell types, the labeled clonal descendants would only contribute to restricted domains of the nephron tubule (Figure 5B). We optimized administration of tamoxifen to identify a dosage (0.1 mg) that, when injected into dams carrying *Six2*$^{GCE/+}$; *R26R*$^{lacZ/+}$ embryos at 12.5 dpc, gave rare and dispersed clusters of labeled cells at 14.5 dpc (3.58 ± 1.31 clusters per kidney, n = 12), indicative of clonal events (data not shown). Oil-injected control kidneys showed no β-gal+ cell (Figures 5C, 5E, 5G, and 5L).

Next, we repeated this 0.1 mg tamoxifen injection at 12.5 dpc but now examined nephrons at 19.5 dpc (Figures 5C–5M). We analyzed serial sections from kidneys with three clonal clusters or less; 24 clusters gave similar results. In several of these, multiple β-gal+ GFP+ cells were observed within the cap mesenchyme, confirming our previous observation that *Six2*+ cells undergo self-renewal (Figures 5H, 5I, 5K, and 5M). All nephron tubules that contained β-gal+ cells were mosaic, with a majority of cells β-gal−, as expected if the pretubular aggregate is derived from multiple *Six2*+ cap mesenchyme cells (Figures 5H, 5J, 5K, and 5K′). Within nephron derivatives, β-gal+ cells were observed in different specialized domains along the developing nephron tubule (Figure 5J). Serial section analysis demonstrated that β-gal+ cells within a single mature nephron tubule contributed to podocytes, proximal and distal tubule structures (Figures 5K and 5K′). These observations were further confirmed by confocal microscopy revealing that β-gal+ cells contribute to

Figure 4. The Nephron Progenitor Population Is Maintained by Duplication of Six2+ Cells

(A and B) Models for maintenance of the nephron progenitor population. (A) A β-gal-labeled (blue) *Six2*+ cell produces another β-gal-labeled *Six2*+ cell, which results in retention of β-gal-labeled cells in the cap mesenchyme (cm). (B) A progenitor population that generates *Six2*+ cells in the cap mesenchyme resides outside of the *Six2*+ population. Non-β-gal-labeled cells from the progenitor population (renal precursor, rp) dilute the β-gal-labeled cells in the cap mesenchyme. pa, pretubular aggregate.

(C–Q) β-gal-stained kidneys at 19.5 dpc from *Six2^{GCE/+}* ; *R26R^{lacZ/+}* embryos after injection of 2 mg tamoxifen at 9.5 dpc (C, H, and M) and 10.5 dpc (E, J, and O), and oil only at 10.5 dpc (D, I, and N) and from *Wnt4^{GCE/+}* ; *R26R^{lacZ/+}* embryos after injection of oil only (F, K, and P) and 2 mg tamoxifen (G, L, and Q) at 12.5 dpc. (C–G) Whole-mount view. (H–L) Sections counterstained with eosin. (M–Q) Higher magnification of the cortical region in (H)–(L), respectively. a, adrenal gland; cb, comma-shaped body; cd, collecting duct; cm, cap mesenchyme; gl, glomerulus; k, kidney; nt, nephron tubule; pa, pretubular aggregate; rp, renal precursor; sb, S-shaped body; ut, ureteric tip.

Figure 5. A *Six2*+ Cell Can Duplicate to Generate *Six2*+ Cells in the Cap Mesenchyme and Contribute to Multiple Domains of the Nephron Tubule

(A and B) Models for developmental potential of *Six2*+ cells. Different cell types are generated along the glomerular-collecting duct (G-CD) axis of the nephron. (A) A *Six2*+ cell retains multipotency for nephrogenesis. (B) Developmental potential of a *Six2*+ cell is restricted to limited cell types of the nephron.

(C–M) Kidneys from *Six2^{GCE/+}; R26R^{lacZ/+}* embryos at 19.5 dpc after injection of oil only (C, E, G, and L), and 0.1 mg (D, F, H, I–K′, and M) tamoxifen at 12.5 dpc. (C–K′) β-gal staining. (C and D) Whole-mount view. The inset in (D) is a higher magnification of a clone in the dashed region. (E and F) Sections counterstained with eosin. Arrows in (D) and (F) indicate β-gal+ clusters. (G–K′) Higher magnification of the cortical region. (H) shows the dashed region in (F). White arrows in (I) indicate β-gal+ cells in the cap mesenchyme. (K) and (K′) are adjacent sections 96 μm apart showing the same nephron. (L and M) Confocal immunofluorescence imaging of the cortical region with anti-β-gal (red), anti-GFP (green), and Hoechst (blue) staining. Arrows and arrowheads in (M) indicate β-gal+ GFP+ cells in the cap mesenchyme and β-gal+ GFP− cells in the developing nephron tubule, respectively. a, adrenal gland; cd, collecting duct; dt, distal tubule; cm, cap mesenchyme; k, kidney; mc, mesangial cell; nt, nephron tubule; pc, podocyte; pt, proximal tubule; sb, S-shaped body; ut, ureteric tip.

Wt1+ (podocytes), LTL-lectin+ (proximal tubule), and uromodulin+ (loop of Henle) cells in a clone (data not shown). These findings suggest that descendants of a single *Six2*+ cell can differentiate into multiple cell types within the nephron. Thus, regional commitment of progenitor cells to segment-specific cell types is likely to occur after an epithelial organization is established in the renal vesicle or its later derivatives (see the Discussion).

Six2 Function Is Cell-Autonomously Required for Maintenance of the Cap Mesenchyme

In the absence of *Six2* function, ectopic tubules form on the dorsal (cortical) side of the ureteric tip at the onset of kidney development, the cap mesenchyme is lost, and nephrogenesis arrests (Self et al., 2006). To determine the fate of the *Six2*-expressing cap mesenchyme cells in *Six2* null kidneys, we utilized the *Cre* knockin alleles to remove *Six2* function and label *Six2*-decendants. In *Six2^{TGC/GCE}; R26R^{lacZ/+}* embryos, activation of the *Six2-TGC* allele was evident from the presence of labeled, β-gal+ cells at 13.5 dpc (Figures 6A and 6B). Thus, the fate of the initial *Six2* population can be assessed on a *Six2* null background. All β-gal+ cells were restricted to laminin+ cytokeratin− ectopic tubules in *Six2* null kidneys (Figures 6C–6J). Some cells within the tubules are not β-gal+. There are likely two possible reasons. First, as noted earlier, the Tet cassette insertion led in some unknown manner to mosaic activity of *Cre*; hence, we would predict that all cells would not be labeled. Second, *Six2* is rapidly downregulated upon renal vesicle formation. This may not enable an adequate period of *Six2* promoter activity for Cre to accumulate to sufficient levels for recombination in all cells. In summary, the data indicate that *Six2* acts directly within nephron progenitors to maintain this population in a mesenchymal progenitor cell state.

To further define the requirement for *Six2* activity, we performed chimera analysis, generating animals composed of wild-type and *Six2* mutant cells (Figure 7A). In this analysis, all wild-type cells were β-gal+, whereas *Six2^{+/−}* and *Six2^{−/−}* cells were β-gal−. Approximately 40%–60% contribution was

Cell Stem Cell

Six2 Regulates Self-Renewing Nephron Progenitors
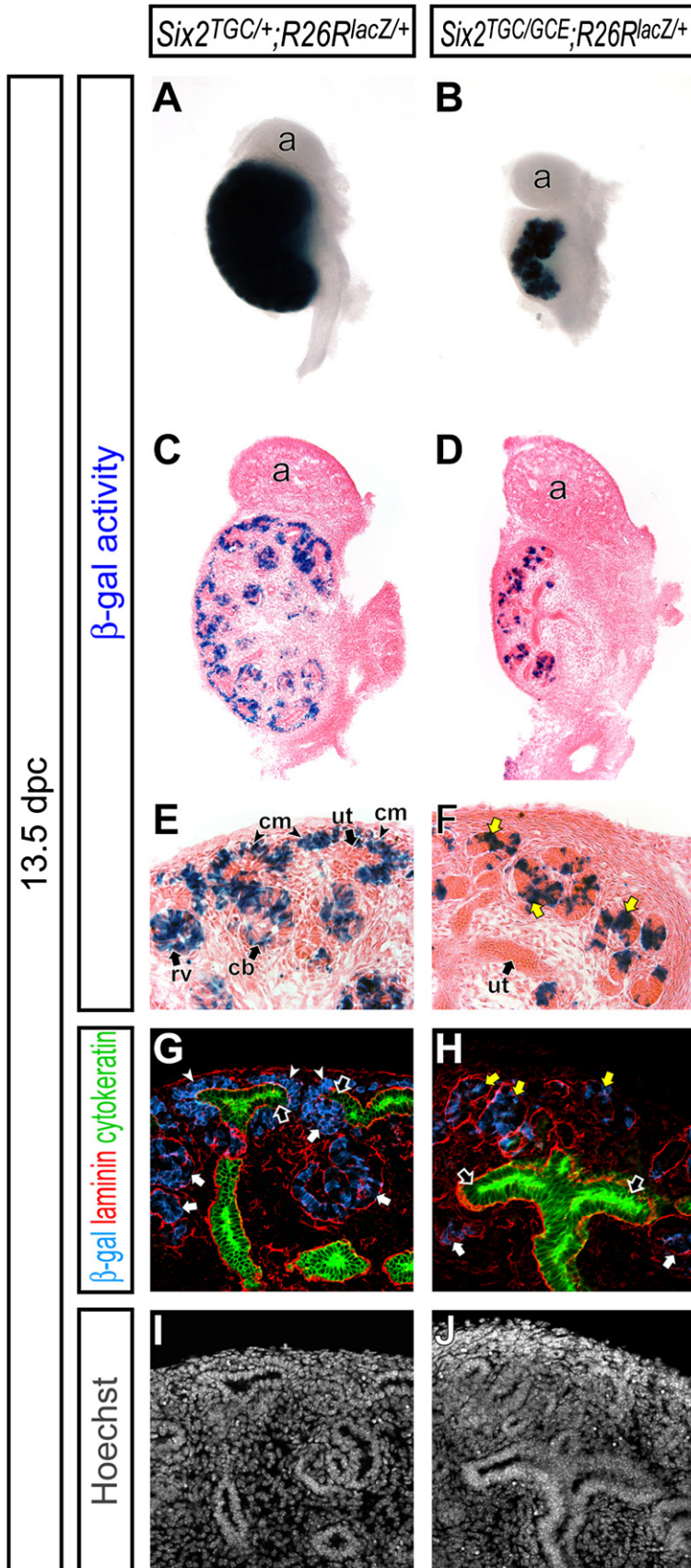
Figure 6. Ectopic Nephron Tubules Are Derived from the Cap Mesenchyme in *Six2* Null Kidneys

Kidneys from *Six2*$^{TGC/+}$; *R26R*$^{lacZ/+}$ (A,C,E,G,I) and *Six2*$^{TGC/GCE}$; *R26R*$^{lacZ/+}$ (B,D,F,H,J) embryos at 13.5 dpc.

(A and B) Whole-mount β-gal staining.

(C and D) β-gal-stained sections counterstained with eosin.

(E and F) Higher magnification of the cortical region in (C) and (D), respectively.

(G–J) Confocal immunofluorescence imaging of the cortical region with anti-β-gal (blue), anti-laminin (red), anti-cytokeratin (green), and Hoechst (gray) staining. Laminin is expressed strongly in the epithelium of the ureteric tip, collecting duct, and developing nephron tubule and weakly in the cap mesenchyme, while cytokeratin is expressed only in the ureteric tip and collecting duct. White arrows, yellow arrows, white arrowheads, and black arrows indicate the nephron tubule, ectopic nephron tubule, cap mesenchyme, and ureteric tip, respectively. a, adrenal gland; cb, comma-shaped body; cm, cap mesenchyme; rv, renal vesicle; ut, ureteric tip.
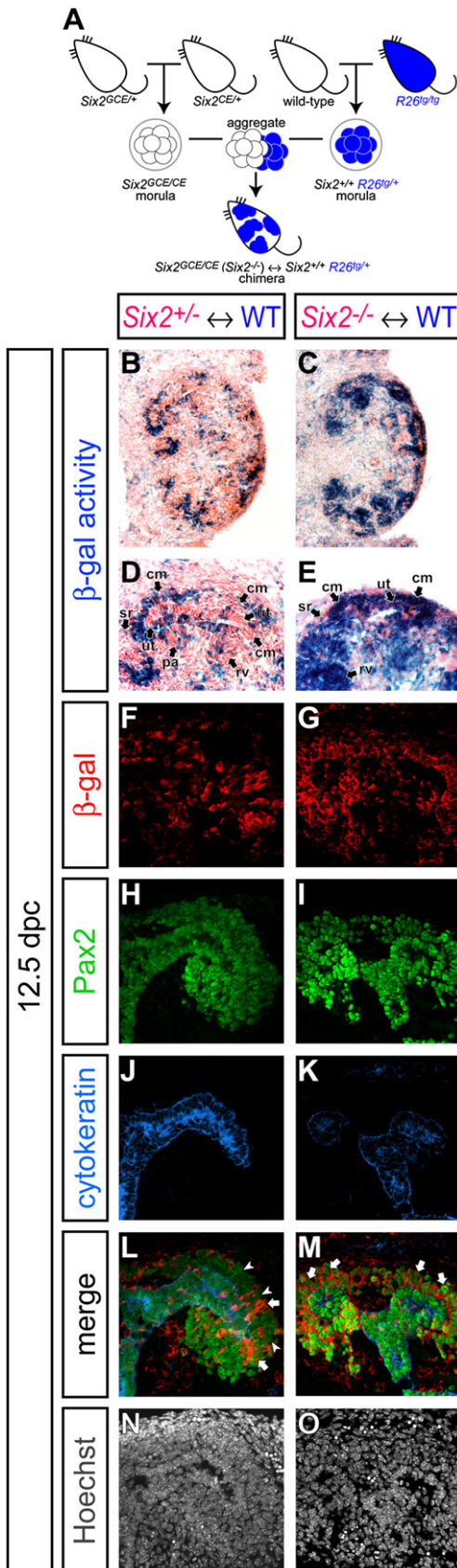
Figure 7. *Six2* Function Is Cell-Autonomously Required in the Cap Mesenchyme

(A) Schematic illustration of the strategy for *Six2* chimera analysis. To facilitate genotyping of chimeras, two different null alleles of *Six2*, *Six2-GCE* and *Six2-CE*, were crossed to generate $Six2^{GCE/CE}$ ($Six2^{-/-}$) morulae. To genetically label wild-type cells, $R26^{tg/+}$ morulae were collected and aggregated with $Six2^{-/-}$ morulae to generate $Six2^{-/-} \leftrightarrow Six2^{+/+} ; R26^{tg/+}$ chimeras. For a control, we used $Six2^{+/-} \leftrightarrow Six2^{+/+} ; R26^{tg/+}$ chimeras.

(B–O) Kidneys from $Six2^{+/-} \leftrightarrow Six2^{+/+} ; R26^{tg/+}$ (B, D, F, H, J, L, and N) and $Six2^{-/-} \leftrightarrow Six2^{+/+} ; R26^{tg/+}$ (C, E, G, I, K, M, and O) chimeras at 12.5 dpc. (B and C) Kidneys with β-gal staining counterstained with eosin. (D and E) Higher magnification of (B) and (C), respectively. (F–O) Confocal immunofluorescence imaging of the cortical region with anti-β-gal (red), anti-Pax2 (green), anti-cytokeratin (blue), and Hoechst (gray) staining. Pax2 is expressed in the ureteric tip, cap mesenchyme, and developing nephron tubule, while cytokeratin is expressed only in the ureteric tip. White arrows and arrowheads in (L) and (M) indicate β-gal+ Pax2+ and β-gal− Pax2+ cells in the cap mesenchyme, respectively. cm, cap mesenchyme; pa, pretubular aggregate; rv, renal vesicle; sr, stroma; ut, ureteric tip.

observed in 18 chimeras. As expected, when control chimeric animals ($Six2^{+/-} \leftrightarrow$ wild-type) were examined at 12.5 dpc, *Six2* heterozygous β-gal− cells contributed to all cell types in the kidney, including the cap mesenchyme, renal vesicle, and its derivatives (Figures 7B, 7D, 7F, 7H, 7J, 7L, and 7N). Surprisingly, in chimeric animals containing *Six2* null cells ($Six2^{-/-} \leftrightarrow$ wild-type), all kidneys examined were morphologically normal; no ectopic nephron structures were observed (Figures 7C and 7E). Interestingly, all cells within the Pax2+ cap mesenchyme and its epithelial nephron derivatives were β-gal+, indicating a wild-type genotype (Figures 7G, 7I, 7K, 7M, and 7O). In contrast, *Six2* null β-gal− cells contributed normally to all other cell populations in the early kidney (Figures 7C, 7E, 7G, 7I, 7K, 7M, and 7O). Thus, whereas *Six2* cell-autonomously is required to maintain nephron progenitors, in chimeras where *Six2* null cells are in close association with wild-type neighbors, no ectopic renal vesicles form.

Formation of Ectopic Tubules in *Six2* Null Mutants Requires *Wnt9b* Activity

Six2 may act by directly inhibiting the process of epithelial formation in mesenchymal progenitors or conversely by cell-autonomously inhibiting the response of these cells to Wnt9b, a signal that is required to induce renal vesicles within a subpopulation of the cap mesenchyme (Carroll et al., 2005). To understand the relationships between *Six2* and *Wnt9b*, we examined the phenotype of $Six2^{-/-} ; Wnt9b^{-/-}$ compound mutants. In $Wnt9b^{+/-}$ (phenotypically normal) and $Six2^{-/-}$ kidneys at 12.5 dpc, the histological appearance of renal vesicles provides a clear indication of nephron formation (Figures 8A and 8C). These laminin+ cytokeratin− structures were confined to the ventral (medullary) side of the laminin+ cytokeratin+ ureteric tips in $Wnt9b^{+/-}$ kidneys but appear also on the dorsal (cortical) side in $Six2^{-/-}$ kidneys (Figures 8E and 8G). In both $Wnt9b^{-/-}$ and $Six2^{-/-} ; Wnt9b^{-/-}$ kidneys at the same stage, no renal vesicle formation was observed, suggesting that ectopic renal vesicle formation in *Six2* null mutants is *Wnt9b* dependent (Figures 8B, 8D, 8F, and 8H).

To examine the inductive process further, we analyzed expression of the early inductive markers *Wnt4* and *Pax8* (Stark et al., 1994) at 11.5 dpc. At this stage, both *Wnt4* and *Pax8* are
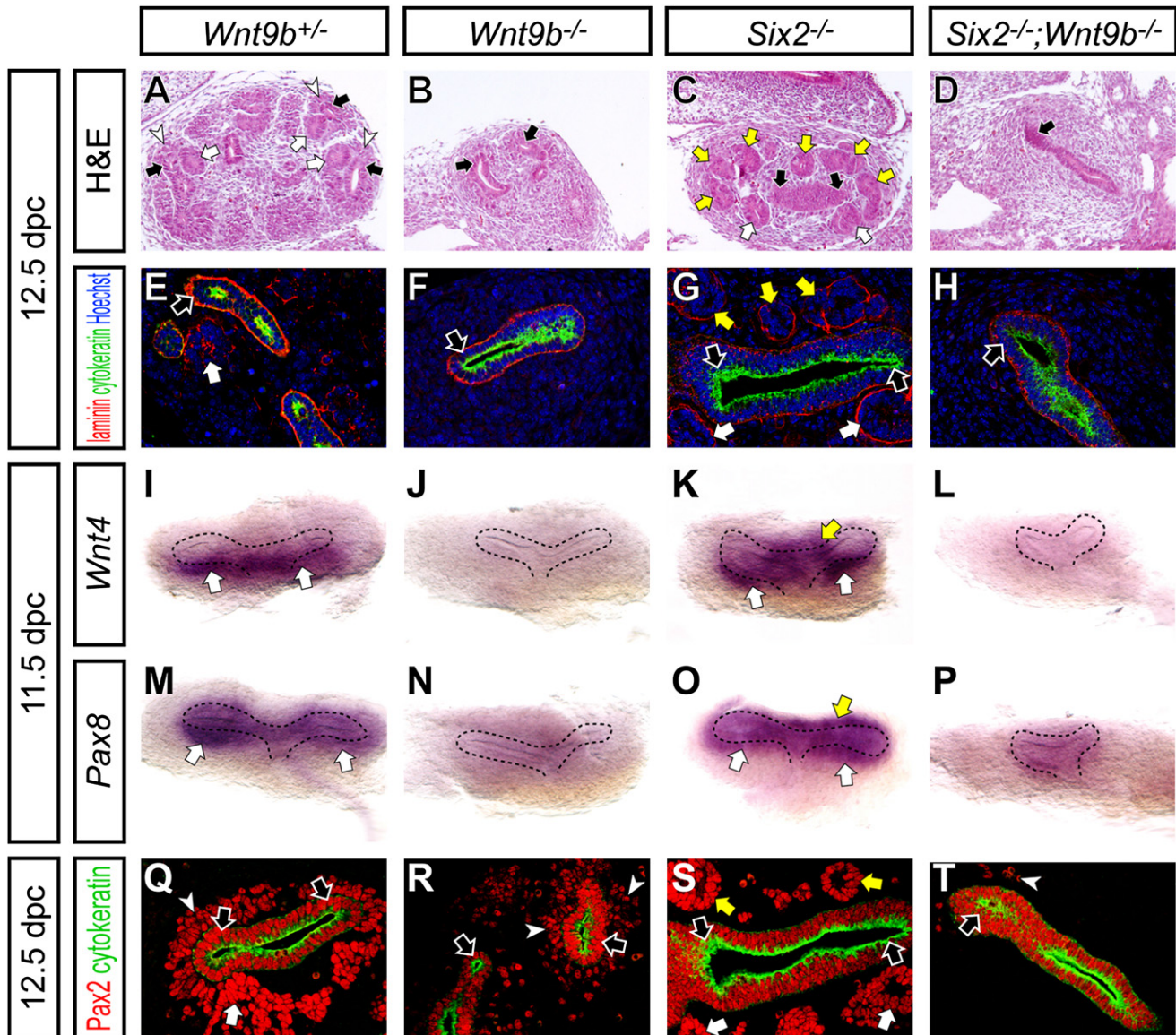
Figure 8. Absence of Nephron Induction in *Six2 ; Wnt9b* Compound Mutants

Kidneys from *Wnt9b*$^{+/-}$ (A, E, I, M, and Q), *Wnt9b*$^{-/-}$ (B, F, J, N, and R), *Six2*$^{-/-}$ (C, G, K, O, and S) and *Six2*$^{-/-}$ *; Wnt9b*$^{-/-}$ (D, H, L, P, and T) embryos at 12.5 dpc (A–H and Q–T) and 11.5 dpc (I–P) with dorsal to top and ventral to bottom.

(A–D) Hematoxylin and eosin staining.

(E–H) Confocal immunofluorescence imaging with anti-laminin (red), anti-cytokeratin (green), and Hoechst (blue) staining.

(I–P) Whole-mount in situ hybridization. (I–L) *Wnt4*. (M–P) *Pax8*. (Q–T) Confocal immunofluorescence imaging with anti-Pax2 (red) and anti-cytokeratin (green) staining. White arrows, yellow arrows, white arrowheads, and black arrows indicate the nephron precursor, ectopic nephron precursor, cap mesenchyme, and ureteric tip, respectively.

activated on the ventral side of the T-bud stage kidneys in initial pretubular aggregates in *Wnt9b*$^{+/-}$ kidneys (Figures 8I and 8M). Both are absent in *Wnt9b*$^{-/-}$ mutants and ectopically activated on the dorsal side of the ureteric bud in *Six2*$^{-/-}$ kidneys (Figures 8J, 8K, 8N, and 8O) (Carroll et al., 2005; Self et al., 2006). In contrast, no inductive response could be observed in *Six2*$^{-/-}$ *; Wnt9b*$^{-/-}$ compound mutants (Figures 8L and 8P).

Whereas this may indicate that ectopic renal vesicle formation in *Six2* mutants requires a direct Wnt9b signaling event, as in normal renal vesicle induction, analysis of the compound mu-

tants suggests additional interactions that may complicate the interpretation. In *Wnt9b*$^{-/-}$ and *Six2*$^{-/-}$ mutants, the timing of ingrowth of the ureteric bud was not markedly different from wild-type (Figures 8I–8K and 8M–8O). However, ingrowth was clearly retarded in *Six2*$^{-/-}$ *; Wnt9b*$^{-/-}$ compound mutants (Figures 8L and 8P). Further, we observed a dramatic reduction of the Pax2+ cap mesenchyme in the compound mutants, more severe than that of *Wnt9b*$^{-/-}$ mutants at 12.5 dpc (Figures 8Q–8T). *Pax2* and *Six2* are coexpressed within the cap mesenchyme renal progenitor (Self et al., 2006), indicating that the renal vesicle-forming

compartment is depleted. Thus, a reduction in this population may influence the observed phenotype.

DISCUSSION

Cellular Dynamics, Progenitor Maintenance, and Cell Fate Specification within the Mammalian Nephron Progenitor Pool

The mammalian kidney undergoes an unusually dynamic developmental program. In this, multiple epithelial nephron precursors, renal vesicles, arise from a mesenchymal progenitor population in response to reiterative inductive signaling mediated by the tips of a branching, epithelial, ureteric network. *Six2+* cells are present within the mesenchymal pools of the kidney anlagen at 10.5 dpc prior to invasion of the inductive ureteric bud, and *Six2+* cells are retained within mesenchyme closely apposed to the branching bud tips until kidney development ceases in the early postnatal animal (Hartman et al., 2007; Oliver et al., 1995). We have used genetic cell fate analysis to examine the contributions of *Six2+* cells to mammalian nephrogenesis. These experiments indicate that *Six2+* cells are nephron progenitors throughout the extended period of nephrogenesis in the mouse. Moreover, the *Six2+* subpopulation of mesenchymal cells is restricted to nephron-forming cell fates. No contribution is seen to other regions of the kidney, and no evidence is observed in this model for an ongoing recruitment of this mesenchymal population to the ureteric epithelium (Herzlinger et al., 1992; Qiao et al., 1995). *Six2*-mediated labeling of adult nephron structures provides new opportunity for the study of kidney regulation. A recent analysis demonstrates that nephron repair in the adult occurs through an intratubular mechanism (Humphreys et al., 2008).

Our results from this analysis are in general agreement with recent cell-fate studies of Boyle et al., (2007) with a different molecular marker, *Cited1*. However, unlike *Six2*, *Cited1* is not expressed in the cap mesenchyme until some days after activation of *Six2*, when nephrogenesis has commenced. Once activated, *Cited1* is reported to substantially overlap the *Six2+* population (Boyle et al., 2007). Thus, *Six2*, but not *Cited1*, marks the nephron progenitor population throughout nephrogenesis.

At the outset of kidney development, approximately 10,000 *Six2+* cells surround a single branch of the prospective ureteric epithelium of the T-bud stage kidney. Each adult mouse kidney comprises approximately 13,000 nephrons (Cullen-McEwen et al., 2003; He et al., 1996), and based on glomerular counts, 8000 are present by 19.5 dpc (Cebrian et al., 2004). As each nephron arises from a multicellular aggregate of *Six2+* cells, the starting *Six2+* population is clearly inadequate for the formation of the full complement of nephrons. Further, direct measurement of *Six2+* cells at 19.5 dpc indicates a 16-fold expansion of the *Six2+* population even though several thousand renal vesicles have formed during the intervening developmental period. At this time, 180,000 *Six2+* cells surround ~1500 branches of the ureteric tip (data herein and Cebrian et al. [2004]). Thus, the *Six2+* pool undergoes a significant expansion in conjunction with the nephrogenic process. This raises the important question of whether the *Six2+* progenitor pool allocated at the onset of nephrogenesis, 11.5 dpc, maintains itself or whether *Six2+* cells are replenished from another *Six2−* cell type.

While our studies cannot rule out a minor role for the latter mechanism, they provide strong support for the former. When a fraction of the *Six2+* progenitor pool is indelibly labeled at the initiation of nephrogenesis (by 11.5 dpc), many of these maintain their progenitor status 8 days later at 19.5 dpc, a few days before nephrogenesis terminates. *Six2+* cells transition to a *Six2− Wnt4+* pretubular aggregate prior to renal vesicle formation. Unlike *Six2+* cells, when *Wnt4*-expressing cells are similarly pulse labeled, *Wnt4* descendants are chased into mature epithelial structures of the nephron over a shorter time course. Thus, self-renewal is restricted within the *Six2+* pool and lost on induction. Importantly, these experiments, while indicating that *Six2+* cells undergo self-renewal, cannot determine whether all *Six2+* cells are equivalent in this ability; self-renewal may be a property restricted to a subset of the population (see below).

An argument for self-renewal of nephron precursors has recently been promoted on the basis of *Cited1*-based cell-labeling studies (Boyle et al., 2007). Though the conclusions reached in these studies agree with our own, they provide a less compelling case. First, the postpulse chase period was considerably shorter, as activity of the *Cited1* transgene was not detected until 13.5 dpc and kidneys were examined at 19.5 dpc. Second, the pulse-labeling period was less restricted. CreER[T2] was nuclear at 24 hr after induction, indicating that Cre activity was ongoing at this time. Thus, while the precise period of Cre activity was not determined, it is clear that the labeling is likely to have occurred over a longer time window than within the *Six2* experiments herein.

The *Six2+* Pool Contains Multipotent Nephron Progenitors

On the basis of clonal analysis in vitro and ex vivo, it was suggested that individual nephron progenitors are multipotent in their capacity to generate distinct regions of the nephron (Herzlinger et al., 1992; Osafune et al., 2006). The analysis of *Six2+* cell fates following low-dose tamoxifen induction in the current study provides additional evidence in support of this conclusion in vivo and defines the population of multipotent nephron progenitor cells to the *Six2+* cap mesenchyme. The appearance of a small number of labeled cell clusters per kidney is consistent with, and indicative of, a clonal level of labeling. These clusters spanned several regions of developing nephrons where distinct regional programs of cell fate specification are underway. Notably, descendants of a *Six2+* cell can be found within molecularly distinct compartments of a single nephron: podocytes, proximal and distal tubule structures. Though these experiments argue that at least some *Six2+* cells are multipotent, they do not address whether this is a general property of the population nor when restriction occurs in the nephron-forming lineage. For example, a clonally labeled multipotent *Six2+* cell may give rise to multiple labeled cells within the mesenchymal nephron progenitor compartment, and these labeled descendants may undergo subsequent restrictions to distinct nephron compartments prior to induction. Indeed, multiple labeled cells can be observed within a *Six2+* cap mesenchymal population, presumably all clonal descendants from a single cell-labeling event. Clonal labeling with *Wnt4-GCE* may resolve this issue. Importantly, the presence of multiple labeled progenitor cells lends additional evidence in favor of self-renewal and suggests that some *Six2+* cells may have

a greater self-renewal capacity than others. The simplest model for nephron patterning, multipotent precursors and regional specific patterning after renal vesicle formation (Herzlinger et al., 1992), is suggested by recent studies of Notch-based signaling in which Notch action proximalizes developing epithelial renal vesicle derivatives (Cheng et al., 2003, 2007; Wang et al., 2003).

Six2 Functions in the Maintenance of Multipotent Nephron Progenitor Cells in the Cap Mesenchyme

Our studies provide new insights into the function of *Six2* and more generally the regulation of the inductive process. Cell-fate analysis in *Six2* mutants indicates that *Six2* is cell autonomously required to prevent premature, appositional renal vesicle formation. However, while we observe this phenotype in *Six2* mutants, we are unable to detect ectopic renal vesicle structures in chimeras consisting of *Six2* mutant and wild-type embryos, nor of contribution of *Six2* mutant cells to normal tubulogenesis. Rather, mutant cells are apparently rapidly lost from the mesenchymal progenitor pool.

There are a number of possible explanations for these different outcomes. For example, formation of a renal vesicle may depend on local induction of a critical number of cells. In the chimera model, the scattering and interspersion of mutant and wild-type cells may prevent the establishment of a critical tubule-forming cell mass. A rapid process of cell removal must follow such that *Six2* mutant cells are undetectable by 12.5 dpc in the cap mesenchyme compartment. Wild-type and mutant cells may also compete for a limiting factor that may promote the propagation of wild-type cells at the expense of mutant cells, leading to rapid depletion of the latter and a failure to contribute to epithelial nephron derivatives. Recent work in *Drosophila* imaginal disc has demonstrated that local cell competition can trigger apoptosis in growth-defective mutants (Moreno et al., 2002).

Wnt9b secreted by the ureteric bud provides a primary inductive signal that initiates nephrogenesis in adjacent nephron progenitors through the canonical Wnt signaling pathway (Carroll et al., 2005; Park et al., 2007). Given that *Six2*+ cells define the nephron progenitor compartment, it follows that the *Six2* population is the likely target of Wnt9b-mediated inductive signaling. *Six2* mutants and *Wnt9b* mutants have opposite phenotypes. In one simple model, *Six2* acts to inhibit a Wnt response within a subset of the *Six2* progenitor pool, maintaining a nephron progenitor pool for additional rounds of nephrogenesis. Our demonstration that compound mutants lack renal vesicles and earlier molecular features of the Wnt9b-inductive response, normally observed in emerging pretubular aggregates, supports this model. However, the resulting phenotypes suggest that this view is likely too simple. In addition to observing a failure of nephrogenesis, compound mutants exhibit reduced survival of the nephron precursor compartment and, likely as a secondary consequence of a loss of signals from this population (notably the branch-growth regulator GDNF) (Costantini and Shakya, 2006), delayed and reduced ingrowth of the ureteric bud.

These observations suggest additional interactions between *Six2* and *Wnt9b*. For example, *Six2* may oppose an inductive Wnt9b signal. However, *Wnt9b* and *Six2* may also act cooperatively to maintain the nephron progenitor pool. The distinct outcomes to Wnt9b signaling may reflect different levels of Wnt signaling—low levels promoting maintenance of *Six2*+ cells and high levels induction, *Six2* providing a tonic level of inhibition to regu-

late the response. Here it is interesting to note lower levels of *Wnt9b* expression in ureteric epithelium underlying the *Six2*+ population compared with ureteric epithelium immediately beneath the branch tip (Carroll et al., 2005) where *Wnt4/Pax8* inductive markers are first observed in *Six2* descendant cells. Alternatively, *Wnt9b* may act in promoting both maintenance and induction of *Six2* cells, the actions of other signals determining the specific outcome to a *Wnt9b* input. Here, several signaling factors have been reported to promote either survival/proliferation of metanephric mesenchyme including Bmp7 (Dudley et al., 1995; Luo et al., 1995), FGF2 (bFGF) (Barasch et al., 1997; Dudley et al., 1999), and TIMP2 (Barasch et al., 1999a) or renal vesicle induction including Wnt4 (Stark et al., 1994), FGF2 (Perantoni et al., 1995), LIF (Barasch et al., 1999b), and TGFβ2 (Plisov et al., 2001).

EXPERIMENTAL PROCEDURES

Mouse Strains

The *Tet-off-eGFPCre-Kan* (*TGC-Kan*) targeting cassette for the *Six2* BAC transgenic allele was generated as follows. A Tet-off cassette (*tTA-2 × pA-tet₀-CMV_min*) was generated by removing *loxP-TKneo-URA-loxP* from mtTAFFF (Bond et al., 2000). The Tet-off construct was combined with *eGFPCre* from pBS592 (Le et al., 1999) and *FRT-Kan-FRT* from pICGN21 (Lee et al., 2001). After adding homologous arms by PCR, the resulting *TGC-Kan* targeting construct was introduced by RED cloning system (Lee et al., 2001) into a mouse BAC clone RPCI23-311C1, which contains the *Six2* locus in the middle of the clone. After screening for correctly recombined clones and removal of the kanamycin selection cassette, the *Six2-TGC* BAC clone was introduced into CD-1 zygotes (Charles River Laboratories) by pronuclear injection (Nagy et al., 2003) to generate transgenic mice. Three founders were generated, and one line exhibited the expected *Six2* expression pattern, though the transgene did not respond to doxycycline. The *Six2-TGC* BAC transgenic was maintained on a CD-1 × Swiss Webster (Taconic) × C57BL/6J (Jackson Laboratory) mixed background.

For *Six2-Cre* knockin alleles, *Six2* targeting vectors were generated with sequence-confirmed homologous arms subcloned by PCR from a BAC clone RPCI23-311C1. The *Six2* initiation codon was replaced by *Tet-off-eGFPCre* (*TGC*), *CreER^T2* (*CE*) (Indra2 et al., 1999), or *eGFPCreER^T2* (*GCE*) constructs followed by an FRT-PGKneobpA-FRT selection cassette. The *eGFPCreER^T2* fusion construct was generated by combining *eGFPCre* from pBS592 (Le et al., 1999) and *CreER^T2* from pCre-ER(AA2) (Feil et al., 1997) constructs. After addition of *MC1-TK* for negative selection, the resulting targeting vectors were introduced by gene targeting (Nagy et al., 2003) into 129/Sv × C57BL/6J F1 hybrid ES cells (Eggan et al., 2001). After G418 and FIAU selection, ES cell colonies were isolated and screened by PCR using both 5′ and 3′ external primers. Chimeric mice were generated by injection of correctly targeted ES cells into C57BL/6J blastocysts. *Six2^TGC/+*, *Six2^CE/+*, and *Six2^GCE/+* mouse lines were maintained on a 129/Sv × C57BL/6J mixed background. The *Wnt4-GCE* allele was generated in a similar way to that of the *Six2-GCE* allele, except a BAC clone RPCI23-246F18 containing the *Wnt4* locus was used.

Six2-Cre alleles were genotyped using the following primers: Cre-Fw1, GGACATGTTCAGGGATCGCCAGGC; Cre-Rv2, CGACGATGAAGCATGTTTAGCTG; mSix2-Fw35, CCACCTTCGGCTTCACGCAGGAGCAAGT; and mSix2-Rv36, CCGCGCAGCTTCTCCGCCTCGATGTAGT, which give a 219 bp band for the *Six2-Cre* alleles (Cre-Fw1 and Cre-Rv2) and a 286 bp band for the *Six2* wild-type allele (mSix2-Fw35 and mSix2-Rv36). The *Wnt4-GCE* allele was genotyped using the following primers: Cre-Fw1, Cre-Rv2, and mWnt4-Fw56, GCCGCCGCGAGCAATTGGCTGTAAGT; and mWnt4-Rv57; GGACGC TTTCCCTCGGGAGACCTGTCA, which give a 219 bp band for the *Wnt4-GCE* allele (Cre-Fw1 and Cre-Rv2) and a 350 bp band for the *Wnt4* wild-type allele (mWnt4-Fw56 and mWnt4-Rv57).

R26R-lacZ Cre reporter (Soriano, 1999) and *R26^tg/tg* *lacZ*-transgene integrated (Friedrich and Soriano, 1991) mice were purchased from Jackson Laboratory and maintained on a C57BL/6J × Swiss Webster mixed and 129/Sv inbred backgrounds, respectively. *R26R-lacZ* mice were genotyped using the

following primers: R26-Fw11, CTCCCAAAGTCGCTCTGAGTTGTTATCAGT; R26-Rv12, CTCGGGTGAGCATGTCTTTAATCTACCT; and pBT-Rv2, GCGAA GAGTTTGTCCTCAACCGCGAGCTGT, which give a 484 bp band for the *R26* wild-type allele (R26-Fw11 and R26-Rv12) and a 320 bp band for *R26R-lacZ* knockin allele (R26-Fw11 and pBT-Rv2).

$Six2^{+/−}$; $Wnt9b^{+/−}$ mice were maintained on a 129/Sv × C57BL/6J × NMRI mixed background and intercrossed to obtain *Six2 ; Wnt9b* compound null mutants (Carroll et al., 2005; Self et al., 2006). Littermates were used for controls. Mice were bred using timed matings, noon on the day of vaginal plug detection considered 0.5 dpc. For induction of the eGFPCreER^{T2} protein, tamoxifen (Sigma, T5648) was dissolved in corn oil (Sigma, C8267) and administrated by intraperitioneal (IP) injection (Danielian et al., 1998).

FACS Analysis

Kidneys from $Six2^{GCE/+}$ mice were dissected and treated in 300 μl Trypsin (Invitrogen, 25200-072) at 37°C for 3–5 min. After adding 600 μl DMEM media (Invitrogen, 11965) containing 10% sheep serum (Sigma, S2263), a single cell suspension was prepared by pipetting. Cells were collected by centrifugation and resuspended in 100 μl of PBS (Mediatech, 21-031-CV) containing 2% sheep serum. FACS analysis was performed using DAKO Cytomation MoFlo.

Chimera Analysis

$Six2^{CE/GCE}$ morulae were aggregated with $Six2^{+/+}$; $R26^{tg/+}$ morulae. After overnight incubation, chimeric embryos were transferred to the uterus of pseudopregnant Swiss Webster females (Nagy et al., 2003). Chimeras were genotyped using the following primers: CE-Fw1, AGTCTTAAGAAGCTTGAATTCCA CCA; XFP-Fw5, CCGTGCTGCTGCCCGACAACCACTA; and Cre-Rv2, CGAC GATGAAGCATGTTTAGCTG, which give a 327 bp band for the *CE* allele (CE-Fw1 and Cre-Rv2) and a 496 bp band for the *GCE* allele (XFP-Fw5 and Cre-Rv2). A total of 18 chimeras were analyzed.

Histology

Dissected kidneys were fixed in 4% paraformaldehyde for 1 hr at 4°C and soaked in 30% sucrose overnight at 4°C. After embedding in OCT (Sakura, 4583), cryosections were generated at 16 μm using a Microm HM 550 cryostat.

β-Gal Staining

β-gal staining was performed as described previously (Nagy et al., 2003). Cryosections were stained with X-gal at 37°C overnight and counterstained with 0.2% Eosin-Y (Polysciences Inc.) or Nuclear Fast Red (Sigma, #N3020). Whole-mount kidneys were fixed in 4% paraformaldehyde for 1 hr at 4°C and stained at 37°C overnight for embryonic samples or at 4°C for 2–3 days for neonate samples.

Immunofluorescence

To generate a Six2 antibody, rabbits were immunized with a KHL-conjugated peptide SEDEKTPSGTPDHSS corresponding to amino acids 241–255 of the mouse Six2 protein sequence, and antiserum was affinity purified against immobilized Six2 peptide (Covance Research Products). The purified antiserum was tested by immunostaining of transiently transfecting (Lipofectamine 2000, Invitrogen) COS7 cells with a mouse *Six2* expression plasmid. Immunostaining on cryosections matched the expected *Six2* mRNA expression pattern in metanephric kidneys at 15.5 dpc.

Sections were incubated with primary antibodies to anti-Wt1 (Santa Cruz, sc-192), anti-Flk1 (PharMingen, 555307), anti-PECAM-1 (anti-CD31, BD PharMingen, 553370), anti-PDGFRb (eBiosciences, 14-1402-82), anti-uromodulin (anti-Tamm-Horsfall glycoprotein, Biomedical Technologies Inc., BT-590), anti-SMA (Sigma, A5228), anti-Pax2 (Covance, PRB-276P), anti-GFP (Aves labs, GFP-1020), anti-β-gal (Cappel, #55976; Abcam, ab9361), anti-cytokeratin (Sigma, C2562), anti-laminin (Sigma, L9393), and LTL-lectin (Vector Laboratories, FL-1321) and detected by the secondary antibodies with Cy2, Cy3, and Cy5 (Jackson ImmunoResearch Laboratories) or Alexa Fluor 488, 568, 633, and 647 (Invitrogen). Sections were stained with Hoechst (Invitrogen, H3570) prior to mounting with Vectashield Mounting Medium (Vector labs, H-1000). Fluorescent images were photographed on a Zeiss LSM510 Axioplan inverted confocal microscope.

Whole-Mount In Situ Hybridization

Whole-mount in situ hybridization was performed as previously described (Carroll et al., 2005; Wilkinson et al., 1987).

SUPPLEMENTAL DATA

The Supplemental Data include three figures and can be found with this article online at http://www.cellstemcell.com/cgi/content/full/3/2/169/DC1/.

REFERENCES

Barasch, J., Qiao, J., McWilliams, G., Chen, D., Oliver, J.A., and Herzlinger, D. (1997). Ureteric bud cells secrete multiple factors, including bFGF, which rescue renal progenitors from apoptosis. Am. J. Physiol. *273*, F757–F767.

Barasch, J., Yang, J., Qiao, J., Tempst, P., Erdjument-Bromage, H., Leung, W., and Oliver, J.A. (1999a). Tissue inhibitor of metalloproteinase-2 stimulates mesenchymal growth and regulates epithelial branching during morphogenesis of the rat metanephros. J. Clin. Invest. *103*, 1299–1307.

Barasch, J., Yang, J., Ware, C., Taga, T., Yoshida, K., Erdjument-Bromage, H., Tempst, P., Parravicini, E., Malach, S., Aranoff, T., et al. (1999b). Mesenchymal to epithelial conversion in rat metanephros is induced by LIF. Cell *99*, 377–386.

Bond, C.T., Sprengel, R., Bissonnette, J.M., Kaufmann, W.A., Pribnow, D., Neelands, T., Storck, T., Baetscher, M., Jerecic, J., Maylie, J., et al. (2000). Respiration and parturition affected by conditional overexpression of the Ca2+-activated K+ channel subunit, SK3. Science *289*, 1942–1946.

Boyle, S., Misfeldt, A., Chandler, K.J., Deal, K.K., Southard-Smith, E.M., Mortlock, D.P., Baldwin, H.S., and de Caestecker, M. (2007). Fate mapping using Cited1-CreERT2 mice demonstrates that the cap mesenchyme contains self-renewing progenitor cells and gives rise exclusively to nephronic epithelia. Dev. Biol. *313*, 234–245.

Carroll, T., Park, J., Hayashi, S., Majumdar, A., and McMahon, A. (2005). Wnt9b plays a central role in the regulation of mesenchymal to epithelial transitions underlying organogenesis of the mammalian urogenital system. Dev. Cell *9*, 283–292.

Cebrian, C., Borodo, K., Charles, N., and Herzlinger, D.A. (2004). Morphometric index of the developing murine kidney. Dev. Dyn. *231*, 601–608.

Cheng, H.T., Miner, J.H., Lin, M., Tansey, M.G., Roth, K., and Kopan, R. (2003). Gamma-secretase activity is dispensable for mesenchyme-to-epithelium transition but required for podocyte and proximal tubule formation in developing mouse kidney. Development *130*, 5031–5042.

Cheng, H., Kim, M., Valerius, M., Surendran, K., Schuster-Gossler, K., Gossler, A., McMahon, A., and Kopan, R. (2007). Notch2, but not Notch1, is required for proximal fate acquisition in the mammalian nephron. Development *134*, 801–811.

Costantini, F. (2006). Renal branching morphogenesis: concepts, questions, and recent advances. Differentiation *74*, 402–421.

Costantini, F., and Shakya, R. (2006). GDNF/Ret signaling and the development of the kidney. Bioessays *28*, 117–127.

Cullen-McEwen, L.A., Kett, M.M., Dowling, J., Anderson, W.P., and Bertram, J.F. (2003). Nephron number, renal function, and arterial pressure in aged GDNF heterozygous mice. Hypertension 41, 335–340.

Danielian, P.S., Muccino, D., Rowitch, D.H., Michael, S.K., and McMahon, A.P. (1998). Modification of gene activity in mouse embryos in utero by a tamoxifen-inducible form of Cre recombinase. Curr. Biol. 8, 1323–1326.

Dressler, G.R. (2006). The cellular basis of kidney development. Annu. Rev. Cell Dev. Biol. 22, 509–529.

Dudley, A.T., Lyons, K.M., and Robertson, E.J. (1995). A requirement for bone morphogenetic protein-7 during development of the mammalian kidney and eye. Genes Dev. 9, 2795–2807.

Dudley, A.T., Godin, R.E., and Robertson, E.J. (1999). Interaction between FGF and BMP signaling pathways regulates development of metanephric mesenchyme. Genes Dev. 13, 1601–1613.

Eggan, K., Akutsu, H., Loring, J., Jackson-Grusby, L., Klemm, M., Rideout, W., Yanagimachi, R., and Jaenisch, R. (2001). Hybrid vigor, fetal overgrowth, and viability of mice derived by nuclear cloning and tetraploid embryo complementation. Proc. Natl. Acad. Sci. USA 98, 6209–6214.

Feil, R., Wagner, J., Metzger, D., and Chambon, P. (1997). Regulation of Cre recombinase activity by mutated estrogen receptor ligand-binding domains. Biochem. Biophys. Res. Commun. 237, 752–757.

Friedrich, G., and Soriano, P. (1991). Promoter traps in embryonic stem cells: a genetic screen to identify and mutate developmental genes in mice. Genes Dev. 5, 1513–1523.

Hartman, H., Lai, H., and Patterson, L. (2007). Cessation of renal morphogenesis in mice. Dev. Biol. 310, 379–387.

He, C., Esposito, C., Phillips, C., Zalups, R.K., Henderson, D.A., Striker, G.E., and Striker, L.J. (1996). Dissociation of glomerular hypertrophy, cell proliferation, and glomerulosclerosis in mouse strains heterozygous for a mutation (Os) which induces a 50% reduction in nephron number. J. Clin. Invest. 97, 1242–1249.

Herzlinger, D., Koseki, C., Mikawa, T., and al-Awqati, Q. (1992). Metanephric mesenchyme contains multipotent stem cells whose fate is restricted after induction. Development 114, 565–572.

Humphreys, B., Valerius, M.T., Kobayashi, A., Mugford, J.W., Soeung, S., Duffield, J.S., McMahon, A.P., and Bonventre, J.V. (2008). Intrinsic epithelial cells repair the kidney after injury. Cell Stem Cell 2, 284–291.

Indra, A.K., Warot, X., Brocard, J., Bornert, J.M., Xiao, J.H., Chambon, P., and Metzger, D. (1999). Temporally-controlled site-specific mutagenesis in the basal layer of the epidermis: comparison of the recombinase activity of the tamoxifen-inducible Cre-ER(T) and Cre-ER(T2) recombinases. Nucleic Acids Res. 27, 4324–4327.

Le, Y., Miller, J.L., and Sauer, B. (1999). GFPcre fusion vectors with enhanced expression. Anal. Biochem. 270, 334–336.

Lee, E.C., Yu, D., Martinez de Velasco, J., Tessarollo, L., Swing, D.A., Court, D.L., Jenkins, N.A., and Copeland, N.G. (2001). A highly efficient Escherichia coli-based chromosome engineering system adapted for recombinogenic targeting and subcloning of BAC DNA. Genomics 73, 56–65.

Luo, G., Hofmann, C., Bronckers, A.L., Sohocki, M., Bradley, A., and Karsenty, G. (1995). BMP-7 is an inducer of nephrogenesis, and is also required for eye development and skeletal patterning. Genes Dev. 9, 2808–2820.

Moreno, E., Basler, K., and Morata, G. (2002). Cells compete for decapentaplegic survival factor to prevent apoptosis in Drosophila wing development. Nature 416, 755–759.

Nagy, A., Gertsenstein, M., Vintersten, K., and Behringer, R.R. (2003). Manipulating the Mouse Embryo: A Laboratory Manual, Third Edition (Cold Spring Harbor, NY: Cold Spring Harbor Laboratory Press).

Oliver, G., Wehr, R., Jenkins, N.A., Copeland, N.G., Cheyette, B.N., Hartenstein, V., Zipursky, S.L., and Gruss, P. (1995). Homeobox genes and connective tissue patterning. Development 121, 693–705.

Osafune, K., Takasato, M., Kispert, A., Asashima, M., and Nishinakamura, R. (2006). Identification of multipotent progenitors in the embryonic mouse kidney by a novel colony-forming assay. Development 133, 151–161.

Park, J., Valerius, M., and McMahon, A. (2007). Wnt/{beta}-catenin signaling regulates nephron induction during mouse kidney development. Development 134, 2533–2539.

Perantoni, A.O., Dove, L.F., and Karavanova, I. (1995). Basic fibroblast growth factor can mediate the early inductive events in renal development. Proc. Natl. Acad. Sci. USA 92, 4696–4700.

Plisov, S.Y., Yoshino, K., Dove, L.F., Higinbotham, K.G., Rubin, J.S., and Perantoni, A.O. (2001). TGF beta 2, LIF and FGF2 cooperate to induce nephrogenesis. Development 128, 1045–1057.

Qiao, J., Cohen, D., and Herzlinger, D. (1995). The metanephric blastema differentiates into collecting system and nephron epithelia in vitro. Development 121, 3207–3214.

Reggiani, L., Raciti, D., Airik, R., Kispert, A., and Brändli, A. (2007). The pre-pattern transcription factor Irx3 directs nephron segment identity. Genes Dev. 21, 2358–2370.

Rodda, S.J., and McMahon, A.P. (2006). Distinct roles for Hedgehog and canonical Wnt signaling in specification, differentiation and maintenance of osteoblast progenitors. Development 133, 3231–3244.

Saxen, L. (1987). Organogenesis of the Kidney (New York: Cambridge University Press).

Schedl, A. (2007). Renal abnormalities and their developmental origin. Nat. Rev. Genet. 8, 791–802.

Self, M., Lagutin, O., Bowling, B., Hendrix, J., Cai, Y., Dressler, G., and Oliver, G. (2006). Six2 is required for suppression of nephrogenesis and progenitor renewal in the developing kidney. EMBO J. 25, 5214–5228.

Soriano, P. (1999). Generalized lacZ expression with the ROSA26 Cre reporter strain. Nat. Genet. 21, 70–71.

Stark, K., Vainio, S., Vassileva, G., and McMahon, A.P. (1994). Epithelial transformation of metanephric mesenchyme in the developing kidney regulated by Wnt-4. Nature 372, 679–683.

Wang, P., Pereira, F.A., Beasley, D., and Zheng, H. (2003). Presenilins are required for the formation of comma- and S-shaped bodies during nephrogenesis. Development 130, 5019–5029.

Wilkinson, D.G., Bailes, J.A., and McMahon, A.P. (1987). Expression of the proto-oncogene int-1 is restricted to specific neural cells in the developing mouse embryo. Cell 50, 79–88.

Wingert, R.A., Selleck, R., Yu, J., Song, H.D., Chen, Z., Song, A., Zhou, Y., Thisse, B., Thisse, C., McMahon, A.P., et al. (2007). The cdx genes and retinoic acid control the positioning and segmentation of the zebrafish pronephros. PLoS Genet. 3, 1922–1938. 10.1371/journal.pgen.0030189.

Chapter 4

Six2 activity is required for the formation of the pyloric sphincter during mouse stomach development

Self M and Oliver G.

Manuscript in preparation

Six2 activity is required for the formation of the pyloric sphincter during mouse stomach development

Michelle Self and Guillermo Oliver[*]

Department of Genetics and Tumor Cell Biology, St. Jude Children's Research Hospital, Memphis, Tennessee, 38105-2794

[*]Correspondence: guillermo.oliver@stjude.org

ABSTRACT

The functional activity of *Six2*, a member of the *so/Six* family of homeodomain-containing transcription factors, is required during mammalian kidney organogenesis. We have now determined that *Six2* activity is also necessary for the formation of the pyloric sphincter, the functional gate at the stomach-duodenum junction that inhibits duodenogastric reflux. Our data reveal that several genes known to be important for pyloric sphincter formation in the chick (e.g., *Bmp4, Bmpr1b, Nkx2.5*, *Sox9*, and *Gremlin*) also appear to be required for the formation of this structure in mammals. Thus, we propose that *Six2* activity regulates this gene network during the genesis of the pyloric sphincter in the mouse.

Keywords: Six2,   pyloric   sphincter,   stomach   development,   mouse

INTRODUCTION

The function of the vertebrate digestive system is to ingest food into the body, digest and absorb nutrients from the food, and excrete waste products. The gut develops soon after gastrulation as a simple tube of endoderm encircled by splanchnic mesoderm (Hogan, 2002; Lawson et al., 1986; Roberts, 2000). Beginning at mouse embryonic day (E) 8.5, the gut tube is patterned on the anterior-posterior (A-P), dorsal-ventral, left-right, and radial axes by reciprocal mesenchymal-epithelial interactions (Franklin et al., 2008; Lawson et al., 1986; Levin, 1997; Lowe et al., 1996; Lyons et al., 1995b; Mendelsohn, 2006; Roberts, 2000; Ryan et al., 1998; Sukegawa et al., 2000). Along the A-P axis, endodermally derived signals pattern the tube into distinct regions including the foregut, which will give rise to the esophagus, liver, lungs, pancreas, and stomach; the midgut, which will form the small intestine (SI); and the hindgut, which is the precursor to the large intestine (Aufderheide and Ekblom, 1988; Duluc et al., 1994; Haffen et al., 1987; Lawson et al., 1986; Roberts, 2000; Wells and Melton, 1999; Yasugi, 1993). The A-P patterning of the gut tube into organ primordia is evident by E10.5, as indicated by the spatially restricted expression of different transcription factors and signaling molecules that participate in mesenchymal-epithelial interactions (Aufderheide and Ekblom, 1988; Kedinger et al., 1990; Lyons et al., 1995b; Roberts, 2000; Wells and Melton, 1999; Yasugi, 1993). Shh and Bmp signaling pathways, as well as Hox transcription factors, participate in these mesenchymal-epithelial interactions (Beck et al., 2000; Grapin-Botton and Melton, 2000; Litingtung et al., 1998; Marigo et al., 1996; Narita et al., 2000; Pepicelli et al., 1998; Pitera et al., 1999; Roberts et al., 1995; Roberts et al., 1998; Sekimoto et al., 1998; Smith and Tabin, 1999; Yokouchi et al., 1995; Zakany and Duboule, 1999). Each region of the gut tube is separated by sphincters, which are thick circular muscles that control the passage of materials through the digestive system.

One of the key organs that form along the gut tube is the stomach. The stomach initially digests the food bolus and converts it into acidic chyme, which is delivered to the small intestine through the pyloric sphincter (PS). Impulses from the nerve plexuses of the enteric nervous system coordinate peristaltic waves of contraction that grind and thrust the contents of the stomach posteriorly. As the peristalsis reaches the pylorus, the

pyloric sphincter reacts by closing, thereby causing retropulsion of the contents and creating shearing forces that grind the food.

The PS consists of a thickened smooth muscle layer covered by mucous-secreting glands at the narrow posterior boundary of the stomach. The mechanisms that underlie the formation of the mammalian PS are not yet known. The only available working model describing the formation of the PS was proposed for chicken embryos. In these animals and in response to Shh signaling, *Bmp4* is expressed in the mesoderm of the small intestine (SI) (Roberts et al., 1995; Roberts et al., 1998; Smith et al., 2000a; Smith et al., 2000b; Smith and Tabin, 1999), whereas the *Bmp receptor 1b* (*Bmpr1b*) is expressed in the mesoderm of the gizzard, the chick's posterior stomach (Smith et al., 2000a; Smith et al., 2000b; Smith and Tabin, 1999). Bmp signaling from the SI specifies the PS in the mesoderm located at the junction of the gizzard and SI (the region where *Bmp4* and *Bmpr1b* expression overlaps) by inducing the expression of the transcription factors *Nkx2.5* and *Sox9* in the posterior gizzard mesoderm (Moniot et al., 2004; Smith et al., 2000b; Smith and Tabin, 1999; Theodosiou and Tabin, 2005). Loss- and gain-of-function approaches concluded that *Nkx2.5* and *Sox9* are necessary and sufficient to specify the typical bleb-like microvilli of the PS epithelium (Moniot et al., 2004; Smith et al., 2000b; Smith and Tabin, 1999; Theodosiou and Tabin, 2005). In the case of *Sox9*, this functional role could be accomplished by inducing *Gremlin* expression, which in turn, modulates Bmp activity (Moniot et al., 2004). Briefly, it is argued that in the chick, Bmp signaling controls the localization where the PS will form as well as the expression of *Sox9* and *Nkx2.5*, two genes that determine the characteristic epithelium of the PS (Moniot et al., 2004; Smith et al., 2000b; Smith and Tabin, 1999; Theodosiou and Tabin, 2005).

In the mouse, *Bmp4* is expressed in the mesenchyme of the stomach and anterior SI (Bitgood and McMahon, 1995; Jones et al., 1991; Smith et al., 2000a); *Bmpr1b* is expressed in the posterior stomach (Smith et al., 2000a); and *Nkx2.5* is expressed in the mesoderm of the PS (Chi et al., 2005; Lints et al., 1993; Smith et al., 2000a). These relatively similar expression patterns of *Bmp4*, *Bmpr1b*, and *Nkx2.5* in the chick and mouse digestive tracts suggest that the mechanisms involved in the formation of the PS may be conserved between the two species.

Six2 belongs to the *so/Six* family of homeobox-containing genes (Oliver et al., 1995). Initial characterization of its expression profile revealed that *Six2* was expressed in tissues such as the developing head, kidneys, limbs, and stomach (Oliver et al., 1995). Further work has shown that this gene's expression in the stomach is also conserved in frog and chick (Smith et al., 2000a). Functional characterization determined that *Six2* plays crucial roles during the development of the kidney and branchial arches (Kutejova et al., 2008; Self et al., 2006). Those initial analyses also identified defects in the development of certain parts of the digestive tract (our unpublished observations).

Here we have investigated the functional role of *Six2* in the development of the murine digestive tract, particularly in the formation of the PS during stomach organogenesis. We identified *Six2* as a key gene required for the formation of the mammalian PS. *Six2* functions in this developmental process by regulating a genetic network that is conserved between mouse and chick.

RESULTS

***Six2 expression in the developing stomach***

First, we performed a detailed characterization of the pattern of expression of *Six2* during organogenesis of the mouse stomach. At around E9.5 and before the stomach morphologically differentiated from the gut tube, *Six2* expression was detected in the region of the splanchnic mesoderm corresponding to the stomach anlage (Figure 1A, arrow) (Oliver et al., 1995). Once the stomach became demarcated from the gut tube at around E10.5, *Six2* expression was observed in the posterior mesenchymal portion (Figure 1B, arrow). By E11.5, the mesenchyme of the posterior half of the stomach continued to express *Six2* (Figure 1C, arrow). The posterior part of the mouse stomach is the glandular stomach (GS); the anterior region of the GS corresponds to the fundus and the most posterior region to the antrum (Hogan, 2002). By E12.5, *Six2* expression was confined to the mesenchyme of the presumptive GS (Figure 1D, E) but was not detected in the endodermally derived epithelial lining of the stomach (Figure 1E, arrowhead). As development of the stomach progressed, *Six2* expression became more restricted, and at E14.5, it was limited to the antrum just anterior to the PS (Figure 1F, arrow). This expression pattern was maintained until birth (data not shown).
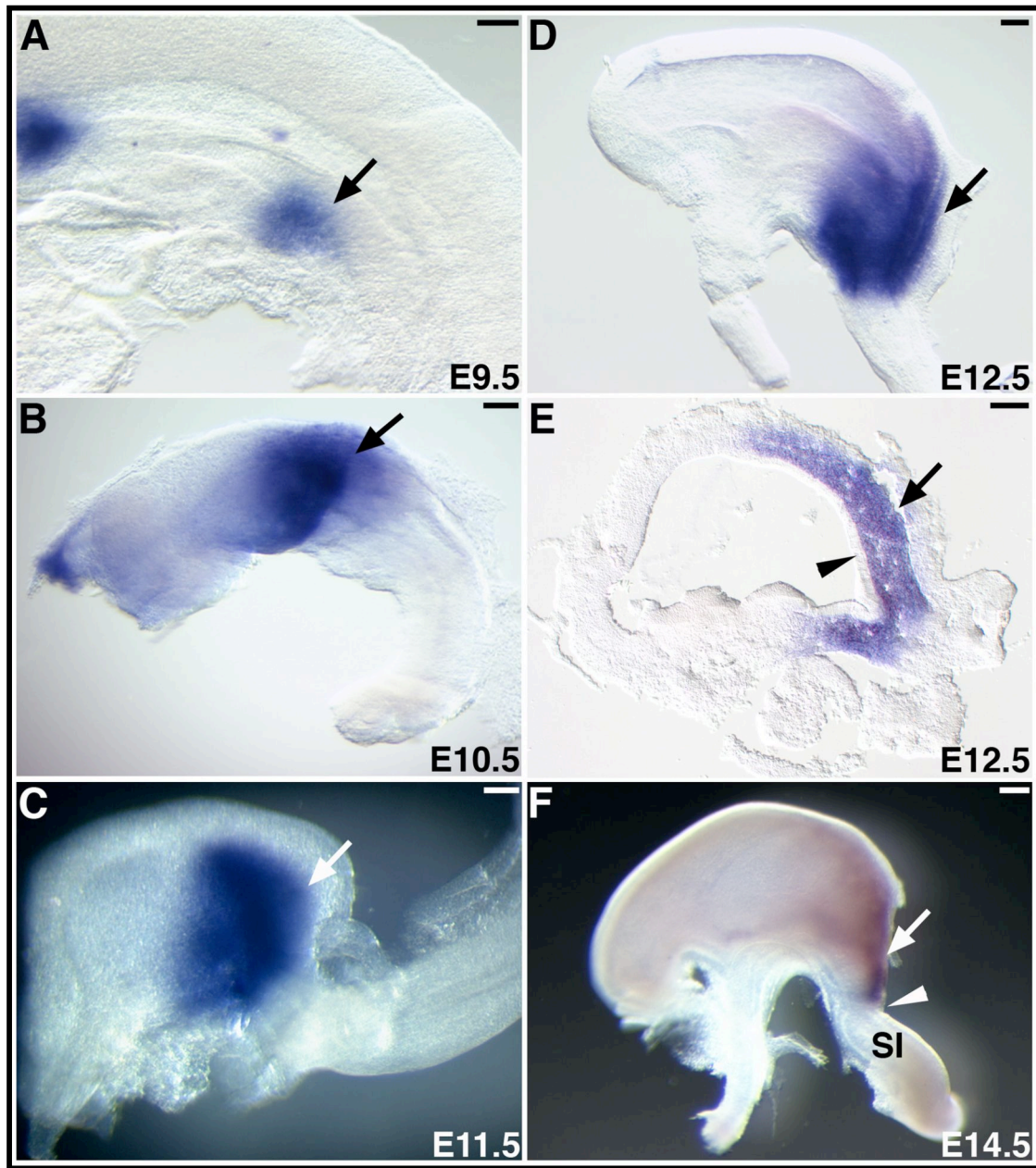
Figure 1. *Six2* is expressed in the mesoderm of the posterior stomach. (A) At E9.5, *Six2* expression is detected in the splanchnic mesoderm of the mouse stomach anlage (arrow). (B) By E10.5, *Six2* expression is detected in the mesoderm of the posterior stomach (arrow). (C) Expression is seen in the presumptive glandular stomach primordium at E11.5. (D, E) At E12.5, *Six2* becomes restricted to the mesenchyme of the antral region of the posterior stomach (arrows); no expression is observed in the epithelial layer (arrowhead). (F) At E14.5, *Six2* remains in the antrum, just anterior to the pyloric sphincter (arrowhead). Small intestine, SI; Scale bars, 100μm.

Pyloric sphincter formation is defective in the Six2-null stomach

As previously reported, *Six2*-null embryos die at birth due to the lack of functional kidneys (Self et al., 2006). To precisely identify morphological defects resulting from the absence of *Six2* activity in the digestive tube, we performed a detailed analysis of the *Six2*-null embryos. Visual inspection of E18.5 *Six2*-null embryos revealed abnormal duodenogastric reflux of amniotic fluid into the mutant stomach (Figure 2B). The cause of the reflux could be a nonfunctional or absent PS. Normally at E18.5, a thickened smooth muscle and constricted region of the stomach identifies the presence of the PS at the junction of the stomach and SI (Figure 2C, E, arrows). This thickened ring of smooth muscle and narrowing of the gut tube was not seen in *Six2*-null littermates (Figure 2D, F). In addition, the mucosa of the *Six2*-null stomach was hypertrophic (Figure 2H). These results indicate that during stomach organogenesis, *Six2* activity controls PS formation and mucosal growth.
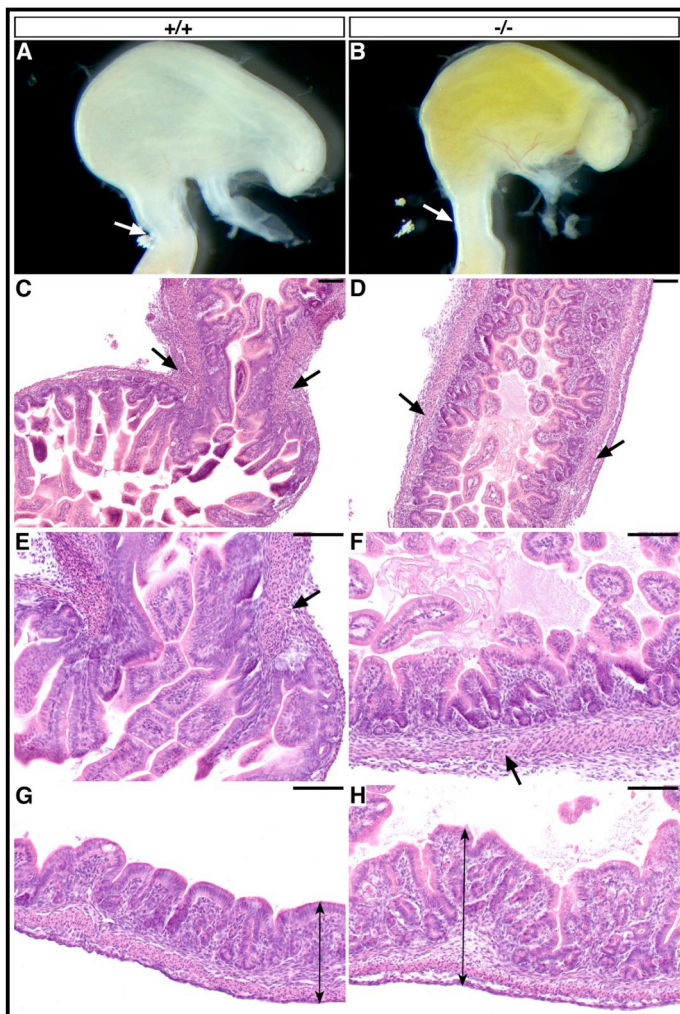

Figure 2. *Six2*-null embryos exhibit duodenogastric reflux and mucosal overgrowth. (A) At E18.5, the wild-type stomach contains a functional pyloric sphincter (arrow) to prevent the reflux of amniotic fluid from the small intestine (to the stomach. (B) The *Six2*-null stomach lacks a functional PS (arrow), thereby allowing reflux of the yellow fluid. (C, E) At this same stage, H & E staining of the wild-type stomach shows the region of the forming PS (arrows), including a thickened circular smooth muscle layer that constricts the gut tube at the junction of the stomach and SI. (D, F) The *Six2*-null gut tube lacks this thickened smooth muscle layer and the constriction at the corresponding level where the PS (arrows) should have formed. (G) At E18.5, the wild-type glandular stomach consists of primitive mucosal glands. (H) The *Six2*-null stomach exhibits overgrowth of the glands at this stage (compare arrows in G and H). Scale bars, 100µm.

To further characterize the identified alterations in PS formation, we analyzed the expression of α-smooth muscle actin (α-SMA), one of the earliest markers of smooth muscle differentiation (McHugh, 1995), in the *Six2*-null stomach. The circular smooth muscle layer begins to differentiate throughout the wild-type stomach at around E13.5 as indicated by expression of α-SMA (Takahashi et al., 1998). By E14.5, the constricted prospective PS region expressing α-SMA was thicker than in the rest of the wild-type stomach and SI (Figure 3A, C, arrows). No thickening or constriction was detected in the similar region of the E14.5 *Six2*-null stomach (Figure 3B, 3D, arrows). This result supports the proposal that PS formation is defective or absent in the *Six2* mutant embryos. In the E18.5 wild-type stomach, the dense muscular wall of the PS can be easily distinguished by α-SMA expression (Figure 3E, arrow). However, at this stage this thickened region of circular smooth muscle was also not readily apparent in the presumptive PS territory of *Six2*-null littermates (Figure 3F). The thickness of the circular smooth muscle layer in the remainder of the *Six2*-null stomach was normal (Figure 3G-3H). These data suggest that lack of *Six2* activity disrupts the initial steps leading to the formation of the PS, e.g., thickening of the smooth muscle layer and constriction of the gut tube in the presumptive pyloric territory. As a consequence, abnormal reflux of embryonic body fluids into the *Six2*-null stomach is observed in the mutant embryos.

A gene expression network is conserved in chick and mice during PS formation

As previously mentioned, not much information is available about the genes and mechanisms responsible for the development of the PS in mammals. We speculated that the functions of some of the genes participating in PS formation in the chick (e.g., *Bmp4, Bmpr1b, Nkx2.5, Sox9*, and *Gremlin*) could have been conserved in mice. However, in the mammalian stomach, only limited data about the expression patterns of some of these genes has been reported (Bitgood and McMahon, 1995; Chi et al., 2005; Jones et al., 1991; Lints et al., 1993; Smith et al., 2000a). Therefore, we first analyzed the expression of those PS markers during mouse stomach development.
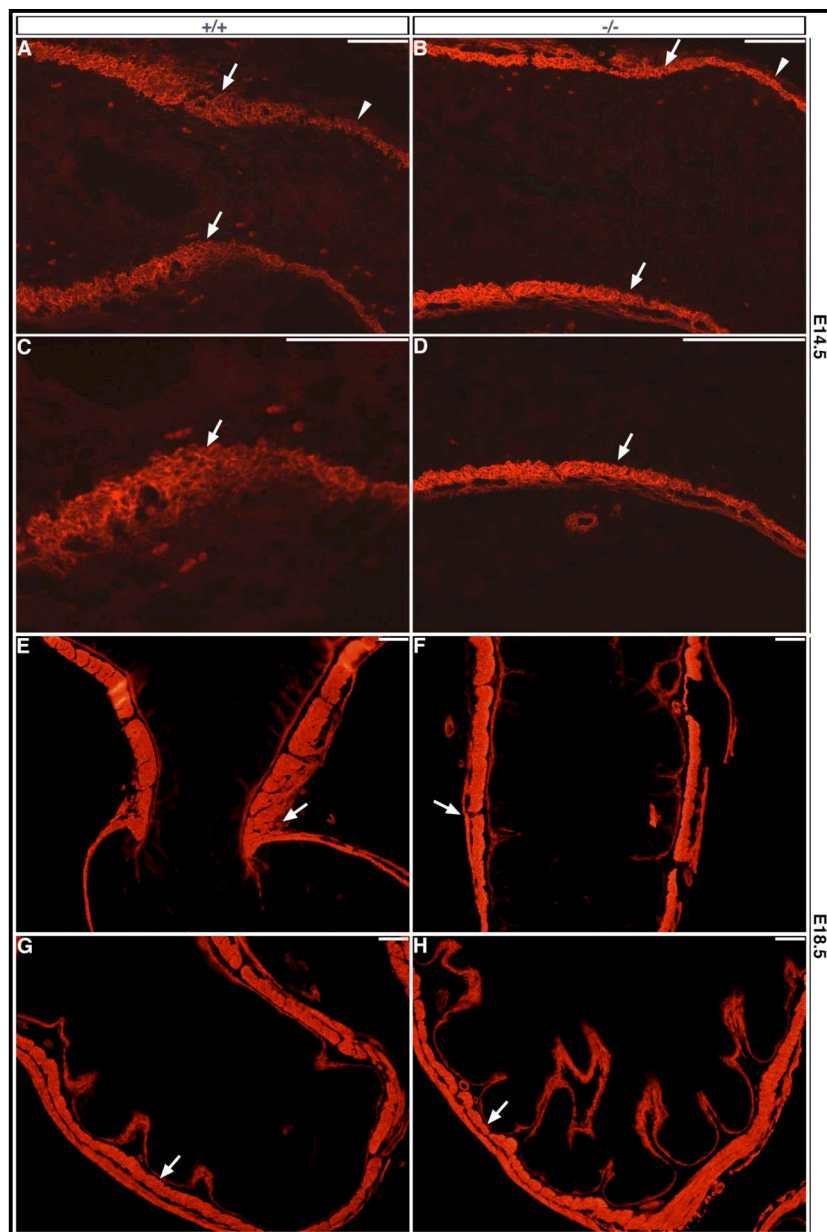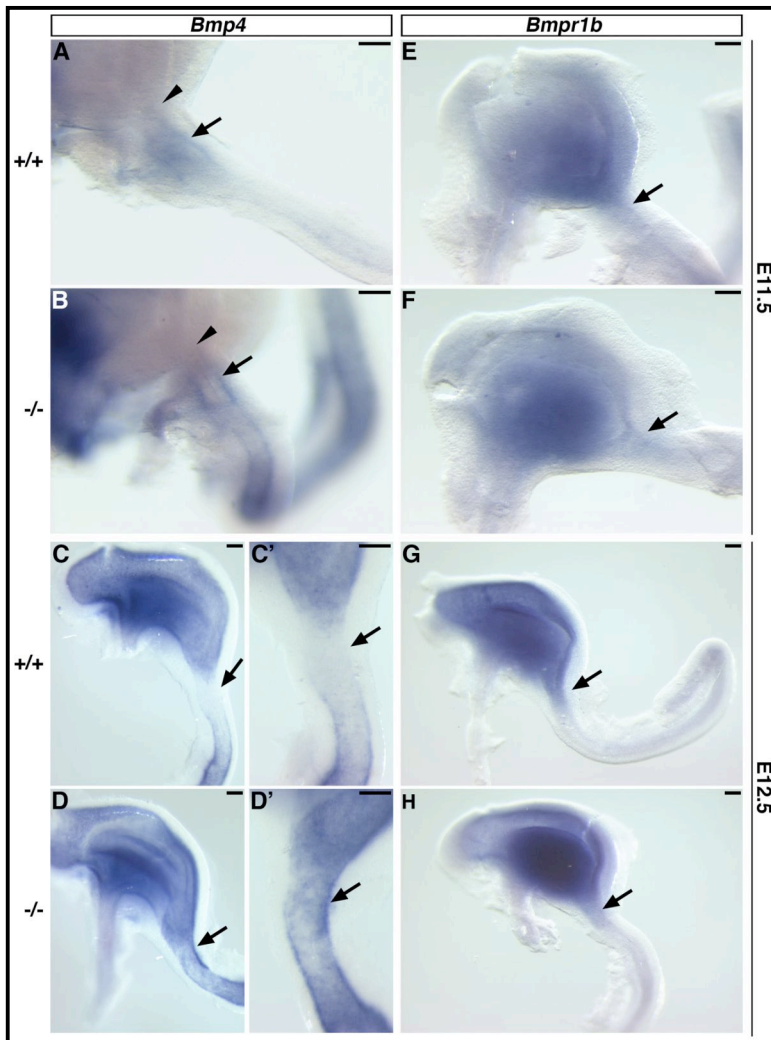
Figure 3. The lack of Six2 activity disrupts the initial steps of pyloric sphincter (PS) formation. (A, C) Expression of α-SMA in the E14.5 wild-type stomach reveals the thickening of the smooth muscle layer and the constriction of the gut tube at the level of the developing PS (arrows). (B, D) In the E14.5 *Six2*-null stomach, the α-SMA$^+$ layer fails to thicken, and the constriction of the gut tube at the boundary of the stomach and small intestine (SI; arrows) does not form. (E) At E18.5, the wild-type stomach shows the characteristic thickening of the smooth muscle layer and constriction of the gut tube in the PS territory (arrow). (F) The *Six2*-null stomach shows no evidence of PS formation at the stomach-SI junction (arrow). (G, H) The thickness of the smooth muscle layer (arrows) in the remainder of the *Six2*-null stomach (H) is similar to that of the wild-type stomach (G), as demonstrated by representative sections of the forestomach. Scale bars, 100μm.

As previously described (Bitgood and McMahon, 1995; Jones et al., 1991; Smith et al., 2000a), at E11.5 *Bmp4* expression was detected in the mesenchyme of the wild-type forestomach, located anterior to the GS (data not shown), and duodenum (Figure 4A, arrow), located posterior to the presumptive PS territory (Figure 4A, arrowhead). In the

Six2⁻ᐟ⁻ stomach, no obvious changes in the expression of *Bmp4* in these regions were observed (Figure 4B and data not shown). At E12.5, *Bmp4* was expressed in the mesenchyme throughout the wild-type stomach and in the mesenchyme of the SI, but it was absent from the mesenchyme of the PS region (Figure 4C, C', arrows). However, in the *Six2⁻ᐟ⁻* stomach, *Bmp4* expression was ectopically expanded into the presumptive PS territory at E12.5 (Figure 4D, D' arrow). At these same stages, *Bmpr1b* expression was detected in the GS mesenchyme of wild-type embryos, extending into the presumptive PS area (Smith et al., 2000a) (Figure 4E, G). This expression pattern was similar in the *Six2*-null stomach (Figure 4F, H). These results suggest that *Six2* might be required to maintain a *Bmp4*-free PS territory for proper morphogenesis of the PS in the mouse stomach.

Figure 4. *Six2* is required to maintain a *Bmp4*-free territory in the prospective PS region. (A) Normally at E11.5, *Bmp4* is expressed in the mesenchyme surrounding the epithelium of the presumptive duodenum (arrow) and is absent from the mesoderm of the presumptive PS region (arrowhead). (B) This expression pattern is not obviously affected in the *Six2*-null gut tube. (C, C') At E12.5, *Bmp4* expression is excluded from the PS territory (arrow) in wild-type embryos. (D, D') In *Six2⁻ᐟ⁻* littermates, expression of *Bmp4* has ectopically expanded into the prospective PS region (arrow). (E) Expression of *Bmpr1b* is detected in the wild-type mesenchyme of the developing glandular stomach and PS region (arrow). (F) This expression pattern appears unaffected in the *Six2*-null stomach. *Bmpr1b* expression remains in the PS territory (arrows) of E12.5 wild-type (G) and *Six2*-null (H) stomachs. Scale bars, 100μm.

The chick model argues that specification of the PS-like epithelial phenotype requires Bmp-mediated mesodermal expression of *Nkx2.5* and *Sox9* (Moniot et al., 2004; Smith et al., 2000b; Smith and Tabin, 1999; Theodosiou and Tabin, 2005). In the mouse, a ring of *Nkx2.5*-expressing mesenchyme is detected in the presumptive PS region at E12.5 (Figure 5A). The expression of *Nkx2.5* was weaker and the expression domain was narrower at this same stage in the *Six2$^{-/-}$* stomach (Figure 5B). At E14.5, no obvious differences in *Nkx2.5* expression in the PS region were detected between wild-type and *Six2*-null stomachs (Figure 5C, D). At the same stages, Sox9-expressing cells were detected in the mesenchyme of the presumptive PS territory in wild-type embryos (Figure 5E, G, arrows). Instead, just a few Sox9$^+$ cells were detected in the *Six2*-null presumptive PS region at E12.5 (Figure 5F, arrow). At E14.5, no Sox9-expressing cells could be identified in the mesenchyme of the *Six2$^{-/-}$* presumptive PS territory (Figure 5H, arrow).
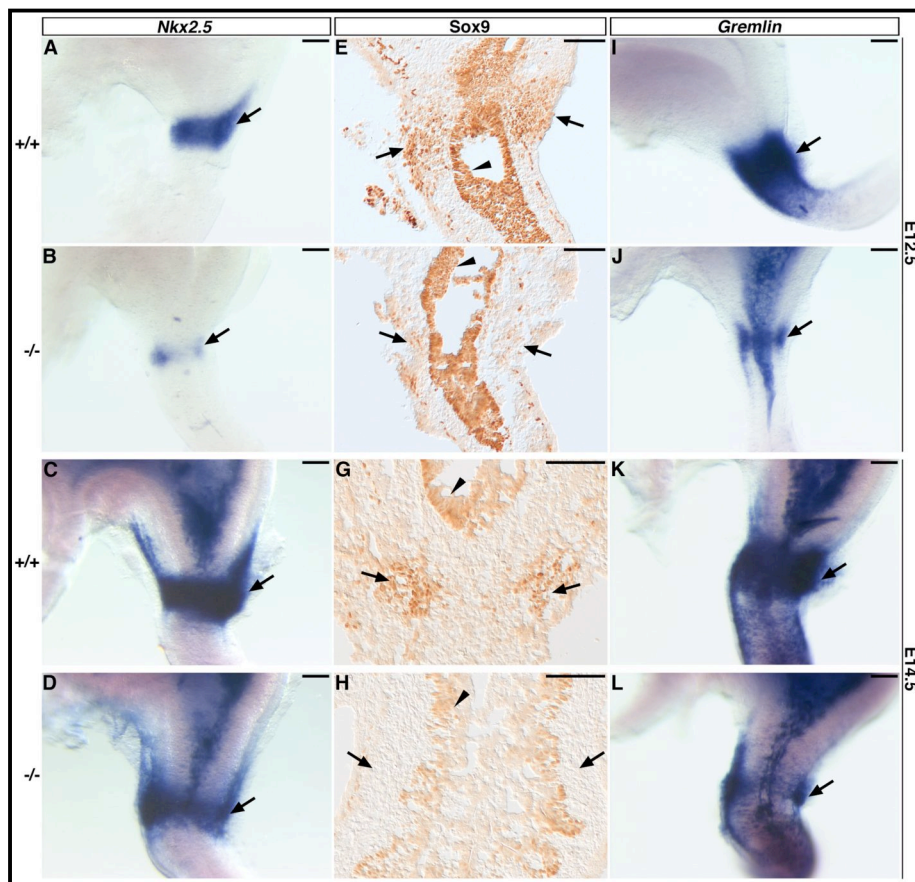
Figure 5. Expression of PS markers is aberrant in the *Six2*-null stomach. (A) *Nkx2.5* is expressed in the E12.5 wild-type PS territory (arrow). (B) *Nkx2.5* expression domain (arrow) is smaller in the prospective PS territory of *Six2$^{-/-}$* littermates. (C) At E14.5, *Nkx2.5* remains in the wild-type presumptive PS territory (arrow). (D) *Nkx2.5* expression appears normal in the *Six2*-null stomach at this stage. (E, G) *Sox9* is expressed in the mesenchyme of the prospective PS region (arrows) and in the epithelium of the stomach (arrowheads) at E12.5 and E14.5. (F, H) In the absence of *Six2*, the domain of mesodermal cells (arrows) expressing Sox9 is smaller at E12.5 and absent at E14.5; its pattern of expression is normal in the stomach epithelium at both stages (arrowheads). *Gremlin* is also expressed in the mesenchyme of the presumptive wild-type PS region (arrows) at E12.5 and E14.5 (I, K). The territory of mesenchymal cells expressing *Gremlin* (arrows) is smaller in the *Six2$^{-/-}$* stomach at E12.5 (J) and E14.5 (L). Scale bars, 100μm.

However, Sox9 remained at normal levels in the stomach epithelium at both of these stages (Figure 5E-H, arrowheads).

The mesenchymal layer of the presumptive PS territory of the E12.5 wild-type stomach also expressed *Gremlin* (Figure 5I). Similar to that of *Nkx2.5* and Sox9, the expression domain of *Gremlin* was smaller in the mesodermal layer of *Six2*-null littermates (Figure 5J). By E14.5, although the level of *Gremlin* expression appeared normal in the $Six2^{-/-}$ stomach, its expression domain remained smaller than that of the wild-type stomach (Figure 5K, 5L). These data suggest that the expression and function of certain genes that are essential for PS formation in chick embryos are also important during PS formation in mammals.

DISCUSSION

The mechanisms that control the formation of the mammalian PS are poorly understood. Conservation of *Six2* expression in the posterior mesodermal compartment of the developing stomach of frog, chick, and mouse embryos suggests that its activity is required for the genesis of a functional PS. Our results shed some light on this process as they identify *Six2* as a gene whose activity is required for the formation of a functional PS, possibly by regulating a gene network conserved between chick and mouse. Our data suggest that ectopic expansion of mesodermal *Bmp4* expression into the presumptive PS territory and decreased expression domains of *Nkx2.5*, *Sox9*, and *Gremlin* could be responsible for the lack of PS formation observed in the *Six2*-null stomach.

In chick embryos, *Bmp4* is expressed throughout the early gut tube except for the stomach, where its expression is detected in the submucosal layer of the gizzard only at later stages of development (Moniot et al., 2004; Roberts et al., 1995; Roberts et al., 1998; Smith et al., 2000a; Smith et al., 2000b; Smith and Tabin, 1999). *Bmpr1a* and *Bmpr1b* exhibit complementary expression patterns: *Bmpr1a* is located in the mesoderm of the SI, and *Bmpr1b*, in the mesoderm of the gizzard (Smith et al., 2000a; Smith et al., 2000b; Smith and Tabin, 1999). Interestingly, in the *Bmp4*-free region of the chick stomach, the smooth muscle layer is thicker than in the rest of the gut tube, a result suggesting that Bmp4 limits the growth of the mesodermal layer along the radial axis

during gut regionalization (Roberts et al., 1998). This proposal is supported by results showing that misexpression of *Bmp4*, *Bmpr1a*, or *Bmpr1b* in the chick stomach results in smaller thin-walled stomachs with altered rates of apoptosis and proliferation (Moniot et al., 2004; Roberts et al., 1998; Smith et al., 2000b; Smith and Tabin, 1999; Theodosiou and Tabin, 2005). Consistent with these results, in the developing mouse stomach *Bmp4* expression is restricted from the presumptive PS region. In the *Six2*-null stomach, ectopic Bmp signaling and decreased expression of the Bmp signal modulator *Gremlin* results in a thinner muscle layer; a result suggesting that in mammals Bmp signaling may also negatively regulate smooth muscle development.

In the chick, the expression of *Nkx2.5* in a precisely delimited region of the gut mesoderm (i.e., located at the boundary between the gizzard and the SI) is one of the first indicators of the territory where the PS will develop (Buchberger et al., 1996; Smith et al., 2000a; Smith and Tabin, 1999; Theodosiou and Tabin, 2005). Injection of constitutively active Bmp receptors or Bmp4 constructs into the embryonic gizzard resulted in the activation of *Nkx2.5* expression in the gizzard mesoderm followed by a morphologic change in the endoderm of the gizzard that acquires the bleb-like microvilli, which is characteristic of the PS epithelia (Smith et al., 2000b; Smith and Tabin, 1999; Theodosiou and Tabin, 2005). On the other hand, blocking Nkx2.5 activity in the PS region resulted in the loss of the PS endodermal phenotype (Smith and Tabin, 1999). Together, these results argued that in the chick, Bmp signaling is involved in the specification of the PS in the mesoderm located at the junction of the gizzard and the SI and that Nkx2.5 activity is sufficient and necessary to specify some aspects of the PS phenotype (Smith et al., 2000b; Smith and Tabin, 1999).

In the chick, *Sox9* is expressed in the endoderm throughout the GI tract, except for the gizzard; it is also expressed in the mesoderm of the PS (Moniot et al., 2004; Theodosiou and Tabin, 2005). Similar expression has been observed in human embryos (Moniot et al., 2004), as well as in the mouse (Figure 5). Misexpression of *Bmp4* in the chick stomach caused the anterior expansion of the *Sox9*^{+} domain (Moniot et al., 2004); however, not all cells in this expanded domain expressed *Sox9*. This result suggested that the mesodermal cells in the stomach differentially respond to *Bmp4* activation. Abrogated Bmp signaling in the stomach by misexpression of *Noggin* caused muscular hypertrophy,

downregulation of *Sox9*, and PS defects (Moniot et al., 2004; Theodosiou and Tabin, 2005). These results suggest that Bmp signaling is both necessary and sufficient for *Sox9* expression in the gizzard mesoderm (Moniot et al., 2004; Theodosiou and Tabin, 2005). Ectopic expression of *Sox9* in the gizzard mesoderm promoted the ectopic induction of *Gremlin* expression in the mesoderm followed by the transformation of the gizzard epithelium into a PS-like epithelium (Moniot et al., 2004). In summary, results in chick embryos suggest a model in which Bmp4 signaling via Bmpr1b at the junction of the gizzard and the SI directs PS formation by inducing the expression of *Nkx2.5* and *Sox9* in the presumptive PS territory. Both of these genes are able to specify the pyloric epithelium, and Sox9 in turn induces the expression of *Gremlin*, which can participate in a negative feedback loop to abrogate *Bmp* signaling.

Based on our results, we propose that a similar gene cascade participates in the development of the mammalian PS. Unfortunately, not much information is yet available regarding the functional roles of these same genes during stomach development in the mouse. *Bmp4-* and *Nkx2.5*-mutant mice exhibit early embryonic lethality precluding analysis of their roles in stomach development (Lyons et al., 1995a; Winnier et al., 1995). Our results confirmed that the expression of genes shown to be important in chick PS formation is at least partially conserved in the mouse and that the expression patterns of those genes are affected in the defective pyloric region of the *Six2*-null stomach. A major difference between chick and mouse PS formation is that in chick, the PS forms at the region where *Bmpr1b* and *Bmp4* expression overlaps in the junction of the gizzard and the SI. Normally in the mouse, *Bmp4* expression is specifically absent from the prospective PS territory. However, in the *Six2*-null stomach, *Bmp4* expression is ectopically expanded into this region, and the smooth muscle layer fails to thicken. In contrast to the chick data, the ectopic expansion of Bmp signaling into the prospective PS territory of the *Six2*-null stomach was not followed by the induction or expansion of the *Sox9-* or *Nkx2.5*-expression domains; the sizes of the *Sox9-*, *Nkx2.5-*, and *Gremlin*-expressing domains were reduced during early stages of stomach development. Therefore, although expression of the genes important for PS formation in chick is conserved during mouse PS development, regulation of this network seems to be different between these species. Another minor difference between chick and mouse PS

formation is that, as far as we are aware, the embryonic mouse PS does not possess the epithelial microvilli characteristic of the chick PS.

We envision two possible roles of *Six2* during mammalian PS formation. Six2 could be required to provide PS competence to a broad region of the antral mesenchyme. In this case, Six2 activity could be required for some of the aforementioned PS markers to reach a certain expression threshold or for the cells expressing the PS markers to reach their proper cell number. In the absence of Six2 activity, the expression levels and the expression domains of the genes discussed above are reduced and smaller; therefore, PS specification does not take place. Alternatively, Six2 may be required to maintain a *Bmp4*-free territory in the prospective PS region so that proper mesodermal differentiation will result in a thicker smooth muscle layer and constriction at this site of the gut tube.

A better understanding about the cellular and molecular mechanisms regulating the development of the mammalian digestive tract may shed light on human metaplasias and congenital disorders. For example, excessive duodenogastric reflux is caused by incomplete closure of the pyloric sphincter, ablation of the pylorus, or imperfect timing of peristalsis, and it can be damaging to the gastric mucosa (DuPlessis, 1960; DuPlessis, 1965; Lawson, 1964; Schrager and Oates, 1978; Vaezi and Richter, 1996; Vaezi et al., 1995). This reflux is also associated with an increased risk of gastric carcinoma (Lundegardh et al., 1988; Miwa et al., 1992; Yasuda et al., 2005). Primary duodenogastric reflux is rare in children, and the origin is unknown (Hermans et al., 2003). Infantile hypertrophic pyloric stenosis (IHPS) is a human condition in which the gastric outlet is obstructed by hypertrophy of the PS muscle, which fills the lumen. IHPS occurs in only two to four of every 1000 infants born, and symptoms arise within the first 2 to 12 weeks of life (Applegate and Druschel, 1995; Hernanz-Schulman et al., 2001; Rollins et al., 1989). This represents a phenotype opposite of that of the *Six2*-null stomach. The generated $Six2^{-/-}$ mice could become a useful animal model in which to study the expression of genes known to be crucial in smooth muscle hypertrophy in patients with IHPS.

MATERIALS AND METHODS

Functional Inactivation of *Six2*

The strategy for the functional inactivation of *Six2* has been previously described (Self et al., 2006).

In Situ Hybridization

Embryos were fixed in 4% paraformaldehyde and processed for whole-mount in situ hybridization (Wilkinson, 1995). Gelatin-embedded stained embryos were cryosectioned (Stern, 1993).

Immunohistochemistry

Embryos were fixed with 4% paraformaldehyde, cryopreserved in 30% sucrose, and cryosectioned for immunohistochemical analysis. Anti-Sox9 (Millipore, Billerica, MA) antibody staining was detected by diaminobenzidine using the VECTASTAIN® ABC kit (Vector Laboratories, Burlingame, CA), and anti–α-SMA antibody (Sigma, St. Louis, MO) was conjugated to Cy3.

References

Applegate, M. S., Druschel, C. M., 1995. The epidemiology of infantile hypertrophic pyloric stenosis in New York State, 1983 to 1990. Arch Pediatr Adolesc Med. 149**,** 1123-9.

Aufderheide, E., Ekblom, P., 1988. Tenascin during gut development: appearance in the mesenchyme, shift in molecular forms, and dependence on epithelial-mesenchymal interactions. J Cell Biol. 107**,** 2341-9.

Beck, F., Tata, F., Chawengsaksophak, K., 2000. Homeobox genes and gut development. Bioessays. 22**,** 431-41.

Bitgood, M. J., McMahon, A. P., 1995. Hedgehog and Bmp genes are coexpressed at many diverse sites of cell-cell interaction in the mouse embryo. Dev Biol. 172, 126-38.

Buchberger, A., Pabst, O., Brand, T., Seidl, K., Arnold, H. H., 1996. Chick NKx-2.3 represents a novel family member of vertebrate homologues to the Drosophila homeobox gene tinman: differential expression of cNKx-2.3 and cNKx-2.5 during heart and gut development. Mech Dev. 56, 151-63.

Chi, X., Chatterjee, P. K., Wilson, W., 3rd, Zhang, S. X., Demayo, F. J., Schwartz, R. J., 2005. Complex cardiac Nkx2-5 gene expression activated by noggin-sensitive enhancers followed by chamber-specific modules. Proc Natl Acad Sci U S A. 102, 13490-5.

Duluc, I., Freund, J. N., Leberquier, C., Kedinger, M., 1994. Fetal endoderm primarily holds the temporal and positional information required for mammalian intestinal development. J Cell Biol. 126, 211-21.

DuPlessis, D. J., 1960. Some aspects of the pathogenesis and surgical management of peptic ulcers. South Afr Med J. 34, 101-108.

DuPlessis, D. J., 1965. Pathogenesis of gastric ulceration. Lancet. 1, 974-978.

Franklin, V., Khoo, P. L., Bildsoe, H., Wong, N., Lewis, S., Tam, P. P., 2008. Regionalisation of the endoderm progenitors and morphogenesis of the gut portals of the mouse embryo. Mech Dev. 125, 587-600.

Grapin-Botton, A., Melton, D. A., 2000. Endoderm development: from patterning to organogenesis. Trends Genet. 16, 124-30.

Haffen, K., Kedinger, M., Simon-Assmann, P., 1987. Mesenchyme-dependent differentiation of epithelial progenitor cells in the gut. J Pediatr Gastroenterol Nutr. 6, 14-23.

Hermans, D., Sokal, E. M., Collard, J. M., Romagnoli, R., Buts, J. P., 2003. Primary duodenogastric reflux in children and adolescents. Eur J Pediatr. 162, 598-602.

Hernanz-Schulman, M., Lowe, L. H., Johnson, J., Neblett, W. W., Polk, D. B., Perez, R., Jr., Scheker, L. E., Stein, S. M., Heller, R. M., Cywes, R., 2001. In vivo visualization of pyloric mucosal hypertrophy in infants with hypertrophic pyloric stenosis: is there an etiologic role? AJR Am J Roentgenol. 177, 843-8.

Hogan, B. L. M., Zaret K. S., Development of the Endoderm and Its Tissue Derivatives. In: J. Rossant, Tam, P. P. L., (Ed.), Mouse Development: Patterning, Morphogenesis, and Organogenesis. Academic Press, San Diego, 2002, pp. 301-330.

Jones, C. M., Lyons, K. M., Hogan, B. L., 1991. Involvement of Bone Morphogenetic Protein-4 (BMP-4) and Vgr-1 in morphogenesis and neurogenesis in the mouse. Development. 111, 531-42.

Karam, S. M., Li, Q., Gordon, J. I., 1997. Gastric epithelial morphogenesis in normal and transgenic mice. Am J Physiol. 272, G1209-20.

Kedinger, M., Simon-Assmann, P., Bouziges, F., Arnold, C., Alexandre, E., Haffen, K., 1990. Smooth muscle actin expression during rat gut development and induction in fetal skin fibroblastic cells associated with intestinal embryonic epithelium. Differentiation. 43, 87-97.

Kutejova, E., Engist, B., Self, M., Oliver, G., Kirilenko, P., Bobola, N., 2008. Six2 functions redundantly immediately downstream of Hoxa2. Development. 135, 1463-70.

Lawson, H. H., 1964. Effect of Duodenal Contents on the Gastric Mucosa under Experimental Conditions. Lancet. 1, 469-72.

Lawson, K. A., Meneses, J. J., Pedersen, R. A., 1986. Cell fate and cell lineage in the endoderm of the presomite mouse embryo, studied with an intracellular tracer. Dev Biol. 115, 325-39.

Lee, E. R., 1985. Dynamic histology of the antral epithelium in the mouse stomach: I. Architecture of antral units. Am J Anat. 172, 187-204.

Levin, M., 1997. Left-right asymmetry in vertebrate embryogenesis. Bioessays. 19, 287-96.

Lints, T. J., Parsons, L. M., Hartley, L., Lyons, I., Harvey, R. P., 1993. Nkx-2.5: a novel murine homeobox gene expressed in early heart progenitor cells and their myogenic descendants. Development. 119, 419-31.

Litingtung, Y., Lei, L., Westphal, H., Chiang, C., 1998. Sonic hedgehog is essential to foregut development. Nat Genet. 20, 58-61.

Lowe, L. A., Supp, D. M., Sampath, K., Yokoyama, T., Wright, C. V., Potter, S. S., Overbeek, P., Kuehn, M. R., 1996. Conserved left-right asymmetry of nodal expression and alterations in murine situs inversus. Nature. 381, 158-61.

Lundegardh, G., Adami, H. O., Helmick, C., Zack, M., Meirik, O., 1988. Stomach cancer after partial gastrectomy for benign ulcer disease. N Engl J Med. 319, 195-200.

Lyons, I., Parsons, L. M., Hartley, L., Li, R., Andrews, J. E., Robb, L., Harvey, R. P., 1995a. Myogenic and morphogenetic defects in the heart tubes of murine embryos lacking the homeo box gene Nkx2-5. Genes Dev. 9, 1654-66.

Lyons, K. M., Hogan, B. L., Robertson, E. J., 1995b. Colocalization of BMP 7 and BMP 2 RNAs suggests that these factors cooperatively mediate tissue interactions during murine development. Mech Dev. 50, 71-83.

Marigo, V., Scott, M. P., Johnson, R. L., Goodrich, L. V., Tabin, C. J., 1996. Conservation in hedgehog signaling: induction of a chicken patched homolog by Sonic hedgehog in the developing limb. Development. 122, 1225-33.

McHugh, K. M., 1995. Molecular analysis of smooth muscle development in the mouse. Dev Dyn. 204, 278-90.

Mendelsohn, C., 2006. Going in circles: conserved mechanisms control radial patterning in the urinary and digestive tracts. J Clin Invest. 116, 635-7.

Miwa, K., Hasegawa, H., Fujimura, T., Matsumoto, H., Miyata, R., Kosaka, T., Miyazaki, I., Hattori, T., 1992. Duodenal reflux through the pylorus induces gastric adenocarcinoma in the rat. Carcinogenesis. 13, 2313-6.

Moniot, B., Biau, S., Faure, S., Nielsen, C. M., Berta, P., Roberts, D. J., de Santa Barbara, P., 2004. SOX9 specifies the pyloric sphincter epithelium through mesenchymal-epithelial signals. Development. 131, 3795-804.

Narita, T., Saitoh, K., Kameda, T., Kuroiwa, A., Mizutani, M., Koike, C., Iba, H., Yasugi, S., 2000. BMPs are necessary for stomach gland formation in the chicken embryo: a study using virally induced BMP-2 and Noggin expression. Development. 127, 981-8.

Oliver, G., Wehr, R., Jenkins, N. A., Copeland, N. G., Cheyette, B. N., Hartenstein, V., Zipursky, S. L., Gruss, P., 1995. Homeobox genes and connective tissue patterning. Development. 121**,** 693-705.

Pepicelli, C. V., Lewis, P. M., McMahon, A. P., 1998. Sonic hedgehog regulates branching morphogenesis in the mammalian lung. Curr Biol. 8**,** 1083-6.

Pitera, J. E., Smith, V. V., Thorogood, P., Milla, P. J., 1999. Coordinated expression of 3' hox genes during murine embryonal gut development: an enteric Hox code. Gastroenterology. 117**,** 1339-51.

Roberts, D. J., 2000. Molecular mechanisms of development of the gastrointestinal tract. Dev Dyn. 219**,** 109-20.

Roberts, D. J., Johnson, R. L., Burke, A. C., Nelson, C. E., Morgan, B. A., Tabin, C., 1995. Sonic hedgehog is an endodermal signal inducing Bmp-4 and Hox genes during induction and regionalization of the chick hindgut. Development. 121**,** 3163-74.

Roberts, D. J., Smith, D. M., Goff, D. J., Tabin, C. J., 1998. Epithelial-mesenchymal signaling during the regionalization of the chick gut. Development. 125**,** 2791-801.

Rollins, M. D., Shields, M. D., Quinn, R. J., Wooldridge, M. A., 1989. Pyloric stenosis: congenital or acquired? Arch Dis Child. 64**,** 138-9.

Ryan, A. K., Blumberg, B., Rodriguez-Esteban, C., Yonei-Tamura, S., Tamura, K., Tsukui, T., de la Pena, J., Sabbagh, W., Greenwald, J., Choe, S., Norris, D. P., Robertson, E. J., Evans, R. M., Rosenfeld, M. G., Izpisua Belmonte, J. C., 1998. Pitx2 determines left-right asymmetry of internal organs in vertebrates. Nature. 394**,** 545-51.

Schrager, J., Oates, M. D., 1978. Relation of human gastrointestinal mucus to disease states. Br Med Bull. 34**,** 79-82.

Sekimoto, T., Yoshinobu, K., Yoshida, M., Kuratani, S., Fujimoto, S., Araki, M., Tajima, N., Araki, K., Yamamura, K., 1998. Region-specific expression of murine Hox genes implies the Hox code-mediated patterning of the digestive tract. Genes Cells. 3**,** 51-64.

Self, M., Lagutin, O. V., Bowling, B., Hendrix, J., Cai, Y., Dressler, G. R., Oliver, G., 2006. Six2 is required for suppression of nephrogenesis and progenitor renewal in the developing kidney. Embo J. 25**,** 5214-28.

Smith, D. M., Grasty, R. C., Theodosiou, N. A., Tabin, C. J., Nascone-Yoder, N. M., 2000a. Evolutionary relationships between the amphibian, avian, and mammalian stomachs. Evol Dev. 2**,** 348-59.

Smith, D. M., Nielsen, C., Tabin, C. J., Roberts, D. J., 2000b. Roles of BMP signaling and Nkx2.5 in patterning at the chick midgut-foregut boundary. Development. 127**,** 3671-81.

Smith, D. M., Tabin, C. J., 1999. BMP signalling specifies the pyloric sphincter. Nature. 402**,** 748-9.

Stern, C. D., Immunocytochemistry of embryonic material. In: C. D. Stern, Holland, P. W. H., (Ed.), Essential Developmental Biology, A Practical Approach. Oxford University Press, New York, 1993, pp. 193-212.

Sukegawa, A., Narita, T., Kameda, T., Saitoh, K., Nohno, T., Iba, H., Yasugi, S., Fukuda, K., 2000. The concentric structure of the developing gut is regulated by Sonic hedgehog derived from endodermal epithelium. Development. 127, 1971-80.

Takahashi, Y., Imanaka, T., Takano, T., 1998. Spatial pattern of smooth muscle differentiation is specified by the epithelium in the stomach of mouse embryo. Dev Dyn. 212, 448-60.

Theodosiou, N. A., Tabin, C. J., 2005. Sox9 and Nkx2.5 determine the pyloric sphincter epithelium under the control of BMP signaling. Dev Biol. 279, 481-90.

Vaezi, M. F., Richter, J. E., 1996. Role of acid and duodenogastroesophageal reflux in gastroesophageal reflux disease. Gastroenterology. 111, 1192-9.

Vaezi, M. F., Singh, S., Richter, J. E., 1995. Role of acid and duodenogastric reflux in esophageal mucosal injury: a review of animal and human studies. Gastroenterology. 108, 1897-907.

Wells, J. M., Melton, D. A., 1999. Vertebrate endoderm development. Annu Rev Cell Dev Biol. 15, 393-410.

Wilkinson, D. G., 1995. RNA detection using non-radioactive in situ hybridization. Curr Opin Biotechnol. 6, 20-3.

Winnier, G., Blessing, M., Labosky, P. A., Hogan, B. L., 1995. Bone morphogenetic protein-4 is required for mesoderm formation and patterning in the mouse. Genes Dev. 9, 2105-16.

Wright, N. A., 2000. Epithelial stem cell repertoire in the gut: clues to the origin of cell lineages, proliferative units and cancer. Int J Exp Pathol. 81, 117-43.

Yasuda, H., Yamada, M., Endo, Y., Inoue, K., Yoshiba, M., 2005. Elevated cyclooxygenase-2 expression in patients with early gastric cancer in the gastric pylorus. J Gastroenterol. 40, 690-7.

Yasugi, S., 1993. Role of Epithelial-Mesenchymal Interactions in Differentiation of Epithelium of Vertebrate Digestive Organs. Develop. Growth & Differ. 35, 1-9.

Yokouchi, Y., Sakiyama, J., Kuroiwa, A., 1995. Coordinated expression of Abd-B subfamily genes of the HoxA cluster in the developing digestive tract of chick embryo. Dev Biol. 169, 76-89.

Zakany, J., Duboule, D., 1999. Hox genes and the making of sphincters. Nature. 401, 761-2.

Chapter 5

Summary and Discussion

SUMMARY and DISCUSSION

Six2 is a member of the mammalian *Six* family of homeobox-containing transcription factors and is expressed in a wide array of tissues during murine embryonic development[1]. During the organogenesis of the kidney and stomach, reciprocal inductive interactions between the mesenchyme and epithelia are vital to the proper differentiation of these organs[2, 3]. The expression of *Six2* in the mesenchymal populations of these and other tissues suggests that it may function to regulate target genes involved in the patterning and differentiation of organs that rely on mesenchymal-epithelial interactions for proper development.

The embryonic mouse kidney is a well-established model of branching morphogenesis, reciprocal inductive interactions, and mesenchyme-to-epithelium transition. Reciprocal inductive signals from the metanephric mesenchyme (MM) and ureteric bud (UB) result in outgrowth and branching of the UB and mesenchymal-epithelial transition during nephrogenesis[3, 4]. The MM, an undifferentiated renal progenitor population, must be continuously replenished for future rounds of nephrogenesis. The molecular mechanisms accountable for maintenance of this pool of undifferentiated mesenchyme had not yet been identified. Previous studies performed in *Pax2*, *Eya1*, and *Hox11* mutant mice exhibiting kidney agenesis demonstrated that *Six2* expression was downregulated or completely absent in the metanephric blastemas of these mutants[5-9]. These results suggested that *Six2* may also play a key role in the mesenchymal-epithelial inductive interactions involved in kidney organogenesis.

In Chapter 2 of this thesis I describe the functional roles of *Six2* during kidney organogenesis. I determined that this gene is part of a genetic mechanism that opposes epithelial polarization and regulates renal epithelial precursor cell renewal by maintaining the undifferentiated state of the progenitor MM population. Functional inactivation of *Six2* resulted in precocious and ectopic differentiation of mesenchymal cells into nephric vesicles and depletion of the mesenchymal progenitor cell population, decreased UB branching, and mispatterning of the developing nephrons.

In the E11.5 *Six2*-null kidney, the entire MM population exhibited ectopic and premature *Wnt4* expression, indicating that all of the MM had been induced to form renal vesicles at this early stage thus depleting the renal progenitor pool. The failure to renew the cortical progenitor population and an increase in apoptosis resulted in severe renal hypoplasia and death soon after birth. By characterizing the expression of several genes known to be important for kidney development, we determined that the reciprocal interactions between the MM and the UB are defective in the *Six2*-null kidney. In addition, by using a kidney organ culture approach to overexpress Six2 in this mesenchymal population, we showed that Six2 is sufficient to prevent conversion of the mesenchyme into nephrons. Based on these results, we concluded that *Six2* controls the fate of the renal epithelial progenitor population by suppressing the inductive signals that promote epithelial differentiation. This functional role is essential to maintain available pools of cells in an undifferentiated state for future rounds of nephrogenesis.

In a collaborative effort with the McMahon laboratory at Harvard University, we sought to further understand the mechanism behind the activity of *Six2* during nephrogenesis. The results described in Chapter 3 using a genetic lineage tracing approach confirmed that the *Six2*-expressing mesenchyme is a self-renewing population that acts cell-autonomously to maintain a progenitor status. Six2-expressing cells contribute to nephron formation throughout kidney organogenesis. Using this approach we also demonstrated that Six2-expressing cells give rise to all cell types of the nephron and that mesenchyme lacking Six2 activity contributes to the ectopic renal vesicles in *Six2*-null kidneys.

Wnt9b is the primary inductive signal emanating from the ureteric buds involved in pretubular aggregate and renal vesicle formation[10]; therefore, we questioned whether Six2 functions by blocking the response to Wnt9b in the cortical MM. In *Wnt9b*-null kidneys, *Six2* expression was normal in the MM, and *Wnt9b* expression was also normal in *Six2*-null kidneys. To better understand the relationship between *Wnt9b* and *Six2*, we generated and analyzed *Wnt9b^{-/-};Six2^{-/-}* compound mutant embryos. No renal vesicle formation was observed in *Wnt9b^{-}*

$^{/-}$ or in *Wnt9b*$^{-/-}$*;Six2*$^{-/-}$ compound mutant embryos; however, the size of the MM renal progenitor population was much more reduced in *Wnt9b*$^{-/-}$*;Six2*$^{-/-}$ embryos at early stages of kidney development. This finding suggests an earlier genetic interaction between *Wnt9b* and *Six2* that complicates the interpretation of the cooperation of these factors during nephrogenesis.

In conclusion, during kidney development *Six2* is required to maintain a population of mesenchymal renal progenitor cells in an undifferentiated state for the continuous generation of nephrons. *Six2* function is also necessary for repetitive reciprocal inductive interactions and kidney growth. The defects in patterning of nephric tubules and lack of UB branching are likely secondary to the depletion of the renal progenitor population and cessation of reciprocal inductive interactions in the *Six2*$^{-/-}$ kidney. Six2 may regulate the Wnt-promoted nephrogenesis cascade to suppress unnecessary renal vesicle formation, thereby maintaining the undifferentiated state of the mesenchymal progenitor population.

In Chapter 4, I describe results from work in progress related to the functional role of *Six2* during stomach development. Analysis of the stomach of *Six2*-null embryos revealed that this gene is required for the formation of a functional pyloric sphincter (PS), a structure that prevents the reflux of contents from the small intestine into the stomach. In *Six2*$^{-/-}$ embryos, the smooth muscle layer is not properly thickened in the PS region and the hallmark constriction of the pyloric zone of the stomach is absent, a defect resulting in duodenogastric reflux. I show that genes known to be required during chicken PS formation are also expressed during mouse PS formation; however, the expression patterns of some of those are defective in the *Six2*-null stomach. In particular, I determined that *Bmp4* expression is ectopically expanded into the presumptive PS territory and that the expression domains of *Nkx2.5*, Sox9, and *Gremlin* are downregulated or reduced.

Based on our results, it is possible to speculate that these changes in expression observed during early stages of PS specification, may be responsible for the identified failure of smooth muscle thickening in the *Six2*$^{-/-}$ stomach. Six2

activity may provide competence to the mesenchyme of the putative pyloric sphincter territory to express PS-promoting signals, such as *Nkx2.5*, *Sox9*, and *Gremlin*. In the absence of *Six2* function, the expression threshold of these PS-promoting factors is defective; therefore, the appropriate number of cells necessary for PS formation may not be specified. The reduction in *Gremlin* expression may result in aberrant modulation of the Bmp pathway and ectopic expansion of *Bmp4* expression in the PS territory. Alternatively, *Six2* may play a more direct role in the regulation of *Bmp4* expression in the PS region with the reduction in expression domains of the other PS markers being a consequence of the misregulation of Bmp signaling in the *Six2*-null stomach.

Studies in chick have demonstrated that regions of the gut tube where Bmp4 is expressed develop thinner muscle layers than those in the gizzard where Bmp4 expression is absent[11]. Ectopic expression of Bmp4 or Bmp receptors in the gizzard resulted in thin-walled stomachs suggesting that Bmp signaling plays a role in proliferation and differentiation of the splanchnic mesoderm and negatively regulates growth of the smooth muscle layer[11-15]. *Bmp4* expression is also restricted from the presumptive PS region in mice suggesting that Bmp signaling may play a conserved role in controlling differentiation of the smooth muscle layer in both species. In the *Six2*-null stomach, failure of the PS smooth muscle layer to thicken may be a direct result of the ectopic expression of *Bmp4* in this territory.

The studies in this thesis provide novel insights into the mechanisms behind kidney and stomach development. These findings will eventually facilitate a better understanding of clinical manifestations behind developmental disorders of the kidney and stomach. SIX2 is expressed in tissues that are involved in Branchio-oto-renal syndrome, an autosomal dominant developmental disorder characterized by renal and urinary tract anomalies, deafness, and craniofacial abnormalities[16]. Mutations in EYA1, SIX1, and SIX5 that affect the binding of EYA1 to SIX proteins were found in BOR syndrome patients[17-23]. It is possible that SIX2 mutations could also be present in BOR-affected individuals. Mutations in SIX2 and BMP4 were demonstrated in some patients with renal

hypodysplasia[24]. Since our analysis of the *Six2*-null stomach revealed the possibility that Six2 may regulate expression of *Bmp4*, this potential interaction warrants further analysis during kidney development.

In the human digestive tract, ablation of the PS, incomplete closure of the PS, or imperfect timing of peristalsis can cause duodenogastric reflux. The reflux of the contents of the SI can be damaging to the stomach mucosa and increases the risk of acquiring gastric carcinoma[25-33]. The opposite phenotype is Infantile Hypertrophic Pyloric Stenosis (IHPS) in which the PS smooth muscle is overgrown filling the lumen and preventing emptying of the stomach[34-36]. The *Six2*-null stomach could be a useful tool to further define the mechanisms behind these disorders.

References

1. Oliver, G. et al. Homeobox genes and connective tissue patterning. *Development* **121**, 693-705 (1995).
2. Hogan, B.L.M., Zaret K. S. in Mouse Development: Patterning, Morphogenesis, and Organogenesis (ed. Rossant, J., Tam, P. P. L.) 301-330 (Academic Press, San Diego, 2002).
3. Vainio, S. & Lin, Y. Coordinating early kidney development: lessons from gene targeting. *Nat Rev Genet* **3**, 533-43 (2002).
4. Dressler, G.R. The cellular basis of kidney development. *Annu Rev Cell Dev Biol* **22**, 509-29 (2006).
5. Davis, A.P., Witte, D.P., Hsieh-Li, H.M., Potter, S.S. & Capecchi, M.R. Absence of radius and ulna in mice lacking hoxa-11 and hoxd-11. *Nature* **375**, 791-5 (1995).
6. Favor, J. et al. The mouse Pax2(1Neu) mutation is identical to a human PAX2 mutation in a family with renal-coloboma syndrome and results in developmental defects of the brain, ear, eye, and kidney. *Proc Natl Acad Sci U S A* **93**, 13870-5 (1996).
7. Torres, M., Gomez-Pardo, E., Dressler, G.R. & Gruss, P. Pax-2 controls multiple steps of urogenital development. *Development* **121**, 4057-65 (1995).
8. Wellik, D.M., Hawkes, P.J. & Capecchi, M.R. Hox11 paralogous genes are essential for metanephric kidney induction. *Genes Dev* **16**, 1423-32 (2002).
9. Xu, P.X. et al. Eya1-deficient mice lack ears and kidneys and show abnormal apoptosis of organ primordia. *Nat Genet* **23**, 113-7 (1999).

10. Carroll, T.J., Park, J.S., Hayashi, S., Majumdar, A. & McMahon, A.P. Wnt9b plays a central role in the regulation of mesenchymal to epithelial transitions underlying organogenesis of the mammalian urogenital system. *Dev Cell* **9**, 283-92 (2005).

11. Roberts, D.J., Smith, D.M., Goff, D.J. & Tabin, C.J. Epithelial-mesenchymal signaling during the regionalization of the chick gut. *Development* **125**, 2791-801 (1998).

12. Moniot, B. et al. SOX9 specifies the pyloric sphincter epithelium through mesenchymal-epithelial signals. *Development* **131**, 3795-804 (2004).

13. Smith, D.M., Nielsen, C., Tabin, C.J. & Roberts, D.J. Roles of BMP signaling and Nkx2.5 in patterning at the chick midgut-foregut boundary. *Development* **127**, 3671-81 (2000).

14. Smith, D.M. & Tabin, C.J. BMP signalling specifies the pyloric sphincter. *Nature* **402**, 748-9 (1999).

15. Theodosiou, N.A. & Tabin, C.J. Sox9 and Nkx2.5 determine the pyloric sphincter epithelium under the control of BMP signaling. *Dev Biol* **279**, 481-90 (2005).

16. Boucher, C.A. et al. Structure, mapping and expression of the human gene encoding the homeodomain protein, SIX2. *Gene* **247**, 145-51 (2000).

17. Abdelhak, S. et al. Clustering of mutations responsible for branchio-oto-renal (BOR) syndrome in the eyes absent homologous region (eyaHR) of EYA1. *Hum Mol Genet* **6**, 2247-55 (1997).

18. Abdelhak, S. et al. A human homologue of the Drosophila eyes absent gene underlies branchio-oto-renal (BOR) syndrome and identifies a novel gene family. *Nat Genet* **15**, 157-64 (1997).

19. Hoskins, B.E. et al. Transcription factor SIX5 is mutated in patients with branchio-oto-renal syndrome. *Am J Hum Genet* **80**, 800-4 (2007).

20. Kumar, S. et al. Identification of three novel mutations in human EYA1 protein associated with branchio-oto-renal syndrome. *Hum Mutat* **11**, 443-9 (1998).

21. Ozaki, H., Watanabe, Y., Ikeda, K. & Kawakami, K. Impaired interactions between mouse Eyal harboring mutations found in patients with branchio-oto-renal syndrome and Six, Dach, and G proteins. *J Hum Genet* **47**, 107-16 (2002).

22. Ruf, R.G. et al. SIX1 mutations cause branchio-oto-renal syndrome by disruption of EYA1-SIX1-DNA complexes. *Proc Natl Acad Sci U S A* **101**, 8090-5 (2004).

23. Vincent, C. et al. BOR and BO syndromes are allelic defects of EYA1. *Eur J Hum Genet* **5**, 242-6 (1997).

24. Weber, S. et al. SIX2 and BMP4 mutations associate with anomalous kidney development. *J Am Soc Nephrol* **19**, 891-903 (2008).

25. DuPlessis, D.J. Some aspects of the pathogenesis and surgical management of peptic ulcers. *South Afr Med J* **34**, 101-108 (1960).

26. DuPlessis, D.J. Pathogenesis of gastric ulceration. *Lancet* **1**, 974-978 (1965).

27. Lawson, H.H. Effect of Duodenal Contents on the Gastric Mucosa under Experimental Conditions. *Lancet* **1**, 469-72 (1964).

28. Schrager, J. & Oates, M.D. Relation of human gastrointestinal mucus to disease states. *Br Med Bull* **34**, 79-82 (1978).

29. Vaezi, M.F. & Richter, J.E. Role of acid and duodenogastroesophageal reflux in gastroesophageal reflux disease. *Gastroenterology* **111**, 1192-9 (1996).

30. Vaezi, M.F., Singh, S. & Richter, J.E. Role of acid and duodenogastric reflux in esophageal mucosal injury: a review of animal and human studies. *Gastroenterology* **108**, 1897-907 (1995).

31. Lundegardh, G., Adami, H.O., Helmick, C., Zack, M. & Meirik, O. Stomach cancer after partial gastrectomy for benign ulcer disease. *N Engl J Med* **319**, 195-200 (1988).

32. Miwa, K. et al. Duodenal reflux through the pylorus induces gastric adenocarcinoma in the rat. *Carcinogenesis* **13**, 2313-6 (1992).

33. Yasuda, H., Yamada, M., Endo, Y., Inoue, K. & Yoshiba, M. Elevated cyclooxygenase-2 expression in patients with early gastric cancer in the gastric pylorus. *J Gastroenterol* **40**, 690-7 (2005).

34. Applegate, M.S. & Druschel, C.M. The epidemiology of infantile hypertrophic pyloric stenosis in New York State, 1983 to 1990. *Arch Pediatr Adolesc Med* **149**, 1123-9 (1995).

35. Hernanz-Schulman, M. et al. In vivo visualization of pyloric mucosal hypertrophy in infants with hypertrophic pyloric stenosis: is there an etiologic role? *AJR Am J Roentgenol* **177**, 843-8 (2001).

36. Rollins, M.D., Shields, M.D., Quinn, R.J. & Wooldridge, M.A. Pyloric stenosis: congenital or acquired? *Arch Dis Child* **64**, 138-9 (1989).

SAMENVATTING EN DISKUSSIE

Six2 is lid van de familie van zoogdier *Six* homeobox-bevattende transcriptiefactoren en komt tot expressie in een groot aantal weefsels tijdens de embryonale ontwikkeling van de muis. Wederzijdse inductieve interacties tussen mesenchym en epitheel zijn van vitaal belang voor de juiste differentiatie tijdens de organogenese van de nieren en de maag. De expressie van *Six2* in de mesenchymale populaties van deze en andere weefsels suggereert dat het mogelijk een funktie vervult bij de regulatie van target genen betrokken bij de patroonvorming en differentiatie van organen die voor hun juiste ontwikkeling afhankelijk zijn van epitheliale-mesenchymale interacties.

De embryonale muizen nier is een erkend model voor de bestudering van de vertakkings morfogenese, inductieve wederzijdse interacties, en mesenchymale-epitheliale transities. Wederzijdse inductieve signalen van het metanephrische mesenchym (MM) en de ureterische bud (UB) leiden tot uitgroei en vertakking van de UB en de epitheliale-mesenchymale transitie tijdens de nefrogenese. Het MM, een populatie van ongedifferentieerde nier voorlopercellen, moet voordurend worden aangevuld voor volgende rondes van nefrogenese. De moleculaire mechanismen die verantwoordelijk zijn voor de instandhouding van deze poel van ongedifferentieerd mesenchym zijn nog niet geïdentificeerd. Uit vorig onderzoek met *Pax2*, *Eya1*, en *Hox11* mutante muizen die nier-agenesie vertoonden, bleek dat in de metanefrische blastemen van deze mutanten de *Six2* expressie verminderd of zelfs geheel afwezig was. Deze resultaten deden vermoeden dat *Six2* ook een belangrijke rol zou kunnen spelen bij de epitheliale-mesenchymale inductieve interacties die betrokken zijn bij de organogenese van de nier.

In hoofdstuk 2 van dit proefschrift geef ik een beschrijving van de functionele rol van *Six2* tijdens de nier organogenese. Ik heb vastgesteld dat dit gen een onderdeel is van een genetisch mechanisme dat epitheliale polarisering tegen gaat en dat de vernieuwing van de populatie van renale epitheliale voorlopercellen reguleert door de MM voorlopercel in een ongedifferentieerde staat te houden. Functionele inactivering van *Six2* resulteerde in vroegtijdige en

ectopische differentiatie van mesenchymale cellen in de nier vesicles, uitputting van de mesenchymale stamcel populatie, verminderde UB vertakking en abnormale patroonvorming van de zich ontwikkelende nefronen.

De gehele MM populatie in de E11.5 *Six2*-nul nieren was onderhevig aan ectopische en vroegtijdige *Wnt4* expressie, wat aangaf dat in dit vroege stadium alle MM cellen waren geïnduceerd tot het vormen van nier vesicles. Omdat de corticale populatie van voorlopercellen niet in staat is zich te vernieuwen en verhoogde apoptose vertoont resulteerde dat in een ernstige renale hypoplasie en dood kort na de geboorte. Door de expressie van verschillende genen te karakteriseren die belangrijk zijn voor de ontwikkelen van de nieren hebben we vastgesteld dat er in *Six2*-nul nieren een gebrek is aan wederzijdse interactie tussen het MM en de UB. Bovendien, door gebruik te maken van nier-orgaan culturen die *Six2* overexpresseren in de mesenchymale populatie, lieten we zien dat *Six2* voldoende is om de overgang van mesenchym naar nephronen tegen te gaan. Op grond van deze resultaten hebben we de conclusie getrokken dat door onderdrukking van de inductieve signalen die de epitheliale differentiatie bevorderen *Six2* de ontwikkelings richting van de populatie van renale epitheliale voorlopercellen controleert. Deze functionele rol is essentieel voor het in stand houden van de beschikbare voorraad van ongedifferentieerde cellen voor toekomstige rondes van nefrogenese.

In samenwerking met het laboratorium van Dr. McMahon aan de universiteit van Harvard, probeerden we het mechanisme dat bestuurd wordt door *Six2* activiteit tijdens de nefrogenese beter te begrijpen. De resultaten die beschreven worden in Hoofdstuk 3, laten zien hoe we met behulp van "genetische lineage tracing" bevestigden dat het mesenchym dat *Six2* expresseert een zichzelf-vernieuwende populatie is, die de ontwikkelingsstaat van voorlopercel cel-autonomisch in stand houdt. *Six2*-expresserende cellen dragen bij aan nefron vorming tijdens de gehele nier organogenese. Met deze aanpak hebben we ook aangetoond dat *Six2*-expresserende cellen alle celsoorten van het nefron produceren en dat mesenchym zonder *Six2* aktiviteit leidt tot de vorming van ectopische nier blaasjes in *Six2*-nul nieren.

Wnt9b is het primaire inductieve signaal dat geproduceerd wordt door de ureterische buds die betrokken zijn bij de vorming van pretubulaire aggregaten en renale vesicles; daarom stelden we de vraag of *Six2* de reactie van het corticale MM op *Wnt9b* blokkeert. *Six2* expressie is normaal in de MM van *Wnt9b*-nul nieren, en *Wnt9b* expressie is ook normaal in *Six2*-nul nieren. Om een beter inzicht te verkrijgen in de relatie tussen *Wnt9b* en *Six2*, hebben we *Wnt9b*$^{-/-}$; *Six*$^{-/-}$ dubbel mutante embryo's gegenereerd en daarna bestudeerd. De vorming van nier vesicles werd niet waargenomen in *Wnt9b*$^{-/-}$ of *Wnt9b*$^{-/-}$; *Six2*$^{-/-}$ dubbel mutante embryo's; maar de omvang van de MM populatie tijdens de vroege ontwikkeling stadia van de nier voorlopercellen was veel kleiner in *Wnt9b*$^{-/-}$; *Six*$^{-/-}$ embryo's. Deze bevinding suggereert een vroegere genetische interactie tussen *Wnt9b* en *Six2* wat de interpretatie van de samenwerking tussen deze factoren tijdens de nefrogenese bemoeilijkt.

De conclusie is dat *Six2* functie tijdens de nier ontwikkeling noodzakelijk is voor de handhaving van een populatie van ongedifferentieerde mesenchymale nier voorloper cellen nodig voor de constante aanmaak van nefronen. *Six2* functie is ook noodzakelijk voor de wederzijdse repeterende inductieve interacties en groei van de nier. De defecten in de patroonvorming van de nierbuisjes en het gebrek aan UB vertakking zijn waarschijnlijk een secundair effect van het uitputten van de nier voorlopercel populatie en het remmen van de wederzijdse inductieve interacties in *Six2*$^{-/-}$ nieren. Het is mogelijk dat *Six2* de *Wnt*-gestuurde cascade van nefrogenese reguleert door vorming van onnodige nier vesicles tegen te gaan zodat de ongedifferentieerde toestand van de mesenchymale voorlopercellen gehandhaafd blijft.

In hoofdstuk 4 beschrijf ik de resultaten van lopende studies naar de functionele rol van *Six2* tijdens de ontwikkeling van de maag. Uit analyse van de maag van *Six2*-nul embryo's is gebleken dat dit gen nodig is voor de vorming van een functionele pylorische sluitspier (PS), een structuur die het terugstromen van de dunne darminhoud naar de maag blokkeert. De gladde spierlaag in *Six2*$^{-/-}$ embryo's wordt niet naar behoren verdikt in de PS-regio, terwijl de kenmerkende vernauwing van de pylorische zone van de maag portier ontbreekt, een gebrek

dat resulteert in terugstroming tussen de twaalfvingerige darm en de maag. Ik toon aan dat genen waarvan bekend is dat zij nodig zijn tijdens de PS vorming bij de kip ook to expressie komen tijdens de PS vorming bij de muis; Echter, de expressie patronen van sommige van deze genen zijn aangedaan in de *Six2*-nul maag. In het bijzonder heb ik vastgesteld dat de ectopische expressie van *Bmp4* is uitgebreid naar de vermoedelijke PS regio en dat de expressie-domeinen van *Nkx2*.5, *Sox9*, en *Gremlin* onderdrukt of verminderd zijn.

Op grond van onze resultaten kunnen we speculeren dat deze waargenomen veranderingen in expressie tijdens de vroege fase van de PS-specificatie verantwoordelijk kunnen zijn voor het uitblijven van de normale gladde spier verdikking in de *Six2*$^{-/-}$ maag. *Six2* activiteit zou het mesenchym van de toekomstige pylorische kringspier regio de mogelijkheid geven PS-bevorderende signalen te produceren, zoals *Nkx2.5*, *Sox9*, en *Gremlin*. Zonder *Six2* wordt de expressie drempel voor deze PS-bevorderende factoren niet bereikt; daardoor wordt het cel aantal dat nodig is voor de vorming van de PS niet gespecificeerd. De verlaging in *Gremlin* expressie kan leiden tot afwijkende modulatie van de BMP-pathway en ectopisch verhoogde expressie van *Bmp4* in de PS-regio. Het is ook mogelijk dat *Six2* een meer directe rol speelt bij de regulatie van de *Bmp4* expressie in de PS-regio, met als gevolg dat de ontregeling van de BMP-signalen de expressie-domeinen van de andere PS-markers in de *Six2*-nul maag verkleint.

Studies bij de kip hebben aangetoond dat in de delen van het darmkanaal waar *Bmp4* tot expressie komt zich dunnere spierlagen ontwikkelen dan in de spiermaag waar *Bmp4* expressie afwezig is. Ectopische expressie van *Bmp4* of *BMP*-receptoren in de spiermaag resulteerde in dunwandige magen, wat erop wijst dat BMP-signalen een rol spelen bij de proliferatie en differentiatie van het splanchnische mesoderm en dat ze de groei van de gladde spierlaag negatief reguleren. *Bmp4* komt ook niet tot expressie in de vermoedelijke PS regio bij de muis, wat erop duidt dat BMP-signalen een geconserveerde rol spelen bij de controle van de differentiatie van de gladde spierlaag in beide species. Het niet

verdikken van de gladde spierlaag van de PS in de *Six2*-nul maag kan een direct gevolg zijn van de ectopische expressie van Bmp4 in deze regio.

De studies in dit proefschrift bieden nieuwe inzichten in de mechanismen die leiden tot de ontwikkeling van de nieren en de maag. Deze bevindingen zullen uiteindelijk leiden tot een beter begrip van de klinische verschijnselen die veroorzaakt worden door ontwikkelingsstoornissen van de nieren en de maag. SIX2 komt tot expressie in weefsels die betrokken zijn bij Branchio-oto-renaal syndroom (BOR), een autosomaal dominante ontwikkelings-stoornis die gekenmerkt wordt door nier en urinewegen anomalieën, doofheid, en aangezichts afwijkingen. Mutaties in EYA1, SIX1, en SIX5 die de binding van EYA1 aan SIX eiwitten beïnvloeden werden ook aangetroffen bij patienten met het BOR Syndroom. Het is daarom mogelijk dat SIX2 mutaties ook bij BOR-patiënten zouden kunnen voorkomen. Mutaties in SIX2 en BMP4 werden aangetoond bij een aantal patiënten met nier-hypodysplasie. Omdat onze analyse van de *Six2*-nul maag heeft aangetoond dat *Six2* mogelijk de expressie van *Bmp4* bepaalt, is dit een zekere reden om deze interaktie tijdens de ontwikkeling van de nier verder te analyseren.

In het menselijk darmkanaal kunnen ablatie van de PS, onvolledige sluiting van de PS, of imperfecte timing van de peristaltiek een duodeno-gastrische reflux veroorzaken. Het terugstromen van de dunne darminhoud kan schadelijk zijn voor het maagslijmvlies en vergroot de kans op maagkanker. Het tegenovergestelde fenotype, Infantiele Hypertrofische Pylorische Stenose (IHPS), is een aandoening waarbij het lumen opgevuld wordt door de overgroeide gladde spier van de PS wat het legen van de maag tegengaat. De *Six2*-nul maag zou daarom nuttig kunnen zijn om de mechanismen achter deze aandoeningen verder te definiëren.

セ

ACKNOWLEDGEMENTS

The time that I have spent working on my PhD in the department of Genetics and Tumor Cell Biology at St. Jude Children's Research Hospital has been a very exciting and fun time. However, the past six years have also been some of the most difficult of my life, both professionally and personally, and I could not have reached this point in my life without the help and support of many people that surround me.

First I would like to thank my loving husband, Scott, who has been a rock of support in my life. Without him, I would not have achieved this goal. He has provided more love, support, and encouragement than I could have ever imagined. Words alone could never express how eternally grateful I am to him and how much I love him for it.

Next I would like to thank my family. My parents have supported me in countless ways and they always believed in me even when I didn't. Throughout my life, my mom has been the driving force to push me to better myself and accomplish my highest goals. She has always been a huge inspiration to me and "the wind beneath my wings". I also want to thank the rest of my family for being so supportive and understanding. I am especially grateful to my Memaw who always has been and always will be an inspiration in my life. I hope that she knows how much I miss her each day.

At St. Jude, I have been surrounded by compassionate friends who are always willing to help when needed. First, I would like to thank Guillermo and Gerard for allowing me to work as a student through Erasmus University while working at St. Jude. Guillermo has been extremely generous to allow me to work on my own research project as a graduate student in addition to my technical and managerial duties in the lab. As a great mentor, he has always supported me and pushed me to be a better scientist for which I will always be grateful. I am also thankful to Gerard for all of his help during this journey. He has been exceptionally kind and helpful with the preparations of the thesis and defense. I would also like to thank all of the PI's in the Genetics department – Gerard

I have been tremendously blessed to have such great friends and family in my life, and to God I must give thanks for that. Without Him, none of this would have been possible.

Curriculum Vitae

Education

1999-2000 **Master of Science in Natural Sciences**
Delta State University, Cleveland, MS, USA

1992-1995 **Bachelor of Science**
University of Southern Mississippi, Hattiesburg, MS
Mississippi Delta Community College, Moorhead, MS

Professional Experience

2000-2008 Senior Research Technologist/Lab Manager
St. Jude Children's Research Hospital
Department of Genetics
Lab of Dr. Guillermo Oliver
Memphis, TN 38105

1997-2000 Public School Science Teacher
Grenada Middle School
Grenada, MS 38901

Honors

Best Poster Award, 7th Annual Vanderbilt University Medical Center Program in Developmental Biology Retreat, Paris Landing State Park, Buchanan, TN, September 5-6, 2003.

Best Poster Award, 10th Annual Developmental Biology Program Retreat, Paris Landing State Park, Buchanan, TN, September 22-23, 2006.

Student Travel Award, Society for Developmental Biology 62nd Annual Meeting, Boston, MA, July 30-August 3, 2003.

Publications

Self M, Lagutin O, Bowling B, Hendrix J, Cai Y, Dressler G, Oliver G (2006) Six2 is required for suppression of nephrogenesis and progenitor renewal in the developing kidney. *EMBO J* 25:5214-5228.

Kobayashi A, Valerius MT, Mugford JW, Carroll TJ, **Self M**, Oliver G, McMahon AP (2008) Six2 defines and regulates a multipotent self-renewing nephron progenitor population throughout mammalian kidney development. *Cell Stem Cell* 3:169-181.

Kutejova E, Engist B, **Self M**, Oliver G, Bobola N (2008) Six2 functions redundantly immediately downstream of Hoxa2. *Development* 135:1463-1470.

Self M, Oliver G. Six2 activity is required for the formation of the pyloric sphincter during mouse stomach development. *Manuscript in preparation*.

Poster Presentations and Talks

Self M and Oliver G. Six2 controls growth of the glandular stomach and pyloric sphincter formation. 11th Annual Developmental Biology Program Retreat, Paris Landing State Park, Buchanan, TN, September 7-8, 2007.

Self M, Lagutin O, Bowling B, Hendrix J, Dressler G, Carroll T, Valerius T, McMahon A, and Oliver G. Six2 activity is required for suppression of inductive signals and progenitor cell renewal in the developing kidney. Southeast Regional Society for Developmental Biology Meeting, Vanderbilt University, Nashville, TN, April 7-9, 2006.

Self M, Lagutin O, Bowling B, Hendrix J, Dressler G, Carroll T, Valerius T, McMahon A, and Oliver G. Six2 activity is required for suppression of inductive signals and progenitor cell renewal in the developing kidney. 10th Annual Developmental Biology Program Retreat, Paris Landing State Park, Buchanan, TN, September 22-23, 2006.

Self M, Lagutin O, Bowling B, Hendrix J, Dressler G, and Oliver G. Six2 controls critical steps in the development of the mammalian kidney. 8th Annual Vanderbilt University Medical Center Program in Developmental Biology Retreat, Paris Landing State Park, Buchanan, TN, September 10-11, 2004.

Self M, Lagutin O, Bowling B, Hendrix J, and Oliver G. The homeobox gene *Six2* controls critical steps in mammalian kidney development. 7th Annual Vanderbilt University Medical Center Program in Developmental Biology Retreat, Paris Landing State Park, Buchanan, TN, September 5-6, 2003.

Self M, Lagutin O, Bowling B, Hendrix J, and Oliver G. The homeobox gene *Six2* controls critical steps in mammalian kidney development. Society for Developmental Biology 62nd Annual Meeting, Boston, MA, July 30-August 3, 2003.

Self M, Lagutin O, Bowling B, Hendrix J, Dressler G, and Oliver G. Six2 controls critical steps in the development of the mammalian kidney. American Society of Nephrology Renal Week 2004, St. Louis, MO, October 27-November 1, 2004.